VEGETATION TYPE AND DEGRADATION CLASSIFICATION ON THE MONGOLIAN STEPPE USING RANDOM FORESTS

by
Wei Liu

A thesis submitted
in partial fulfillment of the requirements
for the degree ofMaster of Science
(Natural Resources and Environment)
at the University of Michigan
August 2013

Faculty advisors:
Dr.Daniel G. Brown
Dr. Kathleen M. Bergen

Abstract

Creating consistent supervised vegetation classifications in different countries where training data are of different levels of quality and detail is challenging but important. For example, mapping steppe types and degradation of Mongolia and Inner Mongolia Autonomous Region (IMAR), China,using the same classification scheme would be helpful for doing comparative studies between the two regions and acquiringa better understanding of how country level differences affect vegetation on theMongolian Plateau.

Steppe and degradation maps, created through on-screen digitizing that combined image and ground information as input,were available inIMAR but not in Mongolia.We exploredsupervised classificationusing Random Forests (RF) to identifya reasonable sampling and training strategy and applied identical methods toclassify remotely sensed images (Landsat Thematic Mapper 5) in IMAR and Mongolia using the same classification systems for the two countries in three ecological regions (meadow steppe, typical steppe and desert steppe). A number of challenges limit our ability to extend classifications trained in IMAR to Mongolia for creating consistent vegetation maps.

Acknowledgement

This study was funded by NASA LCLUC Program (NNX09AK87G), "Grassland Ecosystems and Societal Adaptations Under Changing Grazing Intensity and Climate on the Mongolian Plateau. “We are thankful to the Inner Mongolian Institute of Grassland Survey and Design, theChinese Academy of Sciences and the Mongolian Academy of Sciences for providing us valuable data. We also express sincere thanks to Dr. YichunXiefrom Eastern Michigan University, Mr. Shannon Brines from Environmental Spatial Analysis Lab at University of Michigan and all the other people who offered us help.

Table of Contents

1. INTRODUCTION

Comprehensive comparative analyses of vegetation types and conditions are necessary across ecological gradients and across administrative boundaries to better understand entire ecosystemsand human impacts under different socio-economic contexts. For example, although grasslands in Mongolia and Inner Mongolia, China, have similar basic landscape, structure and plant composition, comparative studies have shown that different grazing stylesand policies in the two countries have led to differential impacts of grazing activity (Bao et al., 2008). As in other cross-national situations, availability of data with which to build comparable vegetation classifications varies quite dramatically between these two countries. Compared to a large number of studies about steppe vegetation, degradation and grazing in IMAR (e.g. Jiang et al., 2010; Liang et al., 2009; Lin et al., 2010; Xie and Sha, 2012; Pei et al., 2008), data and knowledge are only sparsely available to represent the regional patterns in Mongolia (Retzer et al., 2006). Steppe vegetation and degradation mapsacrossthe Mongolian plateau at relatively fine spatial resolution (<50 meters), or at least using commonclassification schemesfor selected images from both IMAR and Mongolia, can make contributions to the study of this region by providingconsistent base maps for comparative study. The use of remote sensing makes it possible to map land cover over a large area, but classification and mappingof steppe vegetation is still very challenging because the same vegetation types may have different spectral responseunder somewhat different ecological conditions, while at the same time different vegetation types may have similar spectral characteristics (Sha et al. 2008).

Provided with reliable andlarge-scale IMAR steppe-type and degradation maps, digitized from Landsat Thematic Mapper 5 (TM5) imagery, and given the high similarity between Mongolia and IMAR along the ecological gradients, we address the following research questions inthis study:

(1) At what level of accuracy canwereproduce the IMAR map of steppe types and degradation through automatic classification?

(2) Can we classify steppe types and degradation levels of Mongolian Landsat TM5 imagesbased on algorithms developed and trained using IMAR data?

(3) What accuracy rate canwe attain in such a predictive mapping experiment?

Methodsfor classifyinglandcover using remotely sensed data includesupervised and unsupervised approaches, and parametric and non-parametric techniques. Frequently used approaches include Iterative Self-Organizing Data Analysis (ISODATA) unsupervised method (Tou and Gonzalez, 1974), supervised classification using maximum likelihood decision rules (Jensen, 2005), support vector machines (SVM) (Cortes and Vapnik, 1995), artificial neural networks (Mas and Flores, 2008), and classification and regression trees(CART) (Breiman, 1984). To meet thegoals of this study, the classifier should be able to classify external imagesafter being trained and to produce comparable classifications on images without training samples. Unsupervised methods, such as ISODATA, cannot be expected to produce comparable classifications. Other methods, like maximum likelihood technique, cannot meet our requirement because thevery limited information ofsteppe types of Mongolia and little ground truth dataare insufficient for training. Furthermore, we were not able to collect training samples directly from the image, nor label classes for supervised classification. For these reasons, we evaluated the random forests (RF)classifier as a technique that might fulfill our requirements.

RF is a tree-based ensemble classifier, suggested by Breiman (Breiman, 2001). A RF is generated by using bootstrap samples with replacement to grow a large amount of unpruned classification trees and each of these trees in the "forest" provides a single vote, thus the input data will be assigned with the class that gets the most votes. Instead of using the best variables, a RF randomly draws subsets of input predictive features at every splitting node to grow trees that can minimize correlation between trees in the ensemble (Breiman, 2001; Liaw and Wiener, 2002). The RF also provides estimation of the error rate based on the training data, called out-of-bag (OOB) error. During each bootstrap iteration, around one third of samples are left out and not used for training that certain tree, but being passed down that tree and classified instead under the assumption that the class of samples are unknown. At the end of the run, the error rate is calculated by averaging OOB predictions from all trees in the "forest," which provides an unbiased estimation of the generalization error so a separate testing dataset is not necessary (Breiman, 2001). RF can also measure the importance of variables during the run by permuting a variable in OOB elements while holding others unchanged and calculate how much accuracy decreased (Breiman, 2001) which provides users with better understanding of the "black box" than method such as neural networks (Prasad et al., 2006). In addition to characteristics introduced above, the RF algorithm seems to be suitable for our study because of its many other appealing features. For instance, it allows a large amount of predictive factors as input without variable deletion; the computational load is small even with a large dataset; and once the model is created, it can be saved and used to classify other datasets. (Breiman, 2001).Many studies have shown that RF classification attains about the same or better overall accuracy, as many other image classification algorithms. For example, using Landsat TM5 data for land-cover classification in the south of Spain, RF gave a significantly better overall performance than a single decision tree, and the RF is also shown to be robust to training data reduction and noise (Rodriguez-Galiano et al., 2012). Using Landsat Multispectral Scanner (MSS) data to classify forests,RF was shown to outperform the single CART classifier andproduce results comparable to bagging and boosting in terms of accuracy, but faster in training (Gislason et al., 2006). Chan and Paelinckx (2008) used airborne hyperspectral imagery to compare RF and Adaboost (which is another tree-based ensemble classification algorithm). They ended up with less than 1% difference in overall accuracy and both methods outperformed a neural network classifier. Pal (2005) showed that, compared with the support vector machines, the RF classifier had equal performance in terms of classification accuracy and training time but required fewer user-defined parameters.RF has also been integrated with image segmentation to conduct object-based classification in some recent studies (Stumpf and Kerle, 2011;Immitzer et al., 2012; Duro et al., 2012; Guan et al., 2013). However, to date RF has not been used specifically for classification of steppe vegetation and degradation of a large area, or for predictive mapping of steppe vegetation and degradation.

The overall goal of this study was to assess approaches to training a RF classifier to consistently classify similar vegetation types and degradation in both the IMAR and in Mongolia.Our approach includes systematic exploration of commonchoices faced when RF is used for image classification and prediction (such as classification unit, unit size and sampling strategies of training dataset). We compared pixel- and patch-based spatial units for classification, combining RF with image segmentation (REF)for the latter. We also wanted to quantitatively examine how RF's prediction power would change under all these different experimental scenarios.

2. STUDY AREA

The country of Mongolia and the Inner-Mongolia Autonomous Region (IMAR) of China form the Mongolia Plateau. The grasslands within these two countries are part of the Eurasian steppe region, which is the largest contiguous grassland area in the world (Bai et al., 2004). Mongolian steppe is not only important habitat for wildlife but is also important for local herders whose livelihoods depend on grazing. However, steppe degradation has become a serious problem in the IMAR of China due to overgrazing, land-use change and variation in climate and other reasons (Tong et al., 2004).

Our study areas are located in both IMAR and Mongolia. The Mongolian steppe vegetation consists of three types of ecological regions distributing from northeast to southwest:meadow steppe, typical steppe and desert steppe(Yu et al. 2003).The annual precipitation of meadow steppe and typical steppe are around 450 mm and 350 mm respectively, while the desert steppe has annual precipitation between 150 and 250 mm and is also influenced by continental climatic conditions (Kang et al., 2007). Biomass production decreasesalong the climate gradient frommeadow steppe andtypical steppe todesert steppe (Yu et al. 2003).

To thoroughly examine the performance of the RF classification method over areas representative of the broader Mongolia plateau, we selected a pair of study sites in each ecological region, one each in IMAR,China and Mongolia (Figure 1). For meadow steppe, we selected an area focused on the Ewenk Autonomous Region (county level) of Hulunbuir City (prefecture level) in IMAR and Khalkhgol sum (district level) Dornodaimag (province level) in Mongolia. For typical steppe, we chose the area around Xilinhot City of Xilingol League in IMAR and the central part of Sükhbaataraimag (including Khalzan, Asgat, Dariganga and Ongon sums) in Mongolia. For desert steppe, we selected Urat Middle Banner of Bayannur City of IMAR and an area around the border between Ömnögoviaimag and Dornogoviaimag of Mongolia (including Khanbogd sum and Khatanbulag sum).

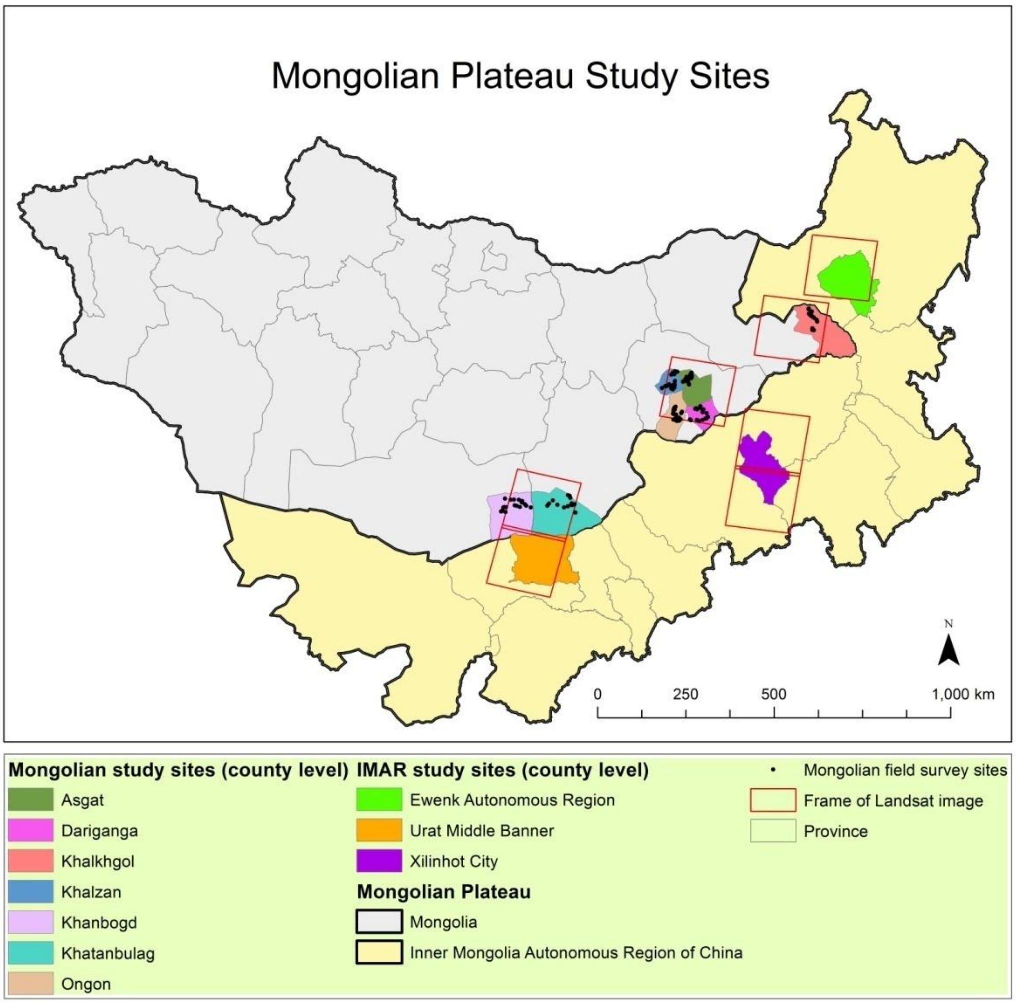

Figure 1. Distribution of study sites on Mongolian Plateau

3. METHODS

3.1 DATA

3.1.1 2009 vegetation and degradation classification maps of IMAR steppe

The IMAR vegetation and degradation maps were provided by the Inner MongolianInstitute ofGrassland Survey and Design (IMIGSD). Scholars of IMIGSDcreated classified vegetation maps by on-screen digitizing based on 2009 Landsat TM5 images while using field survey data, historical data and other ancillary data for reference and validation. Although they mapped the entire autonomous region, we acquired vegetation maps for three counties in IMAR (Ewenk Autonomous Region, XilinhotCity and Urat Middle Banner). Steppes are classified into a two-level classification system (Table 3). This classification scheme integrates landform, soil and vegetation information in steppe classification.To simplify class names, we re-coded each class with a lettercode (Table 3). The digitized polygons in these 2009 vegetation maps were also assigned a degradation level according to a national standard for classifying grassland degradation in China called Parameters for Degradation, Desertification, and Salinization of Rangelands (GB 19377 - 2003) (MOA, 2003). By comparing a target area with conserved grassland nearby, grasslands were classified into three degradation categories, each with three levels (Table 4). This degradation classification system was also recoded in this study. The national standard document states that slight salinization or desertification can be regarded as moderate degradation, and moderate or severe salinization or desertification can be regarded as severe degradation. Thus in our study, we merged those classes in order to just simply show degradation information.

Table 3. Vegetation classification system and class codes
* Absent in study sites
** Excluded from classification

Steppe type - Level 1	Steppe type - Level 2	Letter code
Temperate meadow steppe	Plain/hill meadow steppe	A
	Mountain meadow steppe	B
	Sand land meadow steppe	C
Temperate typical steppe	Plain/hill typical steppe	D
	Mountain typical steppe	K
	Sand land typical steppe	E
Temperate desert steppe	Plain/hill desert steppe	L
	Mountain desert steppe	M
	Sand land desert steppe	N
Temperate steppe desert	Steppe desert	O
Temperate desert	Gravelly desert	P
	Sandy desert	Q
	Saline desert	*
Lowland meadow	Lowland and wetland meadow	F
	Salinized lowland meadow	G
	Swampy lowland meadow	H
Mountain meadow	Low/middle mountain meadow	I
	subalpine meadow	*
Swamp/marsh	Swamp/marsh	J
Improved grassland	Cultivated pasture	**
Non-steppe	Agriculture/urban/etc.	**
Water	Water	**

Table 4. Degradation classification system and class codes

Degradation type - Level 1	Degradation type - Level 2	Letter code	Letter code (merged classes)
No degradation	No degradation	a	a (No degradation)

Degradation	Slight degradation	b	b (Slight degradation)
	Moderate degradation	c	c (Moderate degradation)
	Severe degradation	d	d (Severe degradation)
Desertification	Slight desertification	e	c (Moderate degradation)
	Moderate desertification	f	d (Severe degradation)
	Severe desertification	g	d (Severe degradation)
Salinization	Slight salinization	h	c (Moderate degradation)
	Moderate salinization	i	d (Severe degradation)
	Severe salinization	j	d (Severe degradation)

3.1.2 Landsat TM5 imagery and pre-processing

The existing vegetation and degradation maps were used as reference data for training image classifications. We were also provided with field survey data of Mongolia collected by scientists in Mongolia (see Sec. 3.1.4). Therefore we selected our imagery to be congruent in time with those data. In order to have both IMAR and Mongolia images of growing season with as little time difference to each other and to reference map and field survey data as possible, and also with 10 percent cloud cover or less, seven Landsat TM5 images from 2009to 2011 were selected to cover all study sites. Image dates are listed in Table 1.

With the exception of the thermal band, all Landsat bands were imported and stacked together, and images were then re-projected to the Albers equal-area conic projection. Clouds and their shadows were removed from each image using eCognition software (Trimble®)supplemented by on-screen digitizing for minor edits. All images were then atmospherically corrected using the COST method (Chavez, 1996) within ERDAS Imagine® software (Intergraph Corp., Huntsville, AL). The Xilinhotsite in IMAR is covered by two images (path 124 row 29 and path 124 row 30) that were taken on the same day. Thus these two images, as well as thescenes for desert steppe,were mosaicked and a histogram match was applied to each band within ERDAS Imagine. To address the two-year differences between image pairs and make images more comparable, images of path 123 and row 26 and of path 124 and row 27 were connected by introducing image of path 123 and row 27 (also taken at Aug. 11th, 2011) and all three of them were mosaicked together using histogram matching band by band after atmospheric correction. Lastly, all the IMAR images were clipped to the boundaries of counties in the reference vegetation and degradation maps. To reduce the size of data, Mongolian images were also clipped to the boundaries of counties or districts located within the Landsat scenes where the field survey data were distributed.

Table 1. Selected Landsat TM5 images and acquisition date

Country	Dominant Vegetation Community	Site Name	Path	Row	Date of acquisition
IMAR of China	Meadow Steppe	Ewenk	123	26	08-11-2011
	Typical Steppe	Xilinhot	124	29	08-02-2011
		Xilinhot	124	30	08-02-2011
	Desert Steppe	Urat	129	31	07-01-2010
Mongolia	Meadow Steppe	Khalkhgol	124	27	08-12-2009
	Typical Steppe	Asgat etc.	126	28	06-26-2010
	Desert Steppe	Khatanbulag etc.	129	30	07-01-2010

3.1.3 DEM data

In the classification scheme for the vegetation types, steppes were classified according to both vegetation communities and landforms, so elevation information should be an important input in the process of classification. The 30-meter spatial resolution ASTER global digital elevation model data of study area were downloaded and projected into the same projection coordinates as our processed Landsat images. Terrain features, including slope, aspect, and topographic wetness index, were later derived from this DEM data.

3.1.4 Field survey data of Mongolia

Ground truth data are necessary during the validation of classification result. The Mongolian collaborators on our team from the Institute of Botany, Mongolian Academy of Sciences provided us with field survey data collected in the summer of 2011 (July 11 to July 29). There are 137 ground truth records with coordinates that can be plotted as points, and 119 out of them were located within our image subsets. Each point in this dataset represents a 1 meter by 1 meter plot, and information such as general vegetation community and dominant species in that particular plot was documented. The name of the vegetation community of each plot was actually a combination of species, with the most representative species of that kind of vegetation community ranked the first. Though this field survey dataset cannotform an entire training dataset because the number not enough, it can be used for validation of classification results. However, since these points were not labeled with exactly the same classes as those defined in IMAR steppe vegetation and degradation classification system, they required some modification for use in validation. Scholars from Chinese Academy of Sciences who have been working on Mongolian steppes and very familiar with grassland species provided us with a match table (appendix B) that allowed us to classify the field survey points into our required classes based only on vegetation community and species. Thus we used these data for validation of vegetation type (steppe type specifically). However, these field survey points cannot be used to validate degradation classification results because we did not have additional information that allowed us to label these field survey points with degradation levels.

3.2 Predictor variables

To build and train RF, we calculated a number of predictor variables to help distinguish vegetation classes and degradation levels. These predictor variables included spectral features, terrain features and texture features.

For spectral features, in addition to digital numbers (DNs) of each processed Landsat TM5 band, several indices and other features derived from the Landsat TM5 image were used for classification. The first one is the ratio vegetation index (RVI) which is defined as formula (1) below (Jackson and Huete, 1991). The second one is the normalized difference vegetation index (NDVI), which is probably the most widely used vegetation index and its mathematical transformation is given in formula (2) below. Third is the soil adjusted vegetation index (SAVI), which includes a correctionforthe influence of soil brightness, and we used 0.5 for the value of the soil brightness correction factor L in formula (3).The formulas of RVI, NDVI and SAVI were based on Richardson and Everitt (1992). The tasseled Cap transformation was also applied to all images and, unlike the other three indices, the Tasseled Cap transformation incorporates more information by using different combinations of all six Landsat bands (Crist &Cicone, 1984). Weused the first three components of the transformation (brightness, greenness and wetness) in our study.

$$\mathrm{RVI} = \frac{\mathrm{Band\ 4}}{\mathrm{Band\ 3}} \qquad (1)$$

$$\mathrm{NDVI} = \frac{\mathrm{Band\ 4} - \mathrm{Band\ 3}}{\mathrm{Band\ 4} + \mathrm{Band\ 3}} \qquad (2)$$

$$\mathrm{SAVI} = \frac{(1+\mathrm{L}) * (\mathrm{Band\ 4} - \mathrm{Band\ 3})}{\mathrm{Band\ 4} + \mathrm{Band\ 3} + \mathrm{L}} (3)$$

The second group of features consists of those representing terrain attributes such as elevation, slope and slope aspect. All these features were extracted or derived from the DEM data. These variables describe the local landform that is also a critical constituent of the steppe type classification system. Moreover, terrain may also affect grassland degradation (Xie and Sha, 2012). For instance, in Xilinhot, increase in altitude and slope tended to be negatively correlated with increase in level of degradation from 1991 to 2005 (Li et al., 2012).

Because we needed to calculate the zonal mean of aspect of every patch, we converted the angular value of aspect to a measure ranging from 1 (south-facing) to -1(north facing) by using the formula *cos(aspect - 180)*. Water availability also greatly affects vegetation health in Mongolia (Kogan et al., 2004) thus we introduced the topographic wetness index (TWI) into our analysis which is also derived from the

DEM data. The TWI is defined as*ln(α/tanβ)* where *α* stands for the area drained per unit contour length at a point while *tanβ*is the percent slope (Beven and Kirkby, 1979). The TWI was calculated by using Model Builderin ArcMap v10.0(ESRI, Redlands, CA) with 30-meter resolution and the method of deriving accumulated flow is described in Jenson and Domingue (1988).

Texture features wereincluded only in patch-based classifications, using second-order measures based on thegrey level co-occurrence matrix (GLCM) (Shaban and Dikshit, 2001; Rodriguez-Galiano et al., 2012). GLCM-based texture measures have been shown to improve land-cover classification accuracy in some studies (Lu et al., 2007, Shaban and Dikshit, 2001, Franklin and Peddle, 1990). We selected six GLCM-based measures from among the many possible options (GLCM mean, entropy, contrast, correlation, homogeneity and dissimilarity). Each of them wascalculated using all six Landsat spectral bands and from all directions. To avoid concerns about sensitivity to window size for pixel-based classification and to ensure these two datasets are comparable, we limited our application ofGLCM texture features to thepatch-based classifications.

3.3 Decision-making process

In order to evaluate alternative approaches toclassifying Mongolia images using RF, aseries ofexperiments wasconductedusing the 2009 IMAR data and IMAR Landsat images. This allowed us to test for the most effective way to apply RF in our study. The results of some experimental steps influenced the decision of following steps(Figure 2).

3.3.1 Classification unit

The firstwas whether we would conduct pixel-based or object-based (or patch-based) classification. Pixel-based classification provides finer resolution while patch-based classification can help the fine-scale noise that can accompany pixel-based classifications. Moreover, pixel-based classification involves very large data sets and requires extremely large memory usagein R, making it more difficultto implement than patch-based classification.

To test patch-based (or object-based) classification, images were segmented using eCognition software. Values of parameters were investigated and selected (Table 2). Bands 4, 3, 2 were given higher weight because, during the digitizing of 2009 vegetation and degradation maps, the false color infrared combination was selected for visual interpretation. Values of other parameters weredetermined through a series of trials and visualexamination by comparing boundaries of segments with boundaries of classes in the 2009 China vegetation type and steppe degradation maps. The "color" parameter played a dominant role among the homogeneity criteria,probably because spectral information contributed more during the digitizing process when the vegetation and degradation maps were created. The "scale" parameter determines the size of patches by limiting the maximum allowed heterogeneity of each patch

(Definiens Professional 5 Reference Book).We selected values of 20 and 40 for later comparison by taking both resolution and computational efficiency into consideration. The same parameters within eCognition were used for all of the IMAR and Mongolia Landsat images not only because this set of parameters works well for all sites, but it can also keep the consistency that is helpful in the comparison experiments that involve multiple sites.

Table 2. Parameters used during segmentation

Parameter	Value
Layer Weights	Layers 1, 5, 6 (Band 7): 0.5 Layers 2, 3, 4: 1.0
Scale	20 (and 40)
Color : Shape	0.9 : 0.1
Compactness : Smoothness	0.5 : 0.5

To test which method producedclassifications withhigher accuracy, we collected pixel and patch samples for a comparative experiment. For each study site in IMAR, we created 50,000 random points with 50-meter minimum separation (to make sure no points fall in the same pixel) and extracted all values of predictor variables (except for texture features which is not available for pixels),as well as the steppe class and degradation level codes. All non-steppe points were deleted from the dataset. For each polygon created during image segmentation, we calculated the zonal-mean forevery spectral and terrain feature (texture features were collected during segmentation by not used for this comparison experiment) and then labeled each polygon with steppe class and degradation class represented by the pluralityof pixels within that polygon. Non-steppe patches were deleted from this dataset as well. When we created the RF model, usingthe RandomForest Package (Liaw and Wiener, 2002) in R v2.15.1, we made the model to randomly draw a balanced 200 samples per class from the input dataset to avoid askewed distribution of steppe types that could bias the effect of RF classifier when building the model. However, in Urat Middle Banner, classes have very skewed distribution and some classes have only a few samples in the datasets, which limited the number of samples can be drew to build trees. Thus we assigned smaller sample sizes to these classes. For each RF model, input features and other model parameters were the same. However, we also added texture features to patch-based classification to test for improvements in accuracy and the kept four most important texture variables for later experiments.

3.3.2 Patch size

Based on the result of the comparison ofpixel-based andpatch-based classifications (presented in section 4), we proceeded with patch-based classifications for future experiments. Next, we were interested how the size of those patches as determined by the 'scale' factor during segmentation affects the classification accuracy. For the second experiment, we compared patch-based classifications at "scales" of 20and 40.

Increasing the scale value to 40 resulted in the total number of patches decreasing to around one fourth the number created with a scale of 20.To compare the classification outcomes at these two scales, we used the same predictor variables in RF models but, due to fewer patches using the larger scale value, we sampled 50 patches per class instead of 200 when creating these models. We adjusted the sample numbers of Urat Middle Banner according to values we used in patch and pixel-based comparison experiments due to very skewed distribution steppe classes and to make datasets of two scales comparable.

3.3.3 Local Prediction

Both comparison experiments introduced above used the Out-of-Bag (OOB) error and error matrix (introduced in section 4.4) to assess the classifiers' performance instead of using a separate testing dataset. We then tested if we could maintain a similar accuracy rate if we used justa part of the set of patches to build the RF and classify all patches in the entire IMAR county. We refer to this experiment as "local prediction." To avoid biased classification caused by an unbalanced sample, we used the Hawth's tools for ArcGIS (Beyer, 2004) to do balanced random sampling of the training dataset for input tothe patch-based RF model. Then we used that model to classify the study site in IMAR and compared that with the 2009 classification reference map for accuracy assessment. Since training samples were randomly collected, these patches were distributed all over the image. We sampled 200 patches class in Ewenkimage, and these 200-per-class sampled patchesrepresented7.40% and 2.96% of total patchesrepresenting vegetation type and degradation level, respectively, within the image subset of Ewenk. We did the same for the Xilinhot image, and the percentages of total patches were 5.18% and 2.58%, respectively. However, the sampling ratio varies from class to class due to this balanced sampling design. In Urat Middle Banner, because only a few patches of class N (Sand land desert steppe), Q (Sandy desert) and H (Swampy lowland meadow) were available, these classes were merged with class M (Mountain desert steppe), P (Gravelly desert) and G (Salinized lowland meadow) respectively before the 200-patch-per-class sampling (ratios are 4.60% and 2.63% of total patches). Sampled patches used for training were retained in the dataset of eachcounty when we did prediction.

3.3.4 Prediction within an ecological region

Forclassifying images inMongolia, we have no local samples in training datasets; thus we have to test if RF can help us classify an "unknown" area. Thus in our next experiment, we applied our methodology for use in out-of-sample prediction in our IMAR sites. We split images of our IMAR sites into two halves with both halves having relatively the same area and steppe types. We used one half to build a RF model and the other to test the accuracy of predictions. Then we trained the model and did classification the other way round (switching the training and testing halves). This is what we called"prediction within a certain ecological region (eco-region)."

3.3.5 Prediction across ecological regions

The eco-region boundariesarecoarse and gradients exit where steppes change gradually. Urat Middle Banner in desert steppe is a quite arid area, so it is very different from the other two IMAR sites. However, Ewenk Autonomous Region and Xilinhot City hadsimilar landscape characteristics. Though Ewenk Autonomous Region was in the meadow steppe eco-region, there is still typical steppe within the region. Similarly, although Xilinhot City is mostly covered by typical steppe, meadow steppe also exists in the area. Sites of the Mongolia located in meadow steppe region and typical stepperegion probably also contain both steppe types. We were not sure which IMAR site is most similar to each of sites in Mongolia. To be prudent in training dataset selection, we were interested in looking at what accuracy we could reach if we use Ewenk Autonomous Region data to build the RF model and classify the Xilinhot City and vice versa.We refer to this experiment as "prediction across eco-regions." Since elevation was a very important variable during earlier classification tests, and because there the average elevations weredifferentbetween Ewenk and Xilinhot(770 and 590 respectively), we subtracted the mean elevation within each area from the actual elevation value for both sites to calculate a relative measure of elevation within each county. All the other input variables of RF model remained the same.

3.3.6 Pooling and filtering

After experimentingwithmutual prediction between Ewenk and Xilinhot, both in IMAR, we pooled the training datasetsfor Ewenk and Xilinhot and used the combined datato classify all patches in each region. Unlike local-prediction, external information was added when the RF was built, and this may help the classifier cover greater variety of certain types of steppe and degradation levels. To do this, we combined the 200-per-class randomly sampled datasets used in "local prediction" experiments from Ewenk and Xilinhot into a single training dataset. Those classes that only existed in one site had 50% fewer observations in the combined dataset. However, when we built the model, we still sampled 200 patches per run. We created these pooled datasets for both steppe types and steppe degradation classes. Also, just as what we did in the "prediction across ecological region" experiment, we used the relativeelevation value during both training and prediction.

During our experiments, we noticed that by using a random sampling strategy for collecting training samples, some inappropriate patches were selected into the training dataset. For example, in the 2009 digitized steppe vegetation and degradation maps, road pixels were not well delineated and they were labeled as steppe. Also, becausewe labeled patches using the zonal majority statistics, there were some patches not completely within the digitized steppe boundary but they were labeled with a single steppe type and selected into the training dataset. These mixed patches may not be representative enough for their labeled classes. Thus we manually filtered out those non-steppe and/or significantly mixed patches from the 200-per-class sample sets of Ewenk and Xilinhot based on visual examination and pooled these filtered patches from Ewenk and Xilinhotto see if this "purified" training dataset couldimprove the classification accuracy. We did not do this for degradation classification because there were only four classes in the degradation classification andit was hard to visually interpret degradation levels of different steppe types and tell if a patch is a typical representative of a certain degradation level.

3.3.7 Classify images of Mongolia

With all these experiments above done with IMAR data, we were able to gain a better understanding of the effects of choices about inputs to the RF classifier on steppe classification. Next, we developed a strategy forclassifying image subsets within the country of Mongolia based on our experiments in IMAR and in ways that would ensure that these Mongolian classificationsare congruent with those in IMAR. Because the Mongolian sites in meadow steppe and typical steppe eco-regions were between Ewenk Autonomous Region and Xilinhot City of IMAR in terms of latitudes, we decided to use pooled, non-filtered patchesfrom Ewenk and Xilinhot to train the model and classify those two Mongolian images. For the desert steppe site, we used the samples from Urat Middle Banner as training dataset to classify corresponding Mongolian image subsets. We used the same predictor variables as used in the above experiments on the IMAR sites. These included DNs from Landsat TM5 band 1 to band 5 and band 7; brightness greenness and wetness layers from tasseled cap transformation; the RVI, NDVI and SAVI indices; terrain variables including slope aspect and elevation; and lastly four selected texture features (GLCM entropy, homogeneity, dissimilarity and contrast). For the desert steppe sites, we used the steppe type classification scheme after merging some of classes as we did in earlier experiments of Urat site.

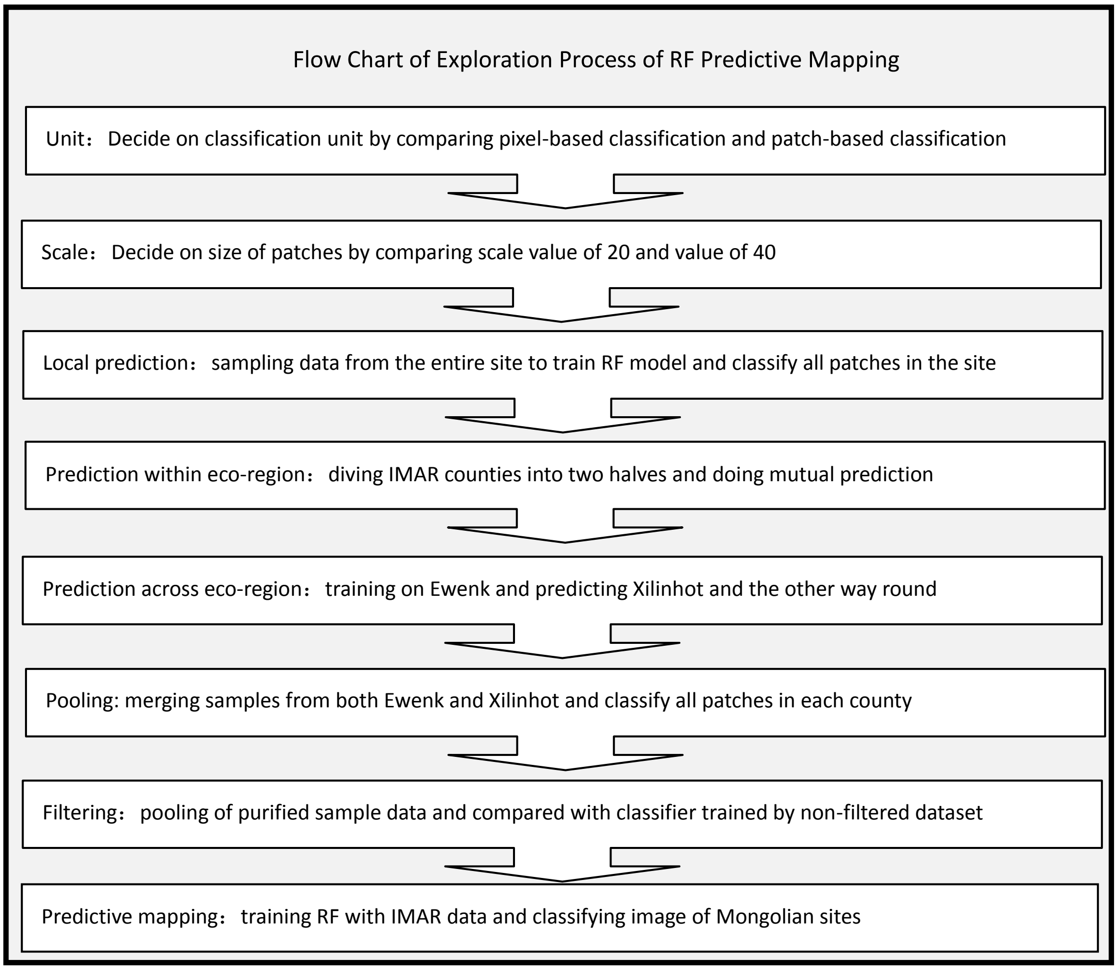

Figure 2. Workflow of exploring Random Forests

3.4 Random Forests

When we created eachRF model, besides predictor variables, there were two key parameters of the model itself that needed to be defined. The firstis the number of trees and the other is the number of variables randomly sampled as candidates at each split of a classification tree. RF does not over fit data and our experiments showed that, for our dataset, error rates became steady after about 500 trees were built. We decided to build 2000 trees for all our models and regarded it as a conservative choice. As for number of variables sampled during split, we simply used the default value built into the software package, which is the closest integer to the square root of total number of features. Studies have shown that the number of random split variables can only slightly alter the classifier's accuracy and the RF,so setting this parameter hardly requires much guidance (Rodriguez-Galiano et al., 2012).

The inherent randomness of this RF method leads to small difference in the final result every time the model is run, but those differences are small enoughto be ignored. Thus we only present one result for each experiment in this paper. To make pixel-based and patch-based classification approaches more comparable, some sample points were deleted from the dataset of pixel samples to make the number of sample in each class be roughly proportional to that of the dataset of patches. The number of deleted points is the difference between total sample number of each class in the reference dataset and total sample number of each class in the reduced dataset (Table 5a and Table 5b, Table 6a and Table 6b, Table 7a and Table 7b). After the deletion, sizes of patch and pixel sample datasets of Ewenk, Xilinhot and Urat were 27027 and 20087, 32305 and 25837, and 27410 and 27410 respectively.

3.5 Accuracy assessment

The OOB error that the RF method provides, which is estimated internally during the run and is also viewed as a unbiased estimation (Breiman, 2001),was used in our study as one measure of classification accuracy after all trees had been built in each model. We also used the traditional error matrix (Congalton et al., 1983) as another accuracy assessment method for each comparative experimentsinIMAR after models had run. The Kappa value was calculated based on traditional error matrices as a reasonable way to estimate overall accuracy when comparing results of different experiments (Congalton and Green, 2009).

For the Mongolian classifications, we used the Mongolia field survey points labeled by using the match table, a total of 119 of which were located within the boundary of image subsets. We extract predicted steppe type of the patches where these field survey points were locatedto those points and compared the class with the class we labeled these field survey points using the match table.

4. RESULTS AND DISCUSSION

4.1 Pixel-based vs. patch-based classification

Comparison of pixel- and patch-based classification shows that, for all three study sites of IMAR, patch-based classification hadhigher accuracy in both steppe vegetation and degradation classification based on both the results of the confusion matrix and the OOB error (Tables 5-10). This may be because the averaging effect of zonal analysis reducedthe influence of extreme values, which could otherwise mislead a classifier during training process. It has been shown in other studies that image segmentation filters out excessive heterogeneity in images and leads to higher accuracy than pixel-based classification (Karl and Maurer, 2010). In addition to a higher accuracy rate, the patch-based classificationsinvolvedmuch smaller datasets so that the classification process can be more efficient.

To keep predictorvariables constant in this comparison experiment, texture variableswereexcluded from theseRFs. Inclusion of the texture variables resulted in no distinct improvement in overall accuracy for both steppe type and degradation classification (Tables 11 and 12). However, a little bit larger difference can be observed in some classes. For example, sand land meadow steppe (code C) was classified with ahigher producer's accuracy (0.51 to 0.6) in Ewenk Autonomous Region and sand land typical steppe (code E) inXilinhot City was classified with slightly higher user's accuracy and producer's accuracy (0.63 to 0.65 and 0.80 to 0.84 respectively). On the other hand, some other classes, such as class D (plain/hill typical steppe), experienced a very small decrease in accuracy when texture features were included. This may be because sandy lands have more texture than other steppe types so that texture features tend to be more useful for distinguishing sand land steppes while they introduce some noise for other classes. The segmentation process has to ensure homogeneity within a patch to a certain degree, thus texture features did not improve classification accuracy dramatically. However, this does not necessarily mean that texture features would be useful or not useful when we classify sites of the Mongolian images. We decided to keep the four most influential texture features (GLCM entropy, contrast, homogeneity and dissimilarity) for future experiments based on variable importance plots (Appendix A).

We also noticed that by altering pixel datasets to make the number of samples in each class proportional to that of patch datasets, the results did not change much (results not shown). This means that the RF classifier is not sensitive to small differences in class distribution. However, for very skewed distribution, classes with much smaller samples will be greatly influenced by dominant classes, especially in terms of user's accuracy. This occurred for all three study sites of IMAR and in both steppe type and degradation classification.

Table 5. Comparison of (a) the error matrix of patch-based steppe vegetation classification, (b) the error matrix of pixel-based steppe vegetation classification and (c) the error matrix of the pixel-based steppe vegetation classification with the pixel dataset reduced to be proportional to the patch dataset of Ewenk autonomous region. UA is user's accuracy, PA is producer's accuracy and OA is overall accuracy. For steppe type, please refer to Table 3.

a. Error matrix of patch-based steppe vegetation classification (Ewenk Autonomous Region)													
	Reference												
Classified		A	B	C	D	E	F	G	H	I	J	total	**UA**
	A	2027	461	98	568	11	260	31	14	296	0	3766	0.54
	B	67	2155	6	8	0	306	1	2	468	0	3013	0.72
	C	390	76	299	179	55	49	67	6	147	0	1268	0.24
	D	500	70	25	3987	40	218	195	84	6	10	5135	0.78
	E	209	7	108	409	459	24	77	11	1	0	1305	0.35
	F	186	284	16	128	0	2060	14	23	360	4	3075	0.67
	G	24	8	14	238	19	68	1264	131	0	101	1867	0.68
	H	21	3	1	136	3	122	167	484	2	121	1060	0.46
	I	209	719	19	20	0	378	0	2	4160	0	5507	0.76

	J	16	4	0	48	1	122	95	174	0	571	1031	0.55
	total	3649	3787	586	5721	588	3607	1911	931	5440	807	27027	**OA**
	PA	0.56	0.57	0.51	0.70	0.78	0.57	0.66	0.52	0.76	0.71		**64.6%**
Kappa = 0.59, OOB = 35.38%													

b. Error matrix of pixel-based steppe vegetation classification (Ewenk Autonomous Region)

	Reference												
		A	B	C	D	E	F	G	H	I	J	total	**UA**
Classified	A	2211	465	129	1518	49	258	35	15	349	1	5030	0.44
	B	167	1950	9	119	0	466	1	2	714	0	3428	0.57
	C	520	162	166	291	43	97	54	6	217	0	1556	0.11
	D	859	153	31	7323	50	215	192	93	37	15	8968	0.82
	E	582	38	121	1429	250	26	77	1	16	2	2542	0.10
	F	321	486	31	170	1	1921	11	35	652	6	3634	0.53
	G	66	11	19	716	40	71	837	129	0	79	1968	0.43
	H	38	16	3	362	2	195	157	443	3	127	1346	0.33
	I	342	1066	17	77	0	774	0	6	3980	0	6262	0.64
	J	30	7	0	85	2	162	93	249	0	551	1179	0.47
	total	5136	4354	526	12090	437	4185	1457	979	5968	781	35913	**OA**
	PA	0.43	0.45	0.32	0.61	0.57	0.46	0.57	0.45	0.67	0.71		**54.7%**
Kappa = 0.46, OOB = 45.33%													

c. Error matrix of pixel-based steppe vegetation classification from reduced dataset of pixel samples (Ewenk Autonomous Region)

	Reference												
		A	B	C	D	E	F	G	H	I	J	total	**UA**
Classified	A	1169	278	107	517	43	159	34	11	223	0	2541	0.46
	B	89	1317	12	44	0	304	2	1	500	1	2270	0.58
	C	294	101	136	100	46	70	49	5	143	0	944	0.14
	D	425	93	26	2570	47	142	181	66	35	11	3596	0.71
	E	320	28	100	511	256	18	75	2	12	2	1324	0.19
	F	164	305	21	80	2	1237	13	33	431	9	2295	0.54
	G	41	7	17	266	40	47	835	92	0	64	1409	0.59
	H	21	12	3	119	2	127	143	315	2	111	855	0.37

	I	174	671	13	19	0	475	0	3	2697	0	4052	0.67
	J	15	2	1	26	1	102	88	164	0	402	801	0.50
	total	2712	2814	436	4252	437	2681	1420	692	4043	600	20087	**OA**
	PA	0.43	0.47	0.31	0.60	0.59	0.46	0.59	0.46	0.67	0.67		**54.4%**
Kappa = 0.47, OOB = 45.57%													

Table 6. Comparison of (a) the error matrix of patch-based steppe vegetation classification, (b) the error matrix of pixel-based steppe vegetation classification and (c) the error matrix of the pixel-based steppe vegetation classification with the pixel dataset reduced to be proportional to the patch dataset of Xilinhot city. UA is user's accuracy, PA is producer's accuracy and OA is overall accuracy. For steppe type, please refer to Table 3.

a. Error matrix of patch-based steppe vegetation classification (Xilinhot City)											
	Reference										
		A	B	D	E	F	G	H	K	Total	**UA**
classified	A	1209	20	2008	165	51	2	1	22	3478	0.35
	B	134	181	193	17	4	0	1	90	620	0.29
	D	34	1	14023	299	115	180	13	34	14699	0.95
	E	64	4	1463	2781	22	42	1	4	4381	0.63
	F	41	0	1337	82	581	185	38	6	2270	0.26
	G	0	0	1277	94	104	1938	72	1	3486	0.56
	H	4	0	336	23	137	301	199	0	1000	0.20
	K	43	27	1765	13	18	11	8	486	2371	0.20
	Total	1529	233	22402	3474	1032	2659	333	643	32305	**OA**
	PA	0.79	0.78	0.63	0.80	0.56	0.73	0.60	0.76		**66.24%**
Kappa=0.48, OOB=33.76%											
b. Error matrix of pixel-based steppe vegetation classification (Xilinhot City)											
	Reference										
		A	B	D	E	F	G	H	K	Total	**UA**
classified	A	2290	54	2626	190	55	2	2	71	5290	0.43
	B	270	189	557	78	9	0	1	126	1230	0.15
	D	50	1	23268	343	202	214	16	68	24162	0.96
	E	80	13	2903	1996	35	54	1	36	5118	0.39
	F	37	1	2796	94	605	187	29	42	3791	0.16
	G	0	0	2042	87	94	1457	78	4	3762	0.39
	H	3	1	469	73	129	426	234	4	1339	0.17
	K	161	26	3162	141	86	18	7	446	4047	0.11
	Total	2891	285	37823	3002	1215	2358	368	797	48739	**OA**
	PA	0.79	0.66	0.62	0.66	0.50	0.62	0.64	0.56		**62.5%**

Kappa=0.37, OOB=37.45%

c. Error matrix of pixel-based steppe vegetation classification from reduced dataset of pixel samples (Xilinhot City)

		Reference									
		A	B	D	E	F	G	H	K	Total	**UA**
classified	A	1137	43	1191	184	33	1	2	48	2639	0.43
	B	151	138	252	85	6	0	1	85	718	0.19
	D	23	3	10793	344	146	187	12	60	11568	0.93
	E	34	11	1366	1987	27	43	1	25	3494	0.57
	F	16	2	1200	92	424	158	24	27	1943	0.22
	G	0	0	988	85	78	1252	70	2	2475	0.51
	H	4	1	257	79	74	328	163	3	909	0.18
	K	77	26	1408	146	64	13	6	351	2091	0.17
	Total	1442	224	17455	3002	852	1982	279	601	25837	**OA**
	PA	0.79	0.62	0.62	0.66	0.50	0.63	0.58	0.58		**62.9%**
Kappa=0.44, OOB=37.13%											

Table 7. Comparison of (a) the error matrix of patch-based steppe vegetation classification and (b) the error matrix of pixel-based steppe vegetation classification of Urat middle banner. UA is user's accuracy, PA is producer's accuracy and OA is overall accuracy. For steppe type, please refer to Table 3.

a. Error matrix of patch-based steppe vegetation classification (Urat Middle Banner)

		Reference											
		F	G	H	J	L	M	N	O	P	Q	Total	**UA**
Classified	F	160	147	0	2	136	7	0	98	57	0	607	0.26
	G	22	594	11	12	726	52	1	131	80	0	1629	0.36
	H	1	71	25	6	35	0	0	2	1	0	141	0.18
	J	9	90	4	47	577	3	0	14	0	0	744	0.06
	L	4	45	0	3	7410	368	0	279	7	0	8116	0.91
	M	0	7	0	0	933	5732	0	911	1	0	7584	0.76
	N	0	2	0	0	19	24	11	71	1	0	128	0.09
	O	1	21	0	0	152	813	7	4476	173	0	5643	0.79
	P	2	21	0	0	12	1	1	518	1892	14	2461	0.77
	Q	1	2	0	0	0	0	0	0	288	66	357	0.18
	Total	200	1000	40	70	10000	7000	20	6500	2500	80	27410	**OA**
	PA	0.80	0.59	0.67	0.67	0.74	0.82	0.55	0.69	0.76	0.83		**74.47%**
Kappa = 0.66, OOB =25.53%													

b. Error matrix of pixel-based steppe vegetation classification (Urat Middle Banner)													
	Reference												
		F	G	H	J	L	M	N	O	P	Q	Total	**UA**
Classified	F	99	114	17	0	701	202	1	96	6	0	1236	0.08
	G	13	580	2	3	378	20	3	419	81	0	1499	0.39
	H	11	13	5	0	73	17	0	8	0	0	127	0.04
	J	3	8	1	67	0	20	0	0	2	0	101	0.66
	L	35	59	9	0	5086	631	0	977	9	0	6806	0.75
	M	16	13	4	0	1098	5780	0	234	33	0	7178	0.81
	N	0	7	0	0	50	3	11	5	19	0	95	0.12
	O	15	137	1	0	2082	138	0	4078	146	1	6598	0.62
	P	8	53	1	0	466	188	5	378	2161	4	3264	0.66
	Q	0	16	0	0	66	1	0	305	43	75	506	0.15
	Total	200	1000	40	70	10000	7000	20	6500	2500	80	27410	**OA**
	PA	0.50	0.58	0.13	0.96	0.51	0.83	0.55	0.63	0.86	0.94		65.46%
Kappa = 0.55, OOB = 34.54%													

Table 8. Comparison of (a) the error matrix of patch-based steppe degradation classification, (b) the error matrix of pixel-based steppe degradation classification of Ewenk autonomous region and (c) the error matrix of the pixel-based steppe degradation classification with the pixel dataset reduced to be proportional to the patch dataset. UA is user's accuracy, PA is producer's accuracy and OA is overall accuracy. For degradation level, please refer to merged class codes in Table 4.

a. Error matrix of patch-based steppe degradation classification (Ewenk Autonomous Region)							
	Reference						
Classified		a	b	c	d	total	**UA**
	a	13463	557	226	41	14287	0.94
	b	2143	3315	758	253	6469	0.51
	c	992	884	1290	253	3419	0.38
	d	403	409	659	1381	2852	0.48
	total	17001	5165	2933	1928	27027	**OA**
	PA	0.79	0.64	0.44	0.72		**72.0%**
Kappa = 0.53, OOB = 28.04%							
b. Error matrix of pixel-based steppe degradation classification (Ewenk Autonomous Region)							
	Reference						
Classifi er		a	b	c	d	total	**UA**
	a	9841	452	212	51	10556	0.93

	b	2000	2247	669	180	5096	0.44
	c	798	793	989	156	2736	0.36
	d	285	254	443	717	1699	0.42
	total	12924	3746	2313	1104	20087	**OA**
	PA	0.76	0.60	0.43	0.65		**68.7%**
Kappa = 0.47, OOB = 31.33%							
c. Error matrix of pixel-based steppe degradation classification from reduced dataset of pixel samples (Ewenk Autonomous Region)							
	Reference						
Classifier		a	b	c	d	total	**UA**
	a	7429	344	143	45	7961	0.93
	b	1532	1809	481	171	3993	0.45
	c	563	605	705	177	2050	0.34
	d	211	199	349	711	1470	0.48
	total	9735	2957	1678	1104	15474	**OA**
	PA	0.76	0.61	0.42	0.64		**68.9%**
Kappa = 0.49, OOB = 31.15%							

Table 9. Comparison of (a) the error matrix of patch-based steppe degradation classification, (b) the error matrix of pixel-based steppe degradation classification and (c) the error matrix of the pixel-based steppe degradation classification with the pixel dataset reduced to be proportional to the patch dataset of Xilinhot city. UA is user's accuracy, PA is producer's accuracy and OA is overall accuracy. For degradation level, please refer to merged class codes in Table 4.

a. Error matrix of patch-based steppe degradation classification (Xilinhot City)							
	Reference						
Classified		a	b	c	d	Total	**UA**
	a	4760	2329	1097	144	8330	0.57
	b	1087	4814	1991	582	8474	0.57
	c	380	2170	4456	1362	8368	0.53
	d	119	881	1789	4344	7133	0.61
	Total	6346	10194	9333	6432	32305	**OA**
	PA	0.75	0.47	0.48	0.68		**56.88%**
	Kappa = 0.42, OOB = 43.12%						
b. Error matrix of pixel-based steppe degradation classification (Xilinhot City)							
	Reference						
Classified		a	b	c	d	Total	**UA**
	a	8088	3756	1470	312	13626	0.59
	b	2356	8150	3557	748	14811	0.55
	c	541	3124	5894	1348	10907	0.54
	d	198	1644	3426	4127	9395	0.44
	Total	11183	16674	14347	6535	48739	**OA**

		a	b	c	d	Total	UA
	PA	0.72	0.49	0.41	0.63		**53.88%**
	Kappa = 0.38, OOB = 46.12%						

c. Error matrix of pixel-based steppe degradation classification from reduced dataset of pixel samples (Xilinhot City)

		Reference					
		a	b	c	d	Total	**UA**
Classified	a	5141	2418	997	306	8862	0.58
	b	1481	5099	2291	764	9635	0.53
	c	343	1937	3776	1340	7396	0.51
	d	116	1050	2238	4125	7529	0.55
	Total	7081	10504	9302	6535	33422	**OA**
	PA	0.73	0.49	0.41	0.63		**54.28%**
	Kappa = 0.39, OOB = 45.72%						

Table 10. Comparison of (a) the error matrix of patch-based steppe degradation classification, (b) the error matrix of pixel-based steppe degradation classification and (c) the error matrix of the pixel-based steppe degradation classification with the pixel dataset reduced to be proportional to the patch dataset of Urat middle banner. UA is user's accuracy, PA is producer's accuracy and OA is overall accuracy. For degradation level, please refer to merged class codes in Table 4.

a. Error matrix of patch-based steppe degradation classification (Urat Middle Banner)

		Reference					
		a	b	c	d	Total	**UA**
Classified	a	6945	1670	361	77	9053	0.77
	b	739	7021	1516	138	9414	0.75
	c	283	2622	5506	213	8624	0.64
	d	401	1164	641	1133	3339	0.34
	Total	8368	12477	8024	1561	30430	**OA**
	PA	0.83	0.56	0.69	0.73		**67.71%**

Kappa = 0.55, OOB = 32.29%

b. Error matrix of pixel-based steppe degradation classification (Urat Middle Banner)

		Reference					
		a	b	c	d	Total	**UA**
Classified	a	6731	2727	762	141	10361	0.65
	b	921	11297	3274	192	15684	0.72
	c	218	4617	10648	283	15766	0.68
	d	533	2065	1149	1142	4889	0.23
	Total	8403	20706	15833	1758	46700	**OA**
	PA	0.80	0.55	0.67	0.65		**63.85%**

Kappa = 0.48, OOB = 36.15%

c. Error matrix of pixel-based steppe degradation classification from reduced dataset of pixel samples (Urat Middle Banner)

		Reference					
		a	b	c	d	Total	**UA**
Classified	a	6722	1675	361	125	8883	0.76
	b	918	6867	1719	176	9680	0.71
	c	238	2786	5398	258	8680	0.62
	d	525	1201	580	1009	3315	0.30
	Total	8403	12529	8058	1568	30558	**OA**
	PA	0.80	0.55	0.67	0.64		**65.44%**
Kappa = 0.51, OOB = 34.56%							

Table 11. The error matrices of patch-based steppe type classification with texture features of (a) Ewenk autonomous region, (b) Xilinhot city and (c) Urat middle banner. UA is user's accuracy, PA is producer's accuracy and OA is overall accuracy. For steppe type, please refer to table 3.

a. Error matrix of patch-based steppe classification with texture features (Ewenk Autonomous Region)													
	Reference												
Classified		A	B	C	D	E	F	G	H	I	J	total	**UA**
	A	1883	423	52	528	16	230	48	18	299	0	3497	0.54
	B	63	2153	9	12	0	314	1	2	502	0	3056	0.70
	C	438	91	354	139	72	96	47	12	153	0	1402	0.25
	D	545	74	3	4097	18	59	164	62	4	5	5031	0.81
	E	220	5	116	366	462	46	75	11	1	0	1302	0.35
	F	207	301	21	89	1	2167	21	27	387	9	3230	0.67
	G	32	8	10	301	12	65	1296	130	0	92	1946	0.67
	H	30	4	1	134	6	119	165	473	3	102	1037	0.46
	I	218	726	20	8	0	372	0	2	4091	0	5437	0.75
	J	13	2	0	47	1	139	94	194	0	599	1089	0.55
	total	3649	3787	586	5721	588	3607	1911	931	5440	807	27027	**OA**
	PA	0.52	0.57	0.60	0.72	0.79	0.60	0.68	0.51	0.75	0.74		**65.0%**
KAPPA = 0.59, OOB = 34.97%													

b. Error matrix of patch-based steppe vegetation classification with texture features (Xilinhot City)										
	Reference									
		A	B	D	E	F	G	H	K	Total	**UA**

Classified	A	1197	18	2051	71	47	3	1	21	3409	0.35
	B	118	182	176	23	6	0	1	91	597	0.30
	D	38	2	14608	211	79	139	4	23	15104	0.97
	E	84	3	1362	2910	29	44	1	10	4443	0.65
	F	49	1	1197	90	594	187	56	8	2182	0.27
	G	0	0	1213	117	116	1960	80	1	3487	0.56
	H	5	0	233	23	144	313	182	0	900	0.20
	K	38	27	1562	29	17	13	8	489	2183	0.22
	Total	1529	233	22402	3474	1032	2659	333	643	32305	**OA**
	PA	0.78	0.78	0.65	0.84	0.58	0.74	0.55	0.76		**68.48%**
Kappa=0.51, OOB=31.52%											

c. Error matrix of patch-based steppe vegetation classification with texture features (Urat Middle Banner)													
	Reference												
		F	G	H	J	L	M	N	O	P	Q	Total	**UA**
Classified	F	164	141	2	1	88	4	0	96	105	0	601	0.27
	G	22	642	13	18	729	71	2	167	67	0	1731	0.37
	H	1	48	20	7	64	0	0	0	0	0	140	0.14
	J	5	83	5	41	592	4	0	10	8	0	748	0.05
	L	0	33	0	2	7392	426	0	237	5	0	8095	0.91
	M	0	6	0	0	931	5553	0	844	2	0	7336	0.76
	N	0	1	0	0	13	17	12	51	1	0	95	0.13
	O	0	18	0	0	165	925	5	4499	160	0	5772	0.78
	P	6	23	0	0	19	0	1	591	1919	14	2573	0.75
	Q	2	5	0	1	7	0	0	5	233	66	319	0.21
	Total	200	1000	40	70	10000	7000	20	6500	2500	80	27410	**OA**
	PA	0.82	0.64	0.59	0.59	0.74	0.79	0.60	0.69	0.77	0.83		**74.09%**
Kappa = 0.66, OOB =25.91%													

Table 12. The error matrices of patch-based steppe degradation classification with texture features of (a) Ewenk autonomous region, (b) Xilinhot city and (c) Urat middle banner. UA is user's accuracy, PA is producer's accuracy and OA is overall accuracy. For degradation level, please refer to merged class codes in Table 4.

a. Error matrix of patch-based steppe degradation classification with texture features (Ewenk Autonomous Region)	
	Reference

		a	b	c	d	total	**UA**
Classified	a	13753	579	217	42	14591	0.94
	b	1783	3185	710	169	5847	0.54
	c	1010	1002	1352	317	3681	0.37
	d	455	399	654	1400	2908	0.48
	total	17001	5165	2933	1928	27027	**OA**
	PA	0.81	0.62	0.46	0.73		**72.8%**
Kappa = 0.54, OOB = 27.15%							

b. Error matrix of patch-based steppe degradation classification with texture features (Xilinhot City)							
	Reference						
		a	b	c	d	Total	**UA**
Classified	a	4664	2349	953	93	8059	0.58
	b	1122	4651	1905	485	8163	0.57
	c	377	2147	4555	1320	8399	0.54
	d	183	1047	1920	4534	7684	0.59
	Total	6346	10194	9333	6432	32305	**OA**
	PA	0.73	0.46	0.49	0.70		**56.97%**
Kappa = 0.43, OOB = 43.03%							

c. Error matrix of patch-based steppe degradation classification with texture features (Urat Middle Banner)							
	Reference						
		a	b	c	d	Total	**UA**
Classified	a	7107	1844	361	81	9393	0.76
	b	569	6699	1263	104	8635	0.78
	c	181	2634	5538	191	8544	0.65
	d	511	1300	862	1185	3858	0.31
	Total	8368	12477	8024	1561	30430	**OA**
	PA	0.85	0.54	0.69	0.76		**67.46%**
Kappa = 0.55, OOB = 32.54%							

4.2 Patch-based classification at the scale of 20 vs. scale of 40

There was not a big difference in overall accuracy, based on Kappa valuesandOOB errors between classifications at two scales (comparing Tables 13-15 to Tables 5a and 10a). This might be because, with larger patch size, more heterogeneity was filtered out but, at the same time, more mixed patches were created making samples less representative of the classes they were labeled. Based the result of this experiment, we decided to keep on using patch data at scale of 20 for a couple of reasons. First, according to our visual examination during image segmentation, smaller ground features such as little sandy patch or small and narrow lowland grassland patch around streams or ponds can be bettercapturedat scale of 20. The size of the dataset with finer-scale patches was not too big, while we can still maintain a lot of details. Second, though larger patch sizes can decrease data size, we were not able to reach a much higher accuracy rate at the cost of losing more information in data. Thus we believe that for our study, 20 was an appropriate value of scale parameter in segmentation.

Table 13. The error matrices of patch-based steppe (a) vegetation and (b) degradation at scale 40 of Ewenk autonomous region. UA is user's accuracy, PA is producer's accuracy and OA is overall accuracy. For steppe type, refer to Table 3. For degradation level, refer to merged class codes in Table 4.

a. Error matrix of patch-based steppe vegetation classification at scale of 40 (Ewenk Autonomous Region)

		Reference											
Classified		A	B	C	D	E	F	G	H	I	J	Total	**UA**
	A	523	128	12	146	3	52	14	3	101	0	982	0.53
	B	22	512	5	3	0	73	0	0	161	0	776	0.66
	C	126	24	84	38	30	19	15	2	38	0	376	0.22
	D	178	21	2	1197	1	11	42	18	3	0	1473	0.81
	E	48	0	32	105	140	10	18	0	0	0	353	0.40
	F	58	76	4	21	0	594	5	11	86	1	856	0.69
	G	12	2	3	70	5	11	385	39	0	19	546	0.71
	H	10	0	1	41	3	45	48	132	0	31	311	0.42
	I	61	219	1	0	0	91	0	0	1172	0	1544	0.76
	J	2	1	0	14	0	51	16	51	0	171	306	0.56
	Total	1040	983	144	1635	182	957	543	256	1561	222	7523	**OA**
	PA	0.50	0.52	0.58	0.73	0.77	0.62	0.71	0.52	0.75	0.77		**65.27%**

Kappa = 0.60 OOB = 34.73%

b. Error matrix of pixel-based steppe degradation classification at scale of 40 (Ewenk Autonomous Region)

		Reference					
Classified		a	b	c	d	Total	**UA**
	a	3760	218	73	12	4063	0.93
	b	490	871	202	54	1617	0.54
	c	303	295	347	80	1025	0.34
	d	124	105	166	423	818	0.52
	Total	4677	1489	788	569	7523	**OA**
	PA	0.80	0.58	0.44	0.74		**71.79%**

Kappa = 0.53, OOB = 28.21%

Table 14. The error matrices of patch-based steppe (a) vegetation and (b) degradation at scale 40 of Xilinhot city. UA is user's accuracy, PA is producer's accuracy and OA is

overall accuracy. For steppe type, please refer to table 3. For degradation level, refer to mergedclass codes in table 4.

a. Error matrix of patch-based steppe vegetation classification at scale of 40 (Xilinhot City)											
	Reference										
		A	B	D	E	F	G	H	K	Total	**UA**
classified	A	311	8	545	25	8	0	0	3	900	0.35
	B	34	46	46	3	2	0	0	20	151	0.30
	D	14	0	4047	58	15	26	2	7	4169	0.97
	E	30	0	314	715	5	11	2	1	1078	0.66
	F	14	1	243	18	168	54	21	5	524	0.32
	G	0	0	360	26	30	527	14	0	957	0.55
	H	2	0	70	11	49	112	56	0	300	0.19
	K	13	5	414	9	2	3	4	104	554	0.19
	Total	418	60	6039	865	279	733	99	140	8633	**OA**
	PA	0.74	0.77	0.67	0.83	0.60	0.72	0.57	0.74		**69.20%**
Kappa=0.51, OOB=30.80%											

a. Error matrix of patch-based steppe degradation classification at scale of 40 (Xilinhot City)						
	Reference					
Classified		a	b	c	d	Total	**UA**
	a	1182	669	278	40	2169	0.54
	b	329	1243	507	116	2195	0.57
	c	95	583	1138	353	2169	0.52
	d	49	308	515	1228	2100	0.58
	Total	1655	2803	2438	1737	8633	**OA**
	PA	0.71	0.44	0.47	0.71		**55.50%**
	Kappa = 0.41, OOB = 44.50%						

Table 15. The error matrices of patch-based steppe (a) vegetation and (b) degradation at scale 40 of Urat middle banner. UA is user's accuracy, PA is producer's accuracy and OA is overall accuracy. For steppe type, please refer to Table 3. For degradation level, please refer to merged class codes in Table 4.

a. Error matrix of patch-based steppe vegetation classification at scale of 40(Urat Middle Banner)													
	Reference												
		F	G	H	J	L	M	N	O	P	Q	Total	**UA**
Classified	F	38	48	1	0	22	0	0	47	34	1	191	0.20
	G	10	135	7	8	117	4	0	21	5	0	307	0.44
	H	0	12	7	0	14	2	0	2	0	0	37	0.19
	J	1	24	0	11	118	7	0	9	0	0	170	0.06
	L	0	11	0	0	1861	128	0	63	0	0	2063	0.90
	M	0	7	0	0	309	1344	1	179	0	0	1840	0.73

	N	0	0	0	0	0	10	3	15	0	0	28	0.11
	O	1	8	0	1	48	253	3	1217	86	0	1617	0.75
	P	0	4	0	0	4	2	0	68	453	2	533	0.85
	Q	0	1	0	0	7	0	0	4	47	17	76	0.22
	Total	50	250	15	20	2500	1750	7	1625	625	20	6862	**OA**
	PA	0.76	0.54	0.55	0.55	0.74	0.77	0.43	0.75	0.72	0.85		**74.12%**
Kappa = 0.66, OOB =25.88%													

b. Error matrix of patch-based steppe degradation classification at scale 40(Urat Middle Banner)							
	Reference						
		a	b	c	d	Total	**UA**
Classified	a	2021	509	119	28	2677	0.75
	b	192	1671	350	30	2243	0.74
	c	31	821	1552	63	2467	0.63
	d	143	339	214	309	1005	0.31
	Total	2387	3340	2235	430	8392	**OA**
	PA	0.85	0.50	0.69	0.72		**66.17%**
Kappa = 0.53, OOB = 33.83%							

4.3 Local prediction

Comparing local prediction results (Tables 16-18) with those of patch-based classification presented (Table 5-10), most of results show no big differences in overall performance of steppe classes and degradation levels in terms of classification accuracy, except that the accuracy of degradation classification of Xilinhot City dropped a few percentage points. The way we sampled the training dataset gave thetraining and testing datasets similar ranges and distributions of predictor variables. Assuming that we have collected abundant training samples in the way that we do for supervised classification for a new image, the classification accuracy we get from the training dataset by using RF might be close to the best we could get if we use RF to classify the entire image.

In this experiment, the difference between commission error and omission error of some classes became even more distinct, which indicated confusion between two classes or among more classes. There were probably two major reasons leading to the misclassification. First, classes shared great similarity so that the predictor variables are not capable of distinguishing them. Second, patches were not labeled appropriately, which affected both training and testing datasets. We used the class of majority of pixels within the patch to label the patch. Those patches with mixed pixels could mislead the classifier. Moreover, the manually digitized boundary may not be accurate or those boundaries had changed in our images due to different climate conditions in a different year, or the degradation had developed (or mitigated) (Figure 2).

During this local prediction experiment, the same input variables were used for both steppe vegetation type and degradation classification. However, if steppe type information is already available, it can be used as another input predictor variable in the RF model of degradation classification. For example, under the assumption that steppe classes were known, using steppe class information as an additional input in degradation classification model of Ewenk Autonomous Regioncan greatly improve accuracy of local prediction (Table 19a). Thisis because there is correlation between degradation and steppe class. For example, lowland meadow with salinizationor sand land meadow or typical steppes are usually degraded which has already reflected in steppe class names. However, when we used the predicted steppe class to label all patches and classify this dataset during local prediction of degradation, the accuracy dropped back (Table 19b). Error in steppe type classification can even further reduced accuracy compared to model with no steppe type as one of the input variables. Thus even if the accuracy was high, it would be risky to use steppe class information in the degradation classification process when validation dataset is too small to assess how reliable isthe steppe type classification result. However, it might be a useful and more efficient way to create degradation map if a steppe type map was available, compared with manually digitizing.

Table 16. The error matrices of local prediction on (a) vegetation and (b) degradation ofEwenk autonomous region. UA is user's accuracy, PA is producer's accuracy and OA is overall accuracy. For steppe type, please refer to Table 3. For degradation level, please refer to merged class codes in Table 4.

a. Error matrix oflocal prediction of steppe types (Ewenk Autonomous Region)													
	Reference												
Classified		A	B	C	D	E	F	G	H	I	J	Total	**UA**
	A	1773	431	36	547	12	244	33	18	313	0	3407	0.52
	B	48	2159	4	18	0	326	0	1	771	0	3327	0.65
	C	421	93	423	185	75	75	49	6	148	0	1475	0.29
	D	610	78	4	3932	17	58	140	40	18	4	4901	0.80
	E	197	2	73	314	468	47	93	19	1	0	1214	0.39
	F	293	329	17	102	3	2204	25	58	357	9	3397	0.65
	G	36	10	5	304	5	37	1278	86	2	68	1831	0.70
	H	42	8	3	264	7	134	211	546	4	105	1324	0.41
	I	218	674	21	14	0	378	2	2	3826	0	5135	0.75
	J	11	3	0	41	1	104	80	155	0	621	1016	0.61
	Total	3649	3787	586	5721	588	3607	1911	931	5440	807	27027	**OA**
	PA	0.49	0.57	0.7	0.69	0.8	0.61	0.67	0.5	0.70	0.7		**63.75**

				2		0			9		7		%
Kappa = 0.58, OOB (training dataset) = 36.70%													

b. Error matrix of local prediction of degradation (Ewenk Autonomous Region)							
	Reference						
		a	b	c	d	Total	**UA**
Classified	a	13775	827	253	36	14891	0.93
	b	1812	2984	744	169	5709	0.52
	c	932	942	1343	308	3525	0.38
	d	482	412	593	1415	2902	0.49
	Total	17001	5165	2933	1928	27027	**OA**
	PA	0.81	0.58	0.46	0.73		**72.21%**
Kappa = 0.53, OOB (training dataset) = 37.25%							

Table 17. The error matrices of local prediction on (a) vegetation and (b) degradation of Xilinhot city. UA is user's accuracy, PA is producer's accuracy and OA is overall accuracy. For steppe type, please refer to Table 3. For degradation level, please refer to merged class codes in Table 4.

a. Error matrix of local prediction of steppe types (Xilinhot City)											
	Reference										
		A	B	D	E	F	G	H	K	Total	**UA**
classified	A	1193	4	1741	95	36	4	1	14	3088	0.39
	B	116	225	194	29	10	0	1	65	640	0.35
	D	50	0	14345	244	52	137	0	20	14848	0.97
	E	84	0	1052	2759	18	23	0	7	3943	0.70
	F	46	0	1503	104	619	146	15	5	2438	0.25
	G	0	0	1334	165	95	1827	33	2	3456	0.53
	H	7	0	540	38	186	510	278	1	1560	0.18
	K	33	4	1693	40	16	12	5	529	2332	0.23
	Total	1529	233	22402	3474	1032	2659	333	643	32305	**OA**
	PA	0.78	0.97	0.64	0.79	0.60	0.69	0.83	0.82		**67.40%**
Kappa=0.50, OOB (training dataset) =30.19%											

b. Error matrix of local prediction of degradation (Xilinhot City)							
	Reference						
		a	b	c	d	Total	**UA**
Classified	a	4281	2399	949	110	7739	0.55
	b	1298	4487	2274	523	8582	0.52
	c	510	2143	4097	1363	8113	0.50
	d	257	1165	2013	4436	7871	0.56
	Total	6346	10194	9333	6432	32305	**OA**
	PA	0.67	0.44	0.44	0.69		**53.56%**

Kappa = 0.38, OOB (training dataset) = 42.62%

Table 18. The error matrices of local prediction on (a) merged vegetation and (b) degradation of Urat middle banner. UA is user's accuracy, PA is producer's accuracy and OA is overall accuracy. For steppe type, please refer to Table 3. For degradation level, please refer to merged class codes in Table 4.

a. Error matrix of local prediction of steppe types (Urat Middle Banner)

		Reference								
		F	GH	J	L	MN	O	PQ	Total	**UA**
Classified	F	274	184	0	774	241	140	9	1622	0.17
	GH	7	793	0	489	57	411	48	1805	0.44
	J	2	1	319	0	2	0	1	325	0.98
	L	9	55	0	6187	295	1167	26	7739	0.80
	MN	2	16	0	1136	7253	654	69	9130	0.79
	O	4	51	0	1921	144	4026	121	6267	0.64
	PQ	1	23	0	419	93	553	2453	3542	0.69
	Total	299	1123	319	10926	8085	6951	2727	30430	**OA**
	PA	0.92	0.71	1.00	0.57	0.90	0.58	0.90		**70.01%**

Kappa = 0.61, OOB (training dataset) = 25.43

b. Error matrix of local prediction of steppe degradation (Urat Middle Banner)

		Reference					
		a	b	c	d	Total	**UA**
Classified	a	7326	2273	466	87	10152	0.72
	b	478	5939	1599	97	8113	0.73
	c	167	3056	5255	202	8680	0.61
	d	397	1209	704	1175	3485	0.34
	Total	8368	12477	8024	1561	30430	**OA**
	PA	0.88	0.48	0.65	0.75		**64.72%**

Kappa = 0.51, OOB (training dataset)= 31.37%

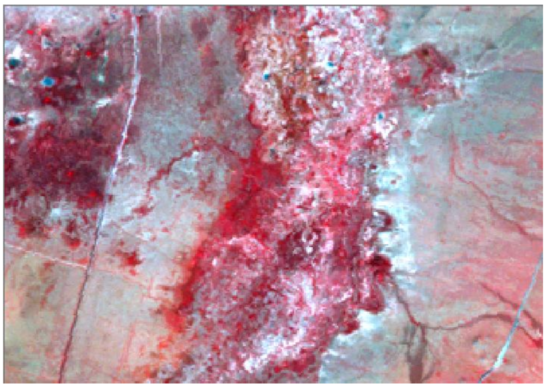

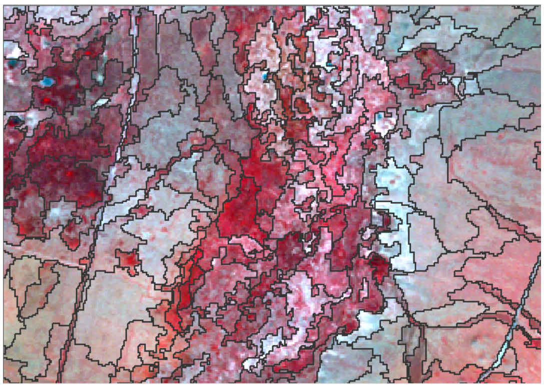

(a) (b)

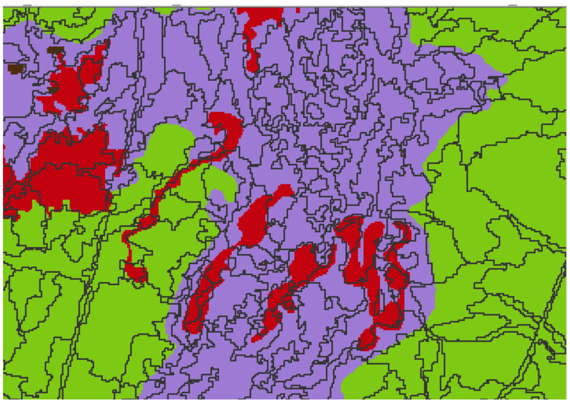

(c)

Figure 2. (a) A lowland meadow subset of 2010 Landsat TM5 image in false color infrared of Xilinhot City, (b) boundaries of segmented patches in the same area, and (c) the 2009 digitized steppe classes. Class G (Salinized lowland meadow) is in purple, class H (Swampy lowland meadow) is in red and class D (Plain/hill typical steppe) is in green.

Table 19. The error matrices of local prediction of degradation of Ewenk autonomous region. (a) Used steppe class information from reference map for both training dataset and testing dataset (all patches in the map). (b) Used steppe class information from reference map for training dataset and used predicted steppe classification for all patches during degradation prediction. UA is user's accuracy, PA is producer's accuracy and OA is overall accuracy. For degradation level, please refer to merged class codes in Table 4.

a. Error matrix of local prediction of degradation with steppe class added into model (Ewenk Autonomous Region)

		Reference					
Classified		a	b	c	d	Total	**UA**
	a	15391	321	109	14	15835	0.97
	b	1278	4071	787	180	6316	0.64
	c	145	569	1484	298	2496	0.59
	d	187	204	553	1436	2380	0.60
	Total	17001	5165	2933	1928	27027	**OA**
	PA	0.91	0.79	0.51	0.74		**82.81%**

Kappa = 0.70, OOB (training dataset) = 29.38%

b. Error matrix of local prediction of degradation with steppe class added into model and by using

predicted steppe class for degradation prediction (Ewenk Autonomous Region)							
	Reference						
Classified		a	b	c	d	Total	**UA**
	a	14068	834	455	174	15531	0.91
	b	2054	3156	734	143	6087	0.52
	c	511	777	1132	236	2656	0.43
	d	368	398	612	1375	2753	0.50
	Total	17001	5165	2933	1928	27027	**OA**
	PA	0.83	0.61	0.39	0.71		**73.00%**
Kappa = 0.53, OOB (training dataset) = 29.38%							

4.4 Predicting within eco-region

Unlike local prediction, dividing every IMAR county into two halvesmeans training and testing datasets came from two different pools, so the ranges and distributions of variables may vary. We divided Ewenk Autonomous Region into northern and southern halves. Since the size of the dataset was halved, we reduced the sample size for input to the RF to 100 per steppe type. Compared to our previous experiments, the accuracy rate of steppe type classification dropped greatly when an RF was trained in the north and tested in the south of the Ewenk site (Table 20a). With no input from the other half part of the image in RF model, it was possible that the classifier tended to "overfit" the northern half. So when the RF was used to classify the southern part, class centers in south Ewenkweredifferent or the distribution of data changed in the multi-dimensional space so that the RF classifier could no longer distinguish different classes. For example class B (Mountain meadow steppe) and class I (Low/middle mountain meadow) were confused with each other which lead to high error rates for both classes (Table 20a). Mountain meadow steppe (B) is distributedto the north of the stream, which runs across the middle subset of the image (Figure 3);Low/middle mountain meadow is in southern part. Both types of steppes are in a mountainous area and they both have high reflectance in near infrared, so they are easily confused with each other. Within the multi-dimensional space defined by all predictor variables, classes overlap with each other so the classifier failed to separate them well.

The degradation classification results also show lower accuracy rates for the within eco-region predictions, but they did not drop as much as that of steppe type classification (Tables 20b and 20d). A main reason is that there were fewer classes in degradation classification. The non-degraded steppe hasmanymore patches than the other degradation levels, which means that it has a large influence onthe overall assessment. On the other hand, degraded steppes, especially slight and moderate degradation levels hadmuch lower accuracy. This same pattern, i.e., dominance of a single class having a negative influence on ability to classify other classes, has been shown in previous experiments' results.

As for Xilinhot City, we divided it into eastern and western halves.Steppe of type B (Mountain meadow steppe) only existed in the east part. The overall performance was better when trained on east and predicted the western half (Tables 21a and 21c).

Class D (Plain/hill typical steppe) contributed a lot to the accuracy rate because it was the dominantsteppe type in the area. Other steppe types that coveredmuch smaller areas had very low user's accuracy or both user's and producer's accuracy. The absence of class B in western half also affected the prediction result. The accuracy rates for mutual prediction of degradation further dropped compared to local prediction (Tables 21b and 21d). Unlike Ewenk, degradation levels had more balanced distributions, in terms of number of patches and relatively mottled pattern (Figure 4 (a)). Moreover, steppes in theeastern half generally appeared to have higher reflectance in near infrared band while band 4 and brightness from tasseled cap transformation were among top three variables in terms of "Mean Decrease Accuracy" plots generated during training process. All these factors mentioned above can explain poor prediction results.

Urat Middle Banner was divided into northeast and southwest halves in order to ensure that both parts cover as many steppe types within the region as possible. Class J (Swamp/marsh) was not in northeast part. The prediction results turned out to have similar pattern as previous experiments on Urat in terms of accuracy rate (Table 22). Steppe M&N (Mountain desert steppe and Sand land desert steppe) and Steppe L (Plain/hill desert steppe) had better classification results and classes P&Q (Gravelly desert and Sandy desert) had higher accuracies when using southwest half to predict the northeast one. Another big steppe type, class O (Steppe desert) could not be well classified as it was confused with Plain/hill desert steppe (L). The rest of the steppe classes, which contained fewer patches, had very high error rates. As for degradation classification, comparing to previous experiments on Urat the accuracy rates of all classes dropped especially the severe degradation class. This was probably also mainly caused by the small size of the classes in the dataset.

In general, the results of "prediction within eco-region" experiments of all IMAR sites had higher error rates than local prediction for both steppe type and degradation classification. By dividing image into two halves, correlation between training and to-be-predicted datasets decreased due to the difference between two parts, such as different elevation, which usually ranked very high in variable importance plots generated during the run of RF model. It becamemore apparent that classes covering a small area in the image, i.e. with manyfewer patches, werevery negativelyaffected by the presence larger classes during classification. This experiment also showedthat steppe classes sometimes only existed in training area or testing area. Though not too many patches were misclassified because of this, it still contributed to higher error rates. More importantly, the explanatory factors used in the RF model were not able to help distinguish classes veryeffectively,thus the overlaps of classes affect the performance of the classifier. It is also possible that even if we introduce more features into the model, using Landsat TM5 imagery and DEM data alone is not capable enough to meet our requirement and serve our goal due to the amount of information they contain.

Table 20. The error matrices of prediction within eco-region ofEwenk autonomous region. (a) Used northern part for training and classify steppe types of southern part.

(b). Used northern part for training and classify degradation of southern part. (c) Used southern part for training and classify steppe types of northern part. (d) Used southern part for training and classify degradation of northern part.UA is user's accuracy, PA is producer's accuracy and OA is overall accuracy. For steppe type, please refer to Table 3. For degradation level, please refer to merged class codes in Table 4.

a. Error matrix of steppe type prediction within eco-region -- train on north and predict on south (Ewenk Autonomous Region)													
	Reference												
Classified		A	B	C	D	E	F	G	H	I	J	Total	**UA**
	A	859	68	41	603	57	123	14	17	26	1	1809	0.47
	B	370	81	21	125	1	48	1	15	27	0	689	0.12
	C	279	28	133	192	315	56	33	21	34	2	1093	0.12
	D	147	7	0	1093	3	23	147	78	0	13	1511	0.72
	E	5	0	1	29	7	1	87	14	0	0	144	0.05
	F	164	138	7	24	0	1142	15	206	114	119	1929	0.59
	G	3	0	0	17	0	2	199	27	0	1	249	0.80
	H	0	0	0	1	0	4	23	63	0	16	107	0.59
	I	101	2693	23	1	0	669	0	1	1685	0	5173	0.33
	J	0	0	0	0	0	0	4	26	0	24	54	0.44
	Total	1928	3015	226	2085	383	2068	523	468	1886	176	12758	**OA**
	PA	0.45	0.03	0.59	0.52	0.02	0.55	0.38	0.13	0.89	0.14		**41.43%**
Kappa = 0.32 OOB (training dataset) = 32.95%													

b. Error matrix of degradation prediction within eco-region -- train on north and predict on south (Ewenk Autonomous Region)							
	Reference						
Classified		a	b	c	d	Total	**UA**
	a	7922	898	261	26	9107	0.87
	b	252	852	575	20	1699	0.50
	c	326	307	495	108	1236	0.40
	d	40	85	228	363	716	0.51
	Total	8540	2142	1559	517	12758	**OA**
	PA	0.93	0.40	0.32	0.70		**75.50%**
Kappa = 0.50, OOB (training dataset) = 29.27%							

c. Error matrix of steppe type prediction within eco-region -- train on south and predict on north (Ewenk Autonomous Region)

	Reference											
Classified		A	B	C	D	E	F	G	H	I	J	Total	**UA**
	A	707	379	23	279	0	85	37	0	381	0	1891	0.37
	B	3	1	0	0	0	12	0	0	229	0	245	0.00
	C	172	63	137	51	2	28	24	0	149	0	626	0.22
	D	277	63	2	1652	0	8	7	12	7	0	2028	0.81
	E	113	9	117	31	10	3	0	0	1	0	284	0.04
	F	97	59	7	10	0	495	0	0	259	0	927	0.53
	G	167	19	58	1175	180	146	1127	169	0	138	3179	0.35
	H	84	44	11	367	11	232	153	211	9	174	1296	0.16
	I	79	121	3	2	0	128	1	0	2519	0	2853	0.88
	J	22	14	2	69	2	402	39	71	0	319	940	0.34
	Total	1721	772	360	3636	205	1539	1388	463	3554	631	14269	**OA**
	PA	0.41	0.00	0.38	0.45	0.05	0.32	0.81	0.46	0.71	0.51		**50.30%**
Kappa = 0.42 OOB (training dataset) = 35.71%												

d. Error matrix of degradation prediction within eco-region -- train on south and predict on north (Ewenk Autonomous Region)							
	Reference						
Classified		a	b	c	d	Total	**UA**
	a	5708	284	120	32	6144	0.93
	b	1584	1593	314	102	3593	0.44
	c	657	824	398	239	2118	0.19
	d	512	322	542	1038	2414	0.43
	Total	8461	3023	1374	1411	14269	**OA**
	PA	0.67	0.53	0.29	0.74		**61.23%**
Kappa = 0.41, OOB (training dataset) = 23.2%							

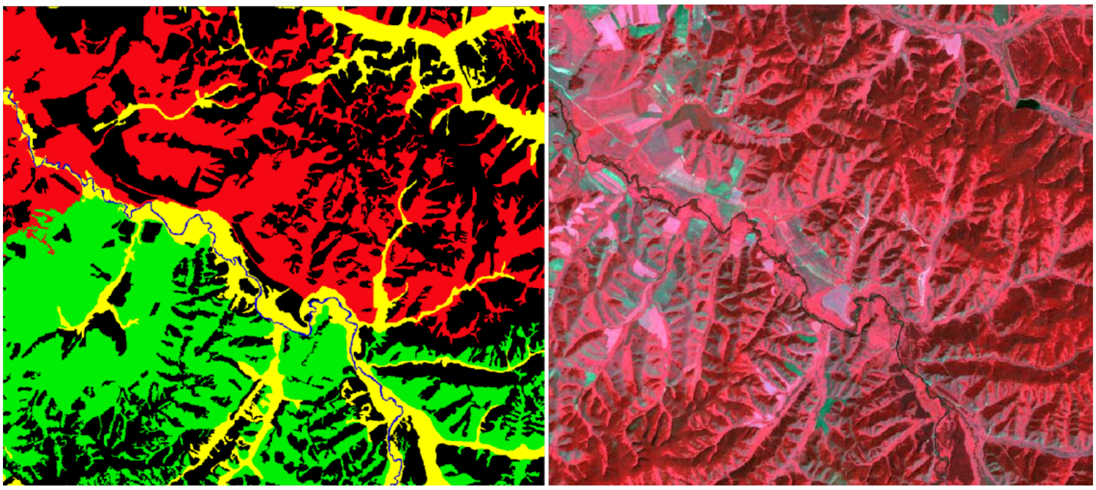

(a) (b)

Figure 3. (a) A subset of 2009 steppe vegetation map (red: "Low/middle mountain meadow", green: "Mountain meadow steppe", yellow: "Lowland and wetland meadow", blue: water, black: non-steppe area), and (b) the same area of 2010 Landsat TM5 image in false color infrared of Ewenk Autonomous Region.

Table 21. The error matrices of prediction within eco-region of Xilinhot city. (a) Used east part for training and classify steppe types of west part. (b) Used east part for training and classify degradation of west part. (c) Used west part for training and classify steppe types of east part. (d) Used west part for training and classify degradation of east part. * Indicated that the class was absent. UA is user's accuracy, PA is producer's accuracy and OA is overall accuracy. For steppe type, please refer to Table 3. For degradation level, please refer to merged class codes in Table 4.

a. Error matrix of steppe type prediction within eco-region -- train on east and predict on west (Xilinhot City)											
	Reference										
		A	B*	D	E	F	G	H	K	Total	**UA**
classified	A	197	0	212	1	6	0	0	0	416	0.47
	B	5	0	9	1	3	0	0	0	18	0.00
	D	2	0	8226	65	35	73	2	32	8435	0.98
	E	17	0	679	778	19	33	1	3	1530	0.51
	F	0	0	88	3	124	44	37	1	297	0.42
	G	1	0	1464	33	198	1171	69	1	2937	0.40
	H	1	0	26	1	34	66	31	0	159	0.19
	K	2	0	545	2	7	6	4	127	693	0.18
	Total	225	0	11249	884	426	1393	144	164	14485	**OA**
	PA	0.88	0.00	0.73	0.88	0.29	0.84	0.22	0.77		**73.55%**
Kappa = 0.49, OOB (training dataset) =35.01%											

b. Error matrix of degradation prediction within eco-region -- train on east and predict on west (Xilinhot City)

	Reference					
		a	b	c	d	Total	**UA**
Classified	a	280	128	31	0	439	0.64
	b	686	1335	386	94	2501	0.53
	c	471	2666	3197	813	7147	0.45
	d	59	694	1609	2036	4398	0.46
	Total	1496	4823	5223	2943	14485	**OA**
	PA	0.19	0.28	0.61	0.69		**47.28%**
	Kappa = 0.25, OOB = 41.73%						

c. Error matrix of steppe type prediction within eco-region -- train on west and predict on east (Xilinhot City)

	Reference										
		A	B	D	E	F	G	H	K	Total	UA
classified	A	873	179	2166	77	48	6	6	268	3623	0.24
	B *	0	0	0	0	0	0	0	0	0	0.00
	D	89	8	5533	165	22	57	0	21	5895	0.94
	E	67	14	533	1744	12	24	0	11	2405	0.73
	F	268	20	1519	400	438	173	44	62	2924	0.15
	G	0	0	408	136	25	754	49	0	1372	0.55
	H	0	0	303	45	61	246	86	4	745	0.12
	K	7	12	691	23	0	6	4	113	856	0.13
	Total	1304	233	11153	2590	606	1266	189	479	17820	**OA**
	PA	0.67	0.00	0.50	0.67	0.72	0.60	0.46	0.24		**53.54%**

Kappa=0.38, OOB=25.22%

d. Error matrix of degradation prediction within eco-region -- train on west and predict on east (Xilinhot City)

	Reference						
		a	b	c	d	Total	**UA**
Classified	a	4291	3477	1511	328	9607	0.45
	b	377	931	879	213	2400	0.39
	c	53	533	974	573	2133	0.46
	d	129	430	746	2375	3680	0.65
	Total	4850	5371	4110	3489	17820	**OA**
	PA	0.88	0.17	0.24	0.68		**48.10%**
	Kappa = 0.30, OOB = 44.50%						

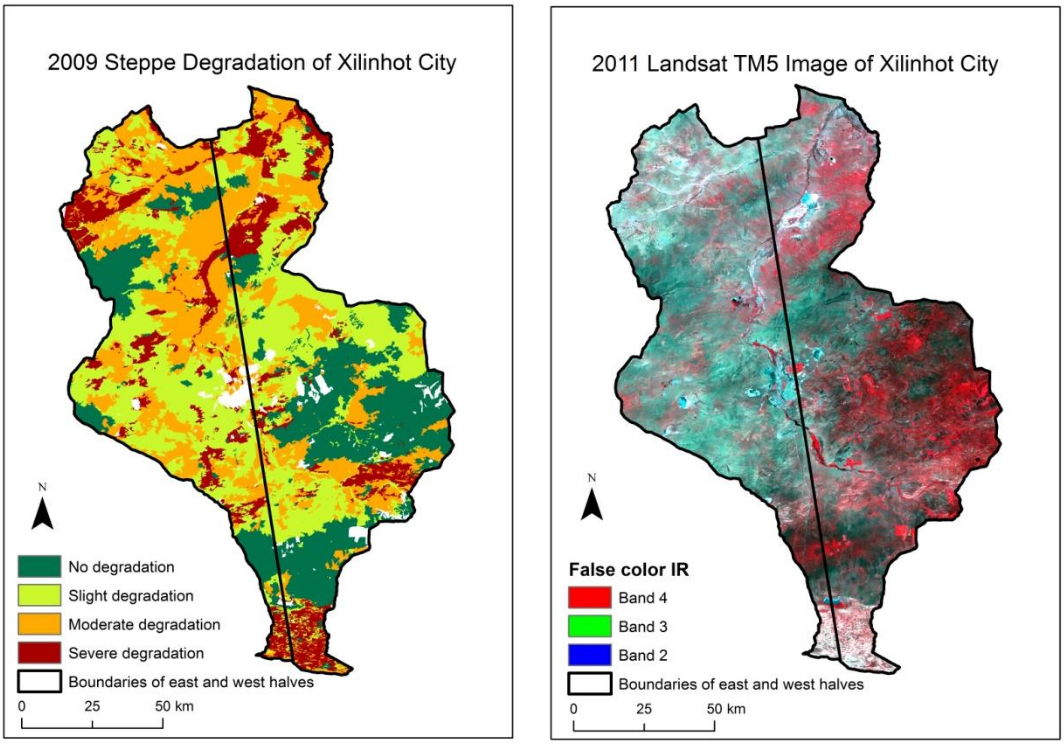

(a) (b)

Figure 4. (a) 2009 steppe degradation map of XilinhotCity which was divided into east and west halves, and (b) 2011 Landsat TM5 image in false color infrared of Xilinhot City.

Table 22. The error matrices of prediction within eco-region of Urat middle banner. (a) used northeast part for training and classify steppe types of southwest part. (b) Used northeast part for training and classify degradation of southwest part. (c) Used southwest part for training and classify steppe types of northeast part. (d) Used southwest part for training and classify degradation of northeast part. * Indicated that the class was absent. UA is user's accuracy, PA is producer's accuracy and OA is overall accuracy. For steppe type, please refer to Table 3. for degradation level, please refer to merged class codes in Table 4.

a. Error matrix of steppe type prediction within eco-region -- train on northeast and predict on southwest (Urat Middle Banner)										
		Reference								
		F	GH	J	L	MN	O	PQ	Total	**UA**
Classified	F	66	169	293	115	69	16	1	729	0.09
	GH	101	239	0	380	94	134	15	963	0.25
	J*	0	0	0	0	0	0	0	0	0.00
	L	34	44	28	2759	178	1374	23	4440	0.62
	MN	16	35	0	491	4683	715	0	5940	0.79
	O	3	7	0	239	96	1231	143	1719	0.72
	PQ	7	95	0	504	618	439	1128	2791	0.40

	Total	227	589	321	4488	5738	3909	1310	16582	**OA**
	PA	0.29	0.41	0.00	0.61	0.82	0.31	0.86		**60.95%**
Kappa = 0.49, OOB (training dataset) = 27.72%										

b. Error matrix of degradation prediction within eco-region -- train on northeast and predict on southwest (Urat Middle Banner)							
	Reference						
Classified		a	b	c	d	Total	**UA**
	a	4473	2080	425	569	7547	0.59
	b	469	1520	1402	48	3439	0.44
	c	123	887	2782	169	3961	0.70
	d	335	458	505	337	1635	0.21
	Total	5400	4945	5114	1123	16582	**OA**
	PA	0.83	0.31	0.54	0.30		**54.95%**
	Kappa = 0.37, OOB = 44.50%						

c. Error matrix of steppe type prediction within eco-region -- train on southwest and predict on northeast (Urat Middle Banner)										
	Reference									
		F	GH	J*	L	MN	O	PQ	Total	**UA**
Classified	F	51	238	0	595	144	46	17	1091	0.05
	GH	2	50	0	96	13	52	32	245	0.20
	J	2	1	0	0	0	0	0	3	0.00
	L	11	147	0	3880	315	1509	327	6189	0.63
	MN	4	8	0	369	1851	21	100	2353	0.79
	O	1	83	0	1337	21	1282	19	2743	0.47
	PQ	1	7	0	162	7	132	924	1233	0.75
	Total	72	534	0	6439	2351	3042	1419	13857	**OA**
	PA	0.71	0.09	0.00	0.60	0.79	0.42	0.65		**58.01%**
Kappa = 0.41, OOB (training dataset) = 23.30%										

d. Error matrix of degradation prediction within eco-region -- train on southwest and predict on northeast (Urat Middle Banner)							
	Reference						
Classified		a	b	c	d	Total	**UA**
	a	1701	503	73	15	2292	0.74
	b	354	2322	484	87	3247	0.72
	c	174	4218	2139	231	6762	0.32
	d	747	489	215	105	1556	0.07
	Total	2976	7532	2911	438	13857	**OA**
	PA	0.57	0.31	0.73	0.24		**45.23%**
Kappa = 0.25, OOB (training dataset) = 27.35%							

4.5 Prediction across eco-region

Mutual prediction of steppe type between Ewenk Autonomous Region and Xilinhot City produced accuracy assessment valuesthat were very lowexcept for class D (Plain/hill typical steppe) (Table 23). These two study sites belong to two eco-regions and it turned out that they were different enough that the RF approach could not learn to accurately predict between them. When we trained on Ewenk, many patches of Xilinhot were misclassified into class C (Sand land meadow steppe) and E (Sand land typical steppe) (Table 23a and 23c). On the other hand, when we trained on Xilinhot, many Ewenk patches were misclassified into Lowland meadow (class F: Lowland and wetland meadow, G: Salinized lowland meadow, H: Swampy lowland meadow). Thiswas probably because the dominant steppe type, Plain/hill typical steppe (class D) was growing on drier soil and grass tend to be more similar to those growing on sand land in Ewenk, while the steppe of Ewenk tended to have more reflectance in near infrared than the same kind of steppe in Xilinhot, thus they were classified as Lowland meadow. This experiment, again, showed that in general, typical steppe and meadow steppe cannot be successfully distinguished by the classifier.The degradation classification results and the accuracy rates were also extremely low (Table 23). When we trained on the Ewenk data, many No degradation (class a) patches inXilinhot were classified as Slight degradation (b) and many Slight degradation patches were misclassified as Moderate degradation patches. On the contrary, when we used training data sampled from Xilinhot, a lot of patches in Ewenk were misclassified as No degradation class. This was probably for similar reasons as the high error rates of steppe type classification. The steppe of Ewenk, which was located in the meadow steppe eco-region, looked healthier especially that growing in mountainous areas. Thus when we use Ewenk as the source of training data, the steppe of Xilinhot was more similar to more degraded grasslands in Ewenk and vice versa when we trained on Xilinhot samples. As introduced earlier in Data section of this paper, the degradation level was determined by comparing with nearby conserved steppe. The difference in situation of those conserved steppes led to different standards of degradation measurement thus when predicted across eco-region, the error rates were high. There were probably many other factors that contributed to low classification accuracy of this experiment.

Table 23. The error matrices of prediction across eco-region. (a) Used 200-per-class sample sets of Ewenk autonomous region for training and classify steppe types of all patches in Xilinhot city. (b) Used 200-per-class sample sets of Xilinhot city for training and classify steppe types of all patches inEwenk autonomous region. (c) Used 200-per-class sample sets of Ewenk autonomous region for training and classify degradation of all patches in Xilinhot city. (d) Used 200-per-class sample sets of Xilinhot city for training and classify degradation of all patches in Ewenk autonomous region. * Indicated that the class was absent. UA is user's accuracy, PA is producer's accuracy and OA is overall accuracy. For steppe type, pleaserefer to Table 3. For degradation level, please refer to merged class codes in Table 4.

a. Prediction across eco-region of steppe type (train on samples of Ewenk Autonomous Region, predict on all patches of Xilinhot City)

		Reference												
		A	B	C*	D	E	F	G	H	I*	J*	K	Total	**UA**
Classified	A	288	6	0	1723	102	88	114	25	0	0	39	2385	0.12
	B	240	122	0	298	9	24	0	0	0	0	102	795	0.15
	C	217	77	0	7277	2043	269	839	110	0	0	418	11250	0.00
	D	509	0	0	6905	19	24	26	4	0	0	0	7487	0.92
	E	51	0	0	4086	1182	212	1053	91	0	0	3	6678	0.18
	F	76	6	0	247	37	215	17	11	0	0	8	617	0.35
	G	17	0	0	799	15	87	574	69	0	0	2	1563	0.37
	H	20	0	0	36	6	85	23	20	0	0	0	190	0.11
	I	111	22	0	1030	61	28	13	3	0	0	71	1339	0.00
	J	0	0	0	1	0	0	0	0	0	0	0	1	0.00
	K*	0	0	0	0	0	0	0	0	0	0	0	0	N/A
	Total	1529	233	0	22402	3474	1032	2659	333	0	0	643	32305	**OA**
	PA	0.19	0.52	N/A	0.31	0.34	0.21	0.22	0.06	N/A	N/A	0.00		**28.81%**

Kappa = 0.12, OOB (training dataset) = 36.50%

b. Prediction across eco-region of steppe type (train on samples of Xilinhot City, predict on all patches of EwenkAutonomous Region)

		Reference												
		A	B	C	D	E	F	G	H	I	J	K*	Total	**UA**
Classified	A	192	244	4	286	0	25	0	5	569	0	0	1325	0.14
	B	27	107	2	3	0	5	0	0	224	0	0	368	0.29
	C*	0	0	0	0	0	0	0	0	0	0	0	0	N/A
	D	928	164	36	2201	55	45	108	27	115	0	0	3679	0.60
	E	6	1	3	1	1	0	3	0	1	0	0	16	0.06
	F	1400	927	73	1600	19	2506	203	340	1133	236	0	8437	0.30
	G	106	7	73	152	162	32	732	50	5	56	0	1375	0.53
	H	681	54	278	1406	338	560	815	507	75	514	0	5228	0.10
	I*	0	0	0	0	0	0	0	0	0	0	0	0	N/A
	J*	0	0	0	0	0	0	0	0	0	0	0	0	N/A
	K	309	2283	117	72	13	434	50	2	3318	1	0	6599	0

	Total	3649	3787	586	5721	588	3607	1911	931	5440	807	0	27027	**OA**
	PA	0.05	0.03	0	0.38	0.00	0.69	0.38	0.54	0	0	N/A		**23.11%**
Kappa = 0.16, OOB (training dataset) = 30.00%														

c. Prediction across eco-region of degradation (train on samples of Ewenk Autonomous Region, predict on all patches of Xilinhot City)							
	Reference						
		a	b	c	d	Total	**UA**
Classified	a	1275	670	305	106	2356	0.54
	b	3156	3861	2770	602	10389	0.37
	c	1696	4590	4455	1865	12606	0.35
	d	219	1073	1803	3859	6954	0.55
	Total	6346	10194	9333	6432	32305	**OA**
	PA	0.20	0.38	0.48	0.60		**41.63%**
Kappa = 0.20, OOB (training dataset) = 36.88%							

d. Prediction across eco-region of degradation (train on samples of Xilinhot City, predict on all patches of Ewenk Autonomous Region)							
	Reference						
		a	b	c	d	Total	**UA**
Classified	a	6669	3598	1640	456	12363	0.54
	b	8086	706	395	104	9291	0.08
	c	1948	490	311	144	2893	0.11
	d	298	371	587	1224	2480	0.49
	Total	17001	5165	2933	1928	27027	**OA**
	PA	0.39	0.14	0.11	0.63		**32.97%**
Kappa = -0.07, OOB (training dataset) = 43.25%							

4.6 Pooling

We combined the balanced sampled patches from Ewenk Autonomous Region and Xilinhot City into one training dataset to test how the pooling affected the classified results compared with local prediction and across eco-region prediction. The pooling of Ewenk and Xilinhot samples generated very similar classification power of the local prediction (Tables 24a and 24b). Although the results of "prediction across eco-region" experiment suggested thatdata from outside of the region could not well represent characteristics of steppes within the region, adding these data to local randomly sampled training dataset did not bring a lot of disturbance. The training dataset had anincreased variety in variable values and samples from classes that were not in either one of the regions, andthe RF classifier worked as well as those trained by local samples. Moreover, different from the results of mutual prediction in the last experiment, in this experiment, few to no patches were misclassified into classes that did not exist in the region. Just like steppe type classification, even if pooling did not increase the classification accuracy, it did not decrease it compared with results of local prediction (Table 24c).

Since RF determines onclassassignments according to votes and because about half thetraining samples were from each local region, any givenpatch hada reasonable chance to be classified as it should be according toits similarity to those local sample patches. Moreover, though differences existed between the two samples of the same class but from different site, the RF classifier might identify two or more class centers for that class during the training process, thus the accuracy was not greatly affected by additional external training samples when classify patches from two regions respectively.

Table 24. The error matrices of classification by pooling Ewenk autonomous region and Xilinhot city sample datasets and classified (a) steppe types of all patches in Ewenk autonomous region, (b) steppe types of all patches in Xilinhot city, (c) degradation of all patches in Ewenk autonomous region and (d) degradation of all patches in Xilinhot city. * Indicated that the class was absent. UA is user's accuracy, PA is producer's accuracy and OA is overall accuracy. For steppe type, please refer to Table 3. For degradation level, please refer to merged class codes in Table 4.

a. Pooling and predicting on Ewenk Autonomous Region - steppe type classification													
		Reference											
		A	B	C	D	E	F	G	H	I	J	K*	Total	**UA**
Classified	A	1687	390	25	617	10	209	39	21	245	0	0	3243	0.52
	B	27	1985	2	10	0	286	0	0	526	0	0	2836	0.70
	C	521	99	456	278	126	121	74	18	145	2	0	1840	0.25
	D	576	72	2	3865	16	49	144	47	19	3	0	4793	0.81
	E	150	4	54	254	421	36	70	9	2	1	0	1001	0.42
	F	277	258	10	98	2	2034	17	57	290	6	0	3049	0.67
	G	36	8	6	229	3	28	1190	66	1	49	0	1616	0.74
	H	42	5	3	248	6	126	237	492	4	80	0	1243	0.40
	I	314	953	28	37	0	510	7	3	4208	0	0	6060	0.69
	J	17	7	0	85	4	207	133	218	0	666	0	1337	0.50
	K	2	6	0	0	0	1	0	0	0	0	0	9	0.00
	Total	3649	3787	586	5721	588	3607	1911	931	5440	807	0	27027	**OA**
	PA	0.46	0.52	0.7	0.68	0.7	0.56	0.62	0.5	0.77	0.8	N/		**62.91**

				8		2			3		3	A		%
Kappa = 0.57, OOB (training dataset) = 35.61%														

b. Pooling and predicting on Xilinhot City - steppe type classification														
		Reference												
		A	B	C*	D	E	F	G	H	I*	J*	K	Total	**UA**
Classified	A	113 9	4	0	2139	83	46	6	0	0	0	10	3427	0.33
	B	122	221	0	204	28	10	0	1	0	0	57	643	0.34
	C	0	0	0	2	0	0	0	0	0	0	0	2	0.00
	D	53	0	0	1372 9	231	57	145	0	0	0	9	1422 4	0.97
	E	86	0	0	1312	277 4	22	36	1	0	0	10	4241	0.65
	F	59	0	0	1027	117	572	91	17	0	0	5	1888	0.30
	G	1	0	0	1262	137	103	192 4	39	0	0	0	3466	0.56
	H	13	0	0	522	41	201	442	267	0	0	0	1486	0.18
	I	0	0	0	0	0	0	0	0	0	0	0	0	N/A
	J	0	0	0	0	0	0	0	0	0	0	0	0	N/A
	K	56	8	0	2205	63	21	15	8	0	0	552	2928	0.19
	Tota l	152 9	233	0	2240 2	347 4	103 2	265 9	333	0	0	643	3230 5	**OA**
	PA	0.74	0.9 5	N/ A	0.61	0.80	0.55	0.72	0.8 0	N/ A	N/ A	0.8 6		**65.56 %**
Kappa = 0.48, OOB (training dataset) = 35.61%														

c. Pooling and predicting on Ewenk Autonomous Region - steppe degradation classification							
		Reference					
		a	b	c	d	Total	**UA**
Classified	a	13956	921	302	42	15221	0.92
	b	1638	2971	783	159	5551	0.54
	c	883	856	1199	301	3239	0.37
	d	524	417	649	1426	3016	0.47
	Total	17001	5165	2933	1928	27027	**OA**
	PA	0.82	0.58	0.41	0.74		**72.34%**
Kappa = 0.53, OOB (training dataset) = 39.50%							

d. Pooling and predicting on Xilinhot City - steppe degradation classification							
		Reference					
		a	b	c	d	Total	**UA**
Classifi ed	a	4149	2111	767	81	7108	0.58
	b	1340	4467	2105	458	8370	0.53

	c	565	2335	4300	1426	8626	0.50
	d	292	1281	2161	4467	8201	0.54
	Total	6346	10194	9333	6432	32305	**OA**
	PA	0.65	0.44	0.46	0.69		**53.81%**
Kappa = 0.38, OOB (training dataset) = 39.50%							

4.7 Pooling of filtered training patches

After filteringout some highly mixed and road patches, we combined the purified sample patches from Ewenk and Xilinhot, as in the pooling experiment. Based on the bootstrapping classification result of training samples using RF, the accuracy rate in this experiment was higher than any training dataset in all of previous experiments. Not only the overall accuracy and Kappa value, but every class also had higher user's accuracy and producer's accuracy (Table 25 a). This is probably due to the filtering process which increased the homogeneity within patches thus the samples were less similar to patches of other classes. However, when we used this new training dataset to classify steppe type for all patches in Ewenk and Xilinhot, the classification results were worse than the pooling experiments without filtered training sample datasets and the local prediction experiments as well (Table 25 b and c).

The randomly sampled training dataset, though containing mixed patches, covered a greater variety of samples for every class. When classifying all patches within the region, patches containing a small portion of pixels from other classes could still be appropriately dealt with. On the contrary, with the filtering process, though within training dataset difference between patches from different classes became more distinct, mixed patches in the map became less similar to class center and were more likely to be classified into other similar classes.

Table 25. The error matrices of classification by pooling Ewenk autonomous region and Xilinhot city filtered samples and classified (a) combined training dataset itself, (b) steppe type of all patches in Ewenk autonomous region and (c) steppe type of all patches in Xilinhot city. * Indicated that the class was absent. UA is user's accuracy, PA is producer's accuracy and OA is overall accuracy. For steppe type, please refer to Table 3.

a. Pooling of filtered sample patches from Ewenk Autonomous Region and Xilinhot City														
		Reference												
		A	B	C	D	E	F	G	H	I	J	K	Total	**UA**
Classified	A	154	19	4	36	3	7	0	3	2	0	5	233	0.66
	B	13	196	0	2	2	3	0	0	10	0	30	256	0.77
	C	4	4	134	0	62	1	6	2	1	0	0	214	0.63
	D	17	3	1	186	8	3	5	6	0	0	3	232	0.80
	E	7	2	19	11	218	1	6	1	0	0	1	266	0.82
	F	9	16	1	6	5	159	1	16	10	3	4	230	0.69

	G	0	0	3	6	13	4	242	27	0	2	0	297	0.81
	H	2	0	3	11	10	30	31	139	0	6	2	234	0.59
	I	2	40	2	1	0	16	0	0	110	0	0	171	0.64
	J	0	0	0	0	0	0	0	34	0	87	0	121	0.72
	K	9	23	0	13	1	0	0	2	0	0	143	191	0.75
	Total	217	303	167	272	322	224	291	230	133	98	188	2445	**OA**
	PA	0.71	0.65	0.80	0.68	0.68	0.71	0.83	0.60	0.83	0.89	N/A		**72.31%**
Kappa = 0.69, OOB = 27.69%														

b. Pooling of purified samples and predicting on Ewenk Autonomous Region - steppe type classification														
		Reference												
		A	B	C	D	E	F	G	H	I	J	K*	Total	**UA**
Classified	A	1245	332	13	1254	19	93	59	26	295	0	0	3336	0.37
	B	18	1451	0	19	0	279	1	1	238	0	0	2007	0.72
	C	952	205	466	510	239	260	169	48	357	7	0	3213	0.15
	D	367	54	1	2912	4	20	126	37	46	1	0	3568	0.82
	E	102	0	40	384	297	31	90	29	1	6	0	980	0.30
	F	604	396	25	337	5	2066	104	269	449	155	0	4410	0.47
	G	27	6	9	145	13	29	1075	92	1	82	0	1479	0.73
	H	72	29	10	112	11	191	167	229	91	49	0	961	0.24
	I	253	1298	22	17	0	488	3	4	3943	0	0	6028	0.65
	J	4	2	0	28	0	147	117	196	4	507	0	1005	0.50
	K	5	14	0	3	0	3	0	0	15	0	0	40	0.00
	Total	3649	3787	586	5721	588	3607	1911	931	5440	807	0	27027	**OA**
	PA	0.34	0.38	0.80	0.51	0.51	0.57	0.56	0.25	0.72	0.63	N/A		**52.51%**
Kappa = 0.45, OOB (training dataset) = 27.69%														

c. Pooling of purified samples and predicting on Xilinhot City - steppe type classification														
		Reference												
		A	B	C*	D	E	F	G	H	I*	J*	K	Total	**UA**
Classified	A	994	7	0	1822	32	31	2	0	0	0	28	2916	0.34
	B	165	209	0	207	33	13	1	0	0	0	90	718	0.29
	C	0	0	0	30	1	0	5	0	0	0	2	38	0.00

	D	67	2	0	13167	191	58	102	2	0	0	9	13598	0.97
	E	98	3	0	1583	2816	36	75	2	0	0	10	4623	0.61
	F	115	2	0	521	92	378	40	23	0	0	9	1180	0.32
	G	5	0	0	1508	93	150	1830	70	0	0	1	3657	0.50
	H	38	0	0	1273	144	347	577	228	0	0	1	2608	0.09
	I	0	0	0	0	0	0	0	0	0	0	0	0	N/A
	J	0	0	0	0	0	0	1	0	0	0	0	1	N/A
	K	47	10	0	2291	72	19	26	8	0	0	493	2966	0.17
	Total	1529	233	0	22402	3474	1032	2659	333	0	0	643	32305	**OA**
	PA	0.65	0.90	N/A	0.59	0.81	0.37	0.69	0.68	N/A	N/A	0.77		**62.27%**
Kappa = 0.44, OOB (training dataset) = 27.69%														

Table 26. The summary table of key experiments on IMAR sites. OA is overall accuracy; K is kappa value.

Classification	Site	Pixel-based		Patch-based		Add texture		Scale of 40		Local prediction		Within eco-region				Across eco-region		Pooling	
												Half 1		Half 2					
		OA (%)	K	OA (%)	K	OA (%)	K	OA (%)	K	OA (%)	K	OA (%)	K	OA (%)	K	OA (%)	K	OA (%)	K
Steppe type	Ewenk	54.4	0.47	64.6	0.59	65.0	0.59	65.3	0.60	63.8	0.58	41.4	0.32	50.3	0.42	23.1	0.16	62.9	0.57
	Xilinhot	62.9	0.44	66.2	0.48	68.5	0.51	69.2	0.51	67.4	0.50	73.6	0.49	53.5	0.38	28.8	0.12	65.6	0.48
	Urat	65.5	0.55	74.5	0.66	74.1	0.66	74.1	0.66	70.0	0.61	61.0	0.49	58.0	0.41				
Degradation	Ewenk	68.9	0.49	72.0	0.53	72.8	0.54	71.8	0.53	72.2	0.53	75.5	0.50	61.2	0.41	33.0	-0.07	72.3	0.53
	Xilinhot	54.3	0.39	56.9	0.42	57.0	0.43	55.5	0.41	53.6	0.38	47.3	0.25	48.1	0.30	41.6	0.20	53.8	0.38
	Urat	65.4	0.51	67.7	0.55	67.5	0.55	66.2	0.52	64.7	0.51	55.0	0.37	45.2	0.25				

4.8 Classifying image subsets in theMongolia

We used an RF trained using the IMAR samplesites toclassify thethree sites in Mongolia, and used the field survey points to assess the result. We used the same training datasetwhen classified Meadow steppe site (Landsat TM 5 image subset of path 124 and row 27) and Typical steppe site in Mongolia (Landsat TM 5 image subset of path 126 and row 28). This training datasethas the non-filtered pooling samples of Xilinhot and Ewenk as we used in pooling experiment with theIMAR data. Almost all patches within these two Mongolian subsets were classified as the "Plain/hill typical steppe". Most of the middle part of image of path 124, row 27was classified as Plain/hill typical steppe (Figure 5). A lot of patches along a long and narrow river in the north were classified as lowland meadow. Some sandy patches with mottled texture on the riverside were classified as the Sand land meadow steppe (class C) and the Sand land typical steppe (class E).Many patches that look like steppe on sandy land in the south of the subset were also classified into class C and E. The classifier recognized sand land but seemed to failed to distinguishSand land meadow steppe and Sand land typical steppe. On the east and south sides of the image, there were many patches labeled as the Plain/hill meadow steppe and these patches seem to have higher reflectance in near infrared band. A few patches in the middle, which were actually agriculture land, were also classified as the Plain/hill meadow steppe or typical steppe. Most of the field survey points clustered in the middle north of this area and a few were near water (Figure 5). Based on the match table, the majority of these pointed (12 out of 19) were labeled as Plain/hill typical steppe and they were all classified as the Plain/hill typical steppe. However, the other seven points (1 Sand land meadow steppe, 6 Salinized lowland meadow) were also classified as Plain/hill typical steppe.

Similar to image of path 124, row 27, the image of path 126 and row 26 was almost all classified as the Plain/hill typical steppe (Figure 6). There was no river in the area, according to our visual image interpretation, but there were some small ponds and their surrounding area appeared bright white to very bright cyan tone. These patches were mostly classified into lowland meadow classes (F, G, H). There were also some patches classified as the Low/middle mountain meadow but they did not form a large area. We also found that, at the edges of the image and around removed clouds, there were more different classified steppe types. This might be caused by some edge effects when we created features (such as TWI) and during zonal mean calculation. In terms of field survey points, there were 71 points falling in this area and according to the match table, 55 of them werePlain/hill typical steppe, 3 class E (Sand land typical steppe), 8 class G (Salinized lowland meadow), 4 class L (Plain/hill desert steppe) and 1class M (Mountain desert steppe). Among these points, 3 of the class D sites were classified into class G and 1 was classified as class C (Sand land meadow steppe). All the other points were classified into class D.

As for the subset of image of path 129 and row 30, the steppe type classification map did not have as a quite homogeneous resultas for the other two areas. Two major classes were the Steppe desert (O) and the merged class P&Q (Gravelly desert and

Sandy desert). Due to the topographyof this area, it looked likethere were many ditch-like ground features and there were all classified as the Lowland meadows (class F, G and H). In general, this area was basically regarded as a desert area, which indicated very little vegetation. In terms of field survey data assessment, this area had the worst result. Among all 29 points, only 4 of them (1 of class O, 3 of class P&Q) were classified as they were labeled. There were 7 points labeled as class L (Plain/hill desert steppe) and 11 as class M&N (Mountain desert steppe and Sand land desert steppe) and they were all classified into class G&H, O or P&Q.

Almost all the correctly classified points, which had their labeled classes according to match table agree with classes assigned by the RF classifier, were the Plain/hill typical steppe points (Table 26). The rest of points were mostly misclassified under the assumption that our labeling of validation points based on the match table wascorrect. However, it was possible that we did not label those points correctly because only used species information to assign the labels. Some species grow on many kinds of steppes and the table cannot cover all the combinations. We also did not take other factors such as neighbor points or how these places look on the image into our consideration to keep this labeling process independent. It was also possible that neither the match table labeling nor the RF classification was correct.

We also classified the degradation levels of these three subsets. However, we do not have ground truth data to assess the accuracy. Most of the area in theimages of path 124, row 27, and path 126, row 28 was classified as slight degradation (Figure 8, 9 and 10). It was interesting that most of the image of path 129, row 30 was classified as severely degraded. It can be misclassification, and it also can be due to the presence of theGobi Desert in the image, which can look degraded. Without other ancillary data, it's hard to better evaluatethe degradation classification results. Because the result of accuracy assessment by using field survey data of Mongolia was not satisfying, we did not use the predicted steppe class as additional input to classify the degradation level again.

Table 27. The error matrix of assessing classification results of subsets of Mongolianimages.* Indicated that the class was absent. UA is user's accuracy, PA is producer's accuracy and OA is overall accuracy. For steppe type, please refer to Table 3.

		Labeled according to match table									
		C	D	E	GH	L	MN	O	PQ	Total	**UA**
classified by RF	C	0	1	0	0	0	0	0	0	1	0.00
	D	1	63	3	14	4	1	0	0	86	0.73
	E*	0	0	0	0	0	0	0	0	0	N/A
	GH	0	3	0	0	1	1	1	1	7	0.00
	L*	0	0	0	0	0	0	0	0	0	N/A
	MN*	0	0	0	0	0	0	0	0	0	N/A
	O	0	0	0	0	3	8	1	3	15	0.07
	PQ	0	0	0	0	3	2	2	3	10	0.30

	Total	1	67	3	14	11	12	4	7	119	**OA**
	PA	0.00	0.94	0.00	0.00	0.00	0.00	0.25	0.43		0.56
Kappa = 0.24											

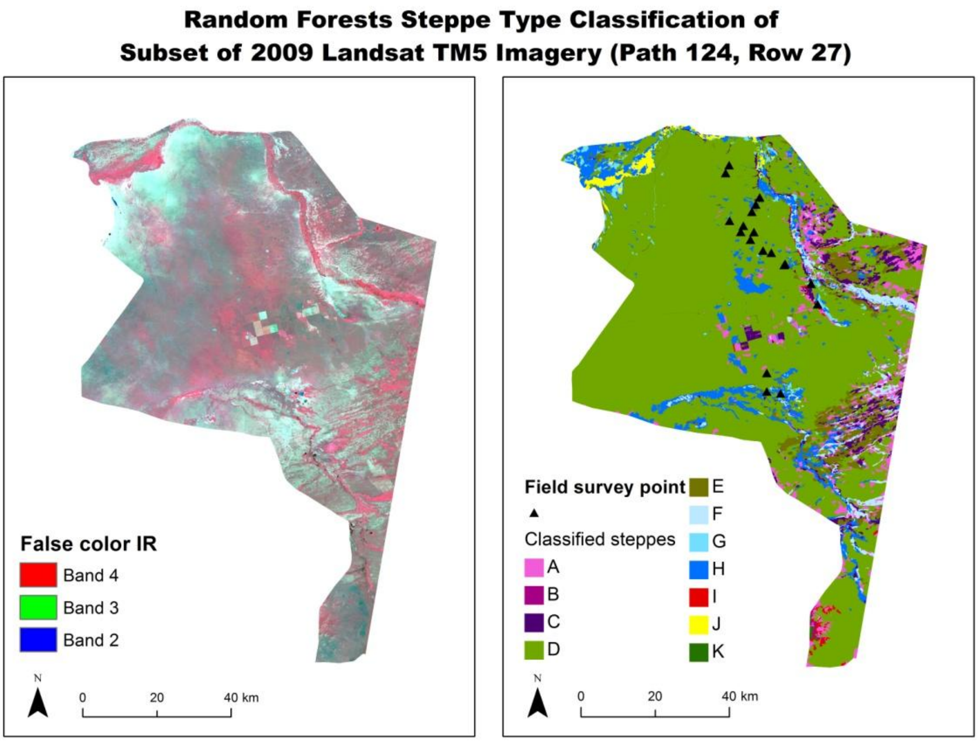

Figure 5. Steppe type classification map of Mongolia image subset (path 124, row 27)

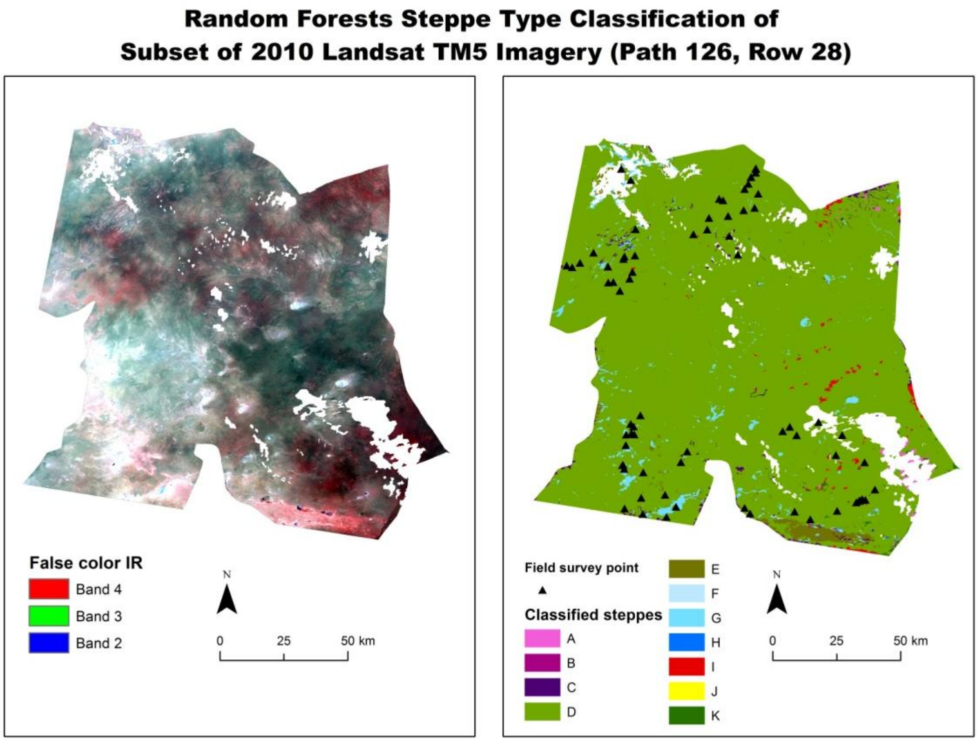

Figure 6. Steppe type classification map of Mongolia image subset (path 126, row 28)

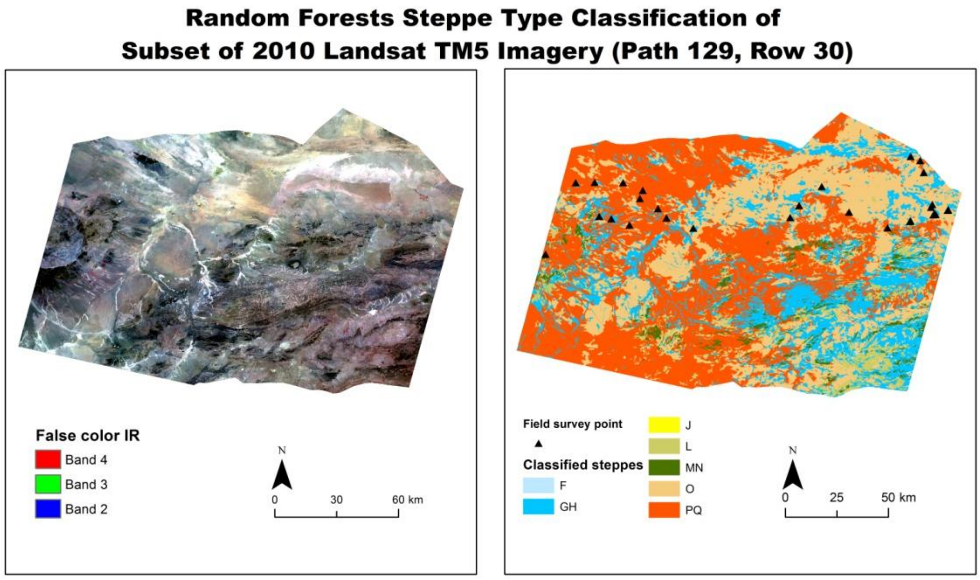

Figure 7. Steppe type classification map of Mongolia image subset (path 129, row 30)

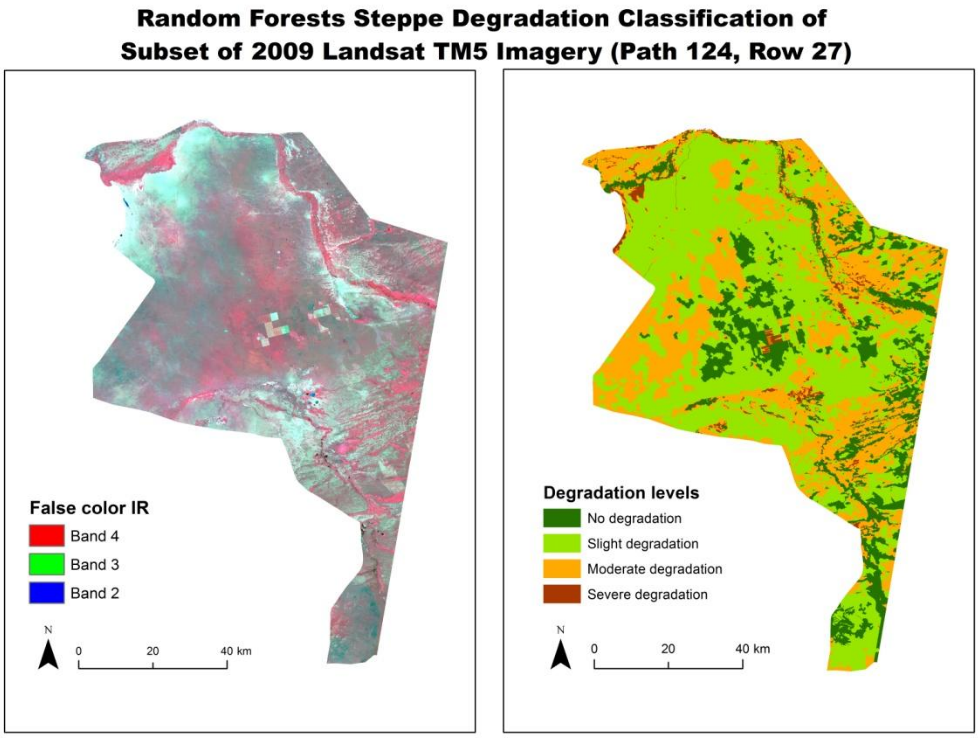

Figure 8. Steppe degradation classification map of Mongolia image subset (path 124, row 27)

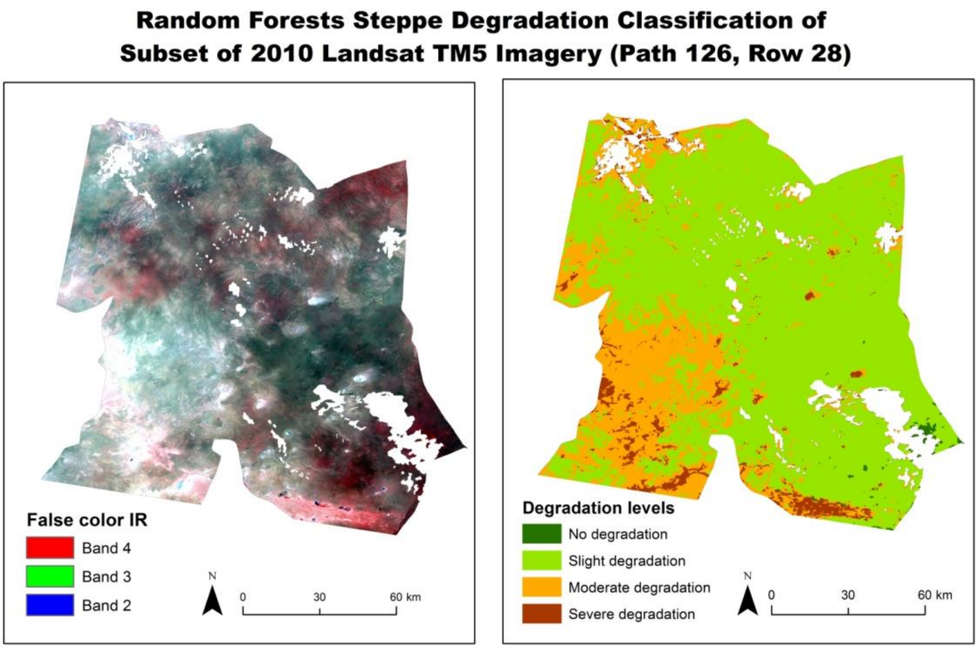

Figure 9. Steppe degradation classification map of Mongolia image subset (path 126, row 28)

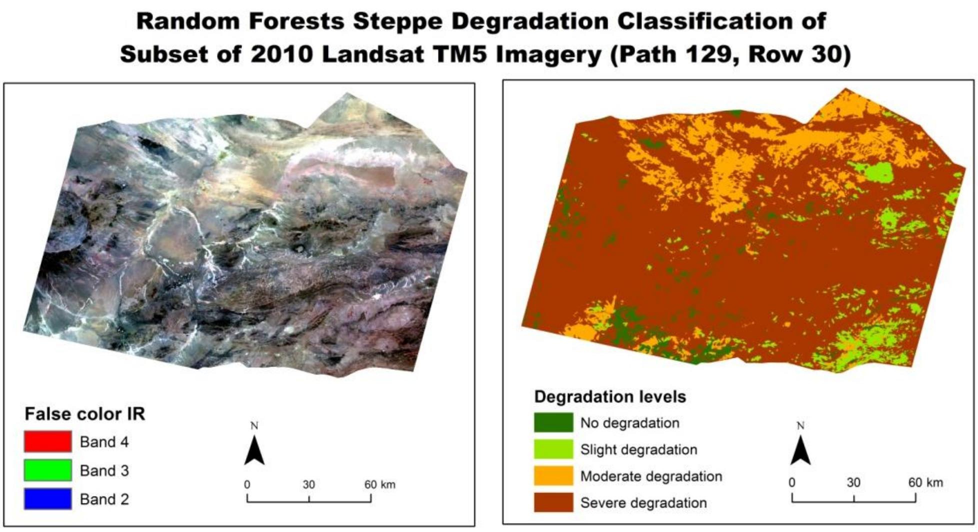

Figure 10. Steppe degradation classification map of Mongolia image subset (path 129, row 30)

5. CONCLUSIONS

Through a series of experiments on sites in Inner Mongolia, we searched for an appropriate way to collect training data for a random forest (RF) model with which to classify Mongolian images. Wefound that patch-based or object-based classification was superior to pixel-based classification in terms of accuracy. By comparing patches created with two "scale" parameter value of segmentation process, we noticed that there was not a big difference in accuracy rates between them, which is probably because, as we increased the size of patches, stronger averaging effects on extreme pixel values and increased heterogeneity within patches exerted influence over the classification these effects mutually offset each other. Byselecting the smaller scale value, i.e. small patch size, we preserved more details while the computational load was still light for the RF. We also found that by using patch-based classification, adding texture features into the list explanatory factors slightly improved classification accuracy, especially for sand land steppe types in this study. The "local prediction," "prediction within eco-region," "prediction across eco-region," and "pooling" experiments demonstrated the importance of the source of the training samples. The similarity between different steppe types and degradation levels made the classifier sensitive to changes in ranges and distributions of values of predictorvariables. Thus error rates got very high when the source areafor thetraining dataset did not intersect with the targetclassification area. It was also found that classes with muchfewer samples werelargely affected by dominant classes and the RF classifier was sensitive to a very skewed class distribution. The "pooling" experiment also showed that with local training samples, although additional external training patches from another area did not further improve the accuracy, neither did they bring much disturbance. The accuracy assessment of classification results for the images in Mongolia was notvery satisfying (overall accuracy was 56% and Kappa was 0.24). Only the Plain/hill typical steppe class showed acceptable accuracy rate (user’s accuracy = 0.73, producer’s accuracy = 0.94). However, we cannot be very confident that the validation data in this region is very reliable. So, the actual accuracy could be better, but could also be even worse. Unfortunately, with no available and suitable data, we cannot further evaluate our classification results. The research questions of this study arose from lacking of Mongolia data which, however, still limited the work.

For all the classification results of our experiments, there were at least four sources of errors that likely affected the performance of the classifier: the source data, the segmentation process, the model variables, and the validation data of Mongolia. Firstly, the source reference data, i.e. the 2009 vegetation and degradation map of IMAR sites, were created by manually digitizing based on Landsat TM5 images. Since we tried to minimize time difference between IMAR and Mongolia images and to have less cloud cover, our remote sensing images of IMAR were from 2010 and 2011 instead of 2009. There were also differences in dates; although images were all from growing season. The climate and phenology of grass at these different times could make images less comparable to each other or to the reference maps. This might be one reason why an area that looked homogenous in the image was classified into two steppe types in the reference map. Secondly, it is possible that, based on all the data we have, we may not be able to fully meet the requirement of the target vegetation and degradation classification systems. Though the reference maps were created based on Landsat TM5 imagery, the interpreters also had better understanding of the study area, historical data for reference, and a lot of ground truth points. The spectral resolution of the Landsat TM5 imagery may not be fine enough for derived features to be able to distinguish well among different types. Also the degradation level is a concept of a relative amount. Steppes were compared with nearby conserved grassland so the standard is not set but varies from place to place. With no such information for Mongolia sites, it is very hard for us to do both classification and validation of the degradation level.

Patch-based classification proved to be more accurate than pixel-based in our study, but the segmentation of patches could also bring errors. Although we did trials to find the best combination of segmentation parameter values, the segmentation algorithm had to ensure homogeneity within patch and boundaries of patches did not perfectly aligned with boundaries of different steppes in the reference map. These mixed patches could increase similarity between classes and affect outcomes.

In the final model, 20 predictor variables (12 spectral features, 4 terrain features and 4 texture features) were included. Even if the RF does not require variable deletion, there were probably better feature combinations and more features could be involved, which may distinguish classes better than current variables and produce better result. In the study, we did not do much about feature selection. According to the variable importance measurement generated during the run (Appendix A), only terrain variables like elevation and slope had big influence on classification accuracy while there were no big differences between the rest of the features in terms of decrease in accuracy or Gini index. Nor did we know what roles these variables would play if we could train the model with Mongolian samples. However, a previous study has shown that feature selection had positive influence on the overall performance in object-based remote sensing image classification by using RF (Stumpf and Kerle, 2011).

Because points in the validation data for Mongolia images, as we have discussed earlier, were labeled according to a species-and-steppe-type match table, they were not as reliable as firsthand ground truth data. All these factors above affected the results of our experiments in this study.

This study was a systematic and comprehensive exploration of the RF classification of steppes of Mongolia Plateau. Though the classification results were not satisfying for the purposes actually carrying accurate classifications of vegetation types in Mongolia that matched those in IMAR, which was our goal, we gained many helpful findings that can guide future work. This study provided a framework of exploring the RF method for prediction which may be helpful for similar studies on different land-cover types. Though our work was limited by availability of data to some degree, the RF method was nonetheless useful in developing accurate classifiers in those situations where we had sufficient data, for example in the local prediction, prediction within eco-region, and pooling experiments. it seems possible that, anIMAR scholar could use RFto update their degradation maps, especially with accurate vegetation map being available as input, which can be more efficient than on-screen digitizing.

Possible further experiments might also improve the effectiveness of the methods demonstrated here.For example,hierarchical classification could be used, by filteringout non-steppe patches and classifying steppes based on the first level of the classification system before classifying the second-level types separately among first-level patches. Additionally, including more features like temperature and precipitation in themodel may improve itsclassification ability. It mightalso be interesting to incorporate multi-temporal images when building the model to deal with time-differences between images and reference data. Lastly, it is important to collect ground truth data from the target area and these data can be used for both training and validation in future research.

References:

Bai, Y., Han, X., Wu, J., Chen, Z., & L. Li, 2004. Ecosystem stability and compensatory effects in the Inner Mongolia grassland. *Nature*, 431(7005),181-184

Bao, X., Jin, Y., Liu, S., Jimuse, G., Wureqimuge, Jigejidesuren, Budebateer, Puchange, W., & L. 2008. Yong. Effects of different grazing on the typical steppe vegetation characteristics on the Mongolian Plateau.*Nomadic Peoples*, 12(2): 53-66.

Beven, K. J., &Kirkby, M. J., 1979. A Physically Based, Variable Contributing Area Model of Basin Hydrology. *Hydrological Sciences Bulletin* 24(1):43 -69

Beyer, H. L. 2004.Hawth's Analysis Tools for ArcGIS.Available at *http://www.spatialecology.com/htools*.

Breiman, L. 1984. Classification and Regression Tree.Chapman& Hall/CRC.

Breiman, L. 2001. Random Forests. *Machine Learning*, 45(1), 5.

Chan, J. C., &Paelinckx, D., 2008.Evaluation of Random Forest and Adaboost Tree-based Ensemble Classification and Spectral Band Selection for Ecotope Mapping Using Airborne HyperspectralImagery. *Remote Sensing of Environment* 112 (6): 2999–3011.doi:10.1016/j.rse.2008.02.011.

Chavez, P.S., 1996. Image-based atmospheric corrections - Revisited and improved, *Photogrammetric Engineering & Remote Sensing*, 62(9): 1025 - 1036.

Congalton, R.G., R.G. Oderwald, and R.A. Mead, 1983. Assessing Landsat classification accuracy using discrete multivariate statistical techniques, *Photogrammetric Engineering & Remote Sensing*, 49(12):1671-1678.

Congalton, R.G., and K. Green, 2009. *Assessing the Accuracy of Remotely Sensed Data: Principles and Practices*, Second edition, CRC Press, Boca Raton, Florida, 208p.

Cortes, C. & V. Vapnik, 1995. "Support-vector networks." *Machine Learning* 20(3): 273-297.

Crist, E. P. and Cicone, R. C., 1984, A physically-based transformation of Thematic Mapper data -- the TM Tasseled Cap, *IEEE Trans. on Geosciences and Remote Sensing*, GE-22: 256-263.

Duro, D.C., Franklin, S.E., & M.G. Dubé, 2012. A comparison of pixel-based and object-based image analysis with selected machine learning algorithms for the classification of agricultural landscapes using SPOT-5 HRG imagery. *Remote Sensing of Environment*, 118(15): 259-272.

Franklin, S. E., and Peddle, D. R., 1990, Classification of SPOT HRV imagery and texture features. *International Journal of Remote Sensing*, 11: 551–556.

Gislason, P.O., Benediktsson, J.A., & J.R. Sveinsson., 2006. Random Forests for land cover classification. *Pattern Recognition Letters*, 27(4): 294-300.

Guan, H., Li, J., Campman, M., Deng, F., Ji, Z., & X. Yang., 2013. Integration of orthoimagery and lidar data for object-based urban thematic mapping using random forests. *International Journal of Remote Sensing*, 34(14):5166-5186.

Han, X., Owens, K., Wu, X. B., Wu, J., and Huang, J., 2009. The Grasslands of Inner Mongolia: A Special Feature. *Rangeland Ecology & Management*, 62(4): 303-304. doi: 10.2307/25549328

Immitzer, M., Atzberger, C., & T. Koukal, 2012.Tree species classification wit Random Forest using very high spatial resolution 8-band WorldView-2 satellite data. *Remote Sensing* 4(9):2661-2693.

Jackson, R. D., &Huete, A. R., 1991. Interpreting vegetation indices. *Preventive Veterinary Medicine*, 11(3–4), 185-200.doi: http://dx.doi.org/10.1016/S0167-5877(05)80004-2

Jenson, S. K., and J. O. Domingue. 1988. Extracting Topographic Structure from Digital Elevation Data for Geographic Information System Analysis. *Photogrammetric Engineering and Remote Sensing* 54 (11): 1593–1600.

Kang, L., Han, X., Zhang, Z., and Sun, O. J., 2007. Grassland ecosystems in China: review of current knowledge and research advancement. Philosophical transactions of the Royal Society of London.Series B, *Biological sciences*, 362(1482), 997.

Karl, J. W., & Maurer, B. A., 2010. Multivariate correlations between imagery and field measurements across scales: comparing pixel aggregation and image segmentation. *Landscape Ecology*, 25(4): 591.

Kogan, F., Stark, R., Gitelson, A., Jargalsaikhan, L., Dugrajav, C., and Tsooj, S., 2004. Derivation of pasture biomass in Mongolia from AVHRR-based vegetation health indices.*International Journal of Remote Sensing*, 25(14), 2889-2896.

Li, S., Verburg, P., Lv, S., Wu, J., and Li, X., 2012. Spatial analysis of the driving factors of grassland degradation under conditions of climate change and intensive use in Inner Mongolia, China. *Regional Environmental Change*, 12(3), 461-474.doi: 10.1007/s10113-011-0264-3

Liang, Y., Han, G., Zhou, H., Zhao, M., Snyman, H.A., Shan, D., &Havstad K.M. 2009.*Rangeland Ecology & Management*, 62(4):328-336.

Liaw, A., & Wiener, M., 2002.Classification and regression by randomForest.*R news*, 2(3), 18-22.

Lin, Y., Han, G., Zhao, M.& S.X. Chang. 2010. Spatial vegetation patterns as early signs of desertification: a case study of a desert steppe in Inner Mongolia, China. *Landscape Ecology*, 25(1): 1519-1527.

Lu, D., Batistella, M., & Moran, E., 2007.Land-cover classification in the Brazilian Amazon with the integration of Landsat ETM+ and Radarsatdata.*International Journal of Remote Sensing*, 28(24), 5447.

MOA (Ministry of Agriculture of the People's Republic of China)., 2003. *Parameters for Degradation, Desertification and Salinization of Rangelands*. By Su, D., Zhang, Z., Chen, Z. and X. Hu. GB19377-2003. Beijing: General Administration of Quality Supervision, Inspection and Quarantine of the People's Republic of China.

Mas, J.F. and Flores, J.J., 2008.The application of artificial neural networks to the analysis of remotely sensed data. *International Journal of Remote Sensing* 29(3):617-663

Pal, M., 2005. Random forest classifier for remote sensing classification. *International Journal of Remote Sensing*, 26(1), 217-222.doi: 10.1080/01431160412331269698

Pei, S., Fu, H., & C. Wan. 2008. Changes in soil properties and vegetation following enclosure and grazing in degraded Alxa desert steppe of Inner Mongolia, China. *Agriculture, Ecosystems & Environment*, 124 (1-2):33-39.

Prasad, A.M., Iverson, L.R., & A. Liaw, 2006. Newer classification and regression tree techniques: bagging and random forests for ecological prediction. *Ecosystems* 9(2), 191-199.

Retzer, V., Madrowski, K., & G. Miehe. 2006. Variation of precipitation and its effect on phytomass production and consumption by livestock and large wild herbivores along an altitudinal gradient during a drought, South Gobi, Mongolia. *Journal of Arid Environments*, 66(1):135-150.

Richardson, A., and J. Everitt, 1992. Using spectral vegetation indices to estimate rangeland productivity, *Geocarto International*, 1:63-77.

Rodriguez-Galiano, V. F., Chica-Olmo, M., Abarca-Hernandez, F., Atkinson, P. M., &Jeganathan, C., 2012.Random Forest classification of Mediterranean land cover using multi-seasonal imagery and multi-seasonal texture.*Remote Sensing of Environment*, 121(0), 93-107.

Rodriguez-Galiano, V.F, Ghimire, B., Rogan, J., Chica-Olmo, M., & J.P. Rigol-Sanchez. 2012. An assessment of the effectiveness of a Random Forest classifier for land-cover classification. *ISPRS Journal of Photogrammetry and Remote Sensing* 67: 93–104.

Sha, Z., Bai, Y., Xie, Y., Yu, M. & L. Zhang. 2008. Using a hybrid fuzzy classifier (HFC) to map typical grassland vegetation in Xilin river Basin, Inner Mongolia, China. International Journal of Remote Sensing, 29 (8): 2317-2337.

Shaban, M. A., andDikshit, O., 2001. Improvement of classification in urban areas by the use of textural features: The case study of Lucknow city, Uttar Pradesh. *International Journal of Remote Sensing*, 22(4), 565.

Stumpf, A., &Kerle, N., 2011. Object-oriented mapping of landslides using Random Forests.*Remote Sensing of Environment*, 115(10), 2564-2577.

Tong, C., Wu, J., Yong, S., Yang, J., & W. Yong. 2004. A landscape-scale assessment of steppe degradation in the Xilin River Basin, Inner Mongolia, China. *Journal of Arid Environments*, 59(1): 133-149.

Tou, J.T., and R.C. Gonzalez, *Pattern Recognition Principles*, Addison-Wesley, London, 1974.

Xie, Y. and Sha, Z., 2012. Quantitative analysis of driving factors of grassland degradation: a case study in Xilin River Basin, Inner Mongolia. *TheScientificWorldJournal* 2012: 169724.

Jiang, Y., Bi, X., Huang, J., & Y. Bai. 2010. Patterns and drivers of vegetation degradation in Xilin River Basin, Inner Mongolia, China. Chinese Journal of Plant Ecology, 34(10):1132-1141.

Yu, F., Price, K. P., Ellis, J., and Shi, P., 2003.Response of seasonal vegetation development to climatic variations in eastern central Asia.*Remote Sensing of Environment*, 87(1), 42-54.

Appendix A

Variable Importance Measurement Plot

Table 5.a

Error matrix of patch-based steppe vegetation classification (Evenk Autonomous Region)

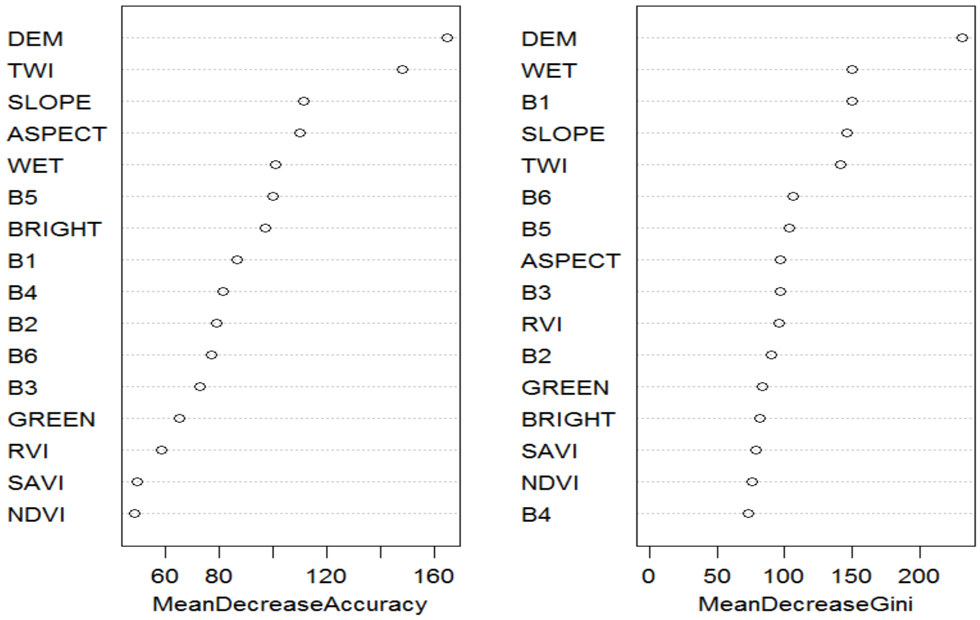

Table 5.b

Error matrix of pixel-based steppe vegetation classification (Evenk Autonomous Region)

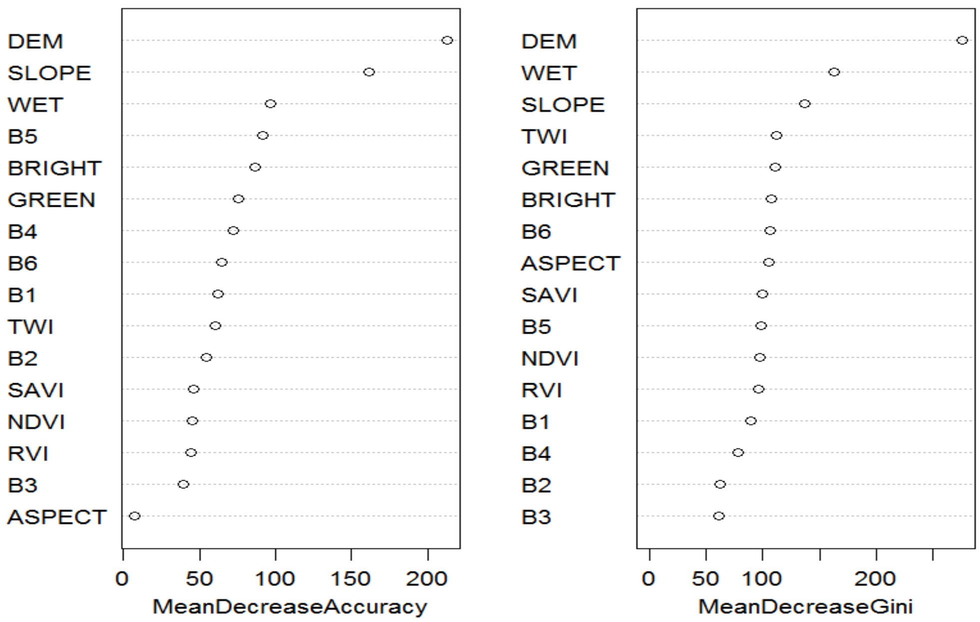

Table 5.c

Error matrix of pixel-based steppe vegetation classification from reduced dataset of pixel samples (Evenk Autonomous Region)

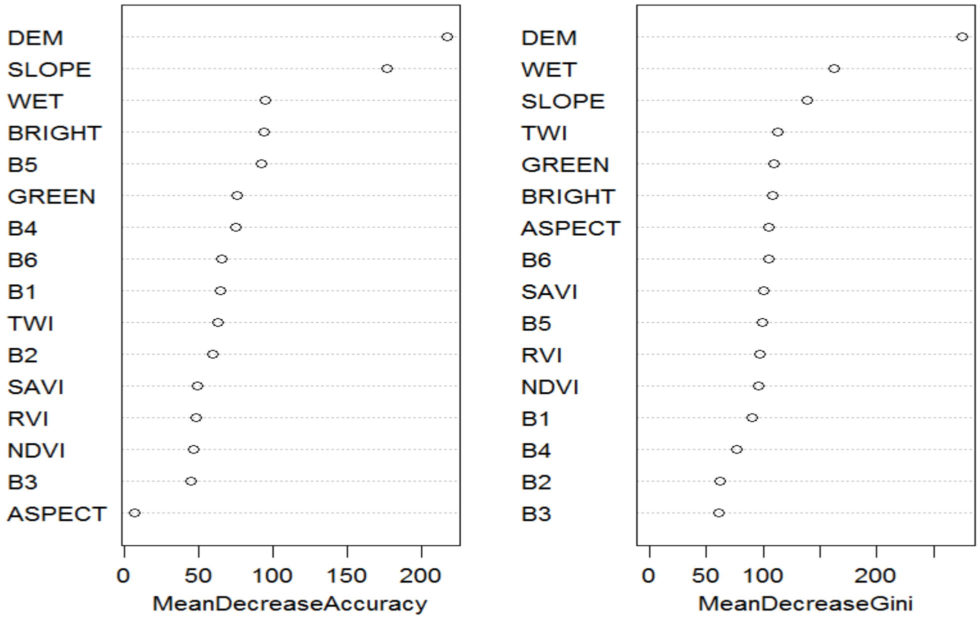

Table 6.a

Error matrix of patch-based steppe vegetation classification (Xilinhot City)

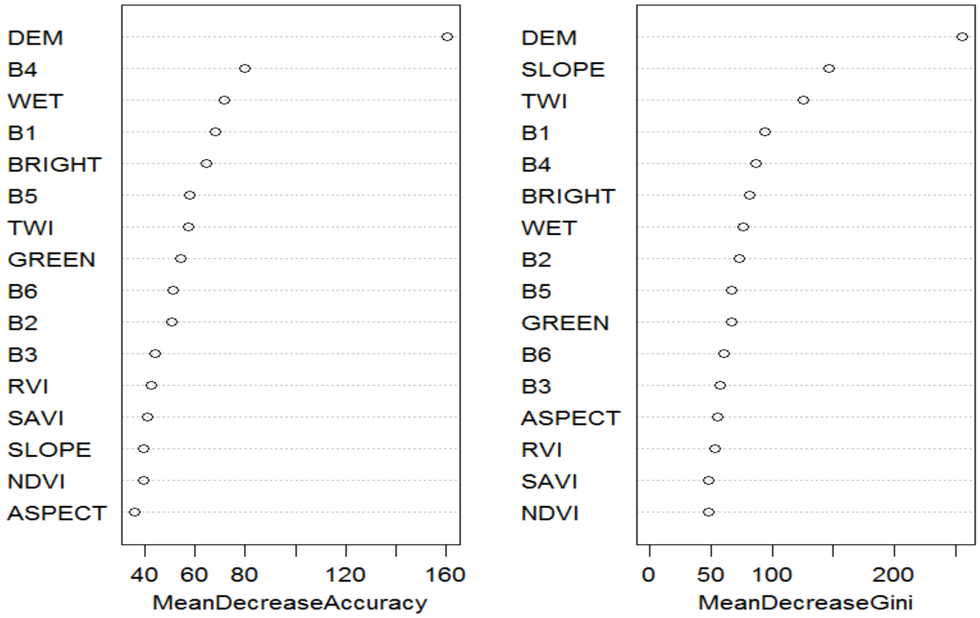

Table 6.b

Error matrix of pixel-based steppe vegetation classification (Xilinhot City)

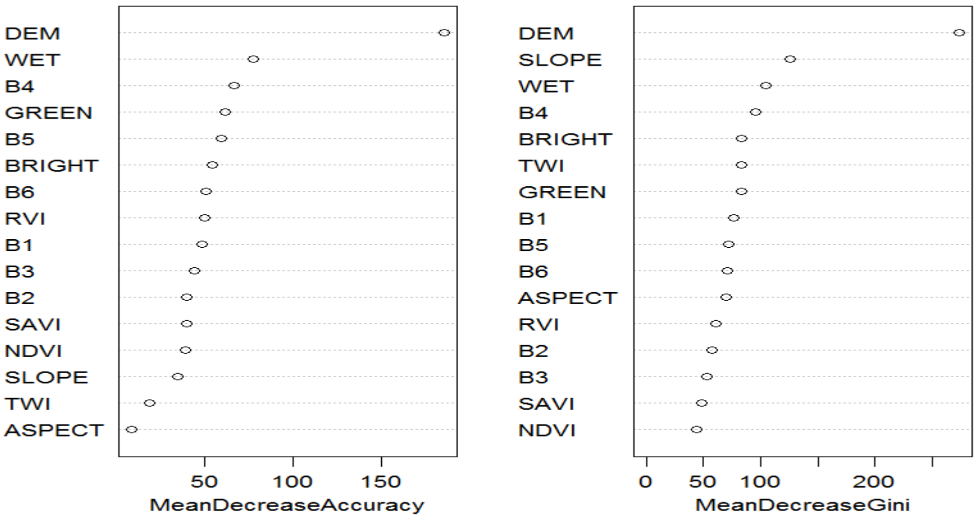

Table 6.c
Error matrix of pixel-based steppe vegetation classification from reduced dataset of pixel samples(Xilinhot City)

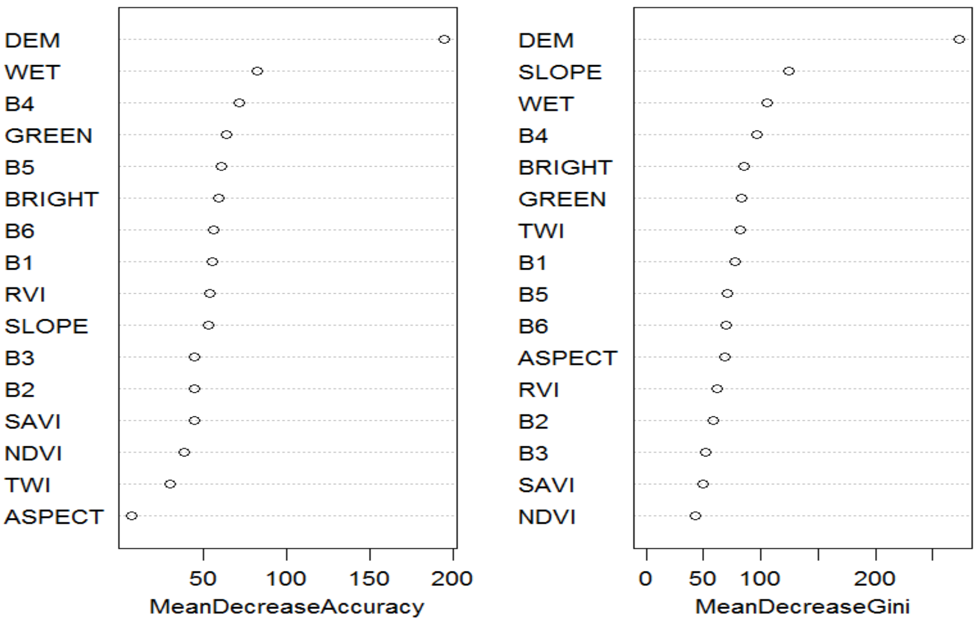

Table 7.a
Error matrix of patch-based steppe vegetation classification (Uraq Middle Banner)

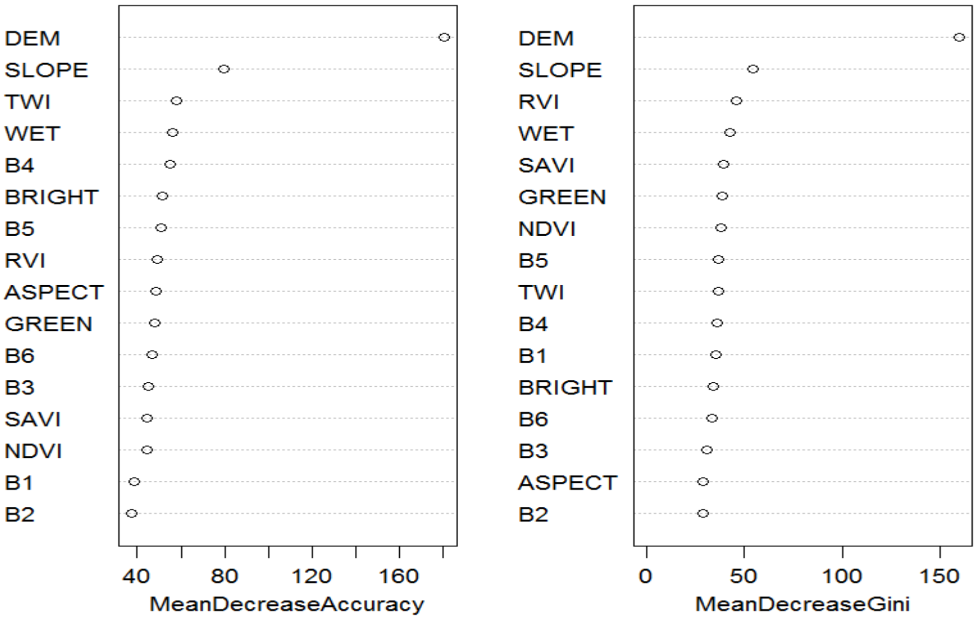

Table 7.b

Error matrix of pixel-based steppe vegetation classification (Urat Middle Banner)

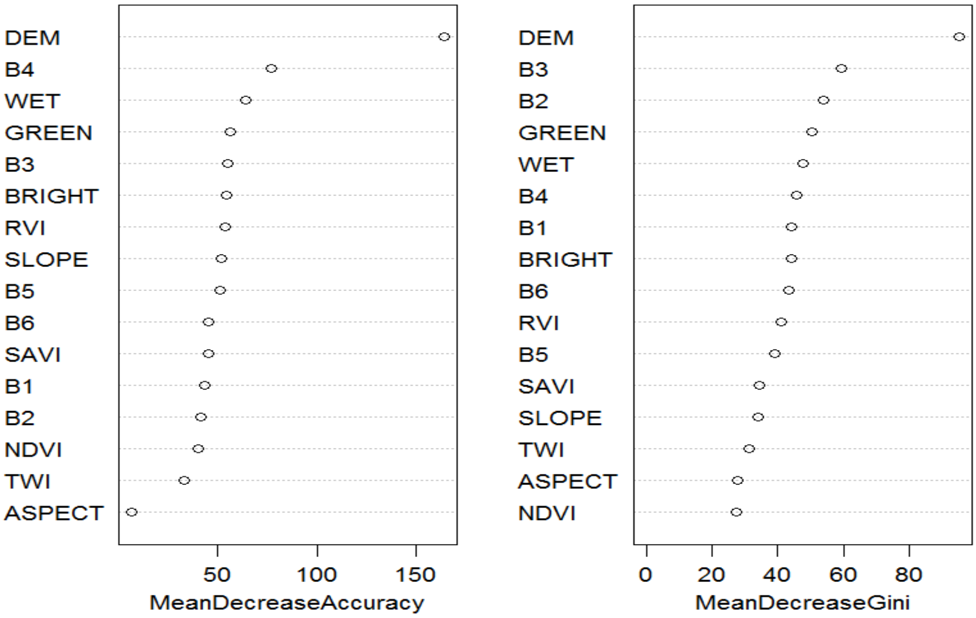

Table 8.a

Error matrix of patch-based steppe degradation classification (Evenk Autonomous Region)

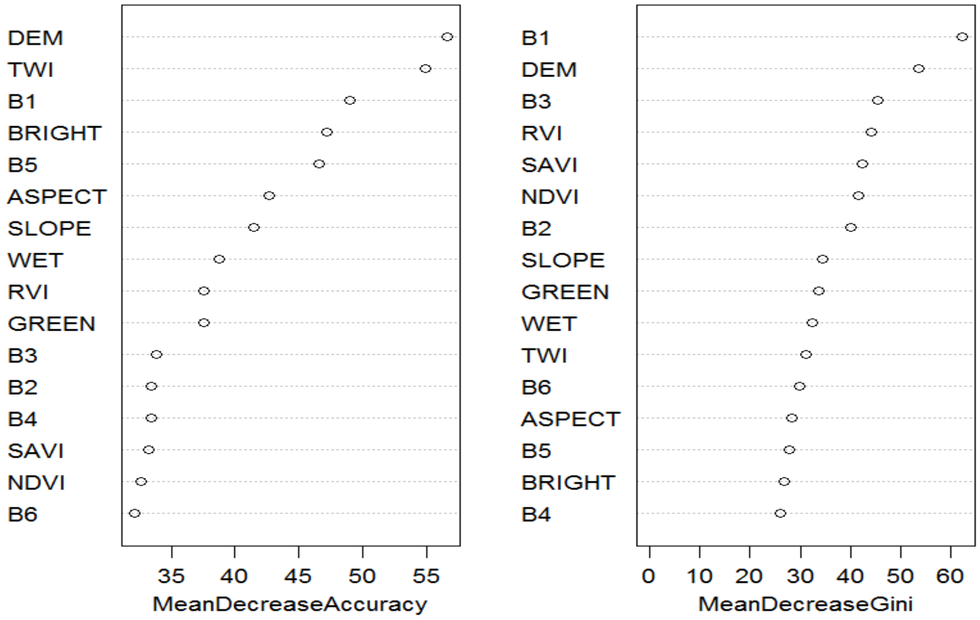

Table 8.b

Error matrix of pixel-based steppe degradation classification (Evenk Autonomous Region)

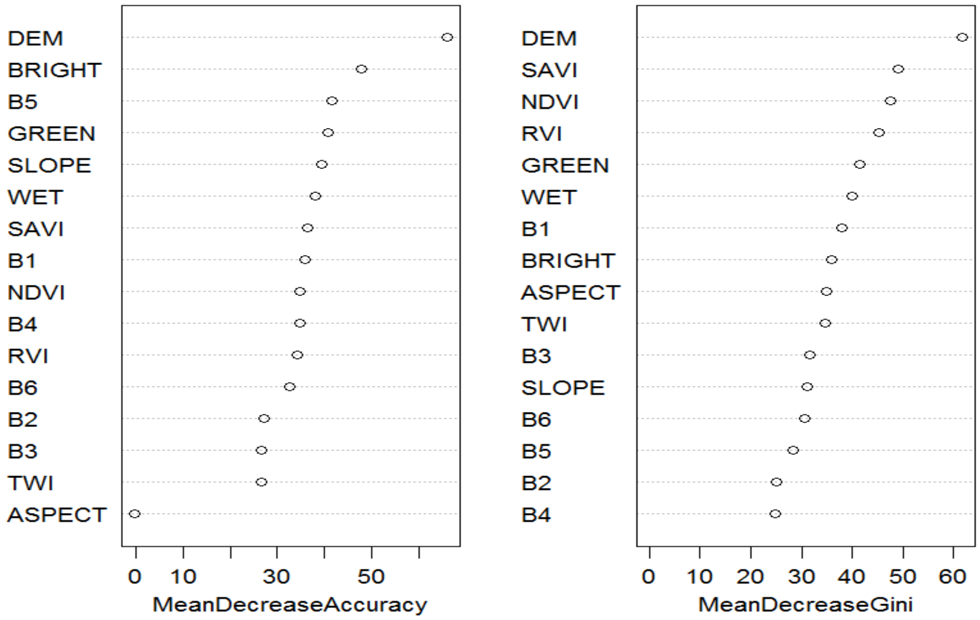

Table 8.c

Error matrix of pixel-based steppe degradation classification from reduced dataset of pixel samples (Evenk Autonomous Region)

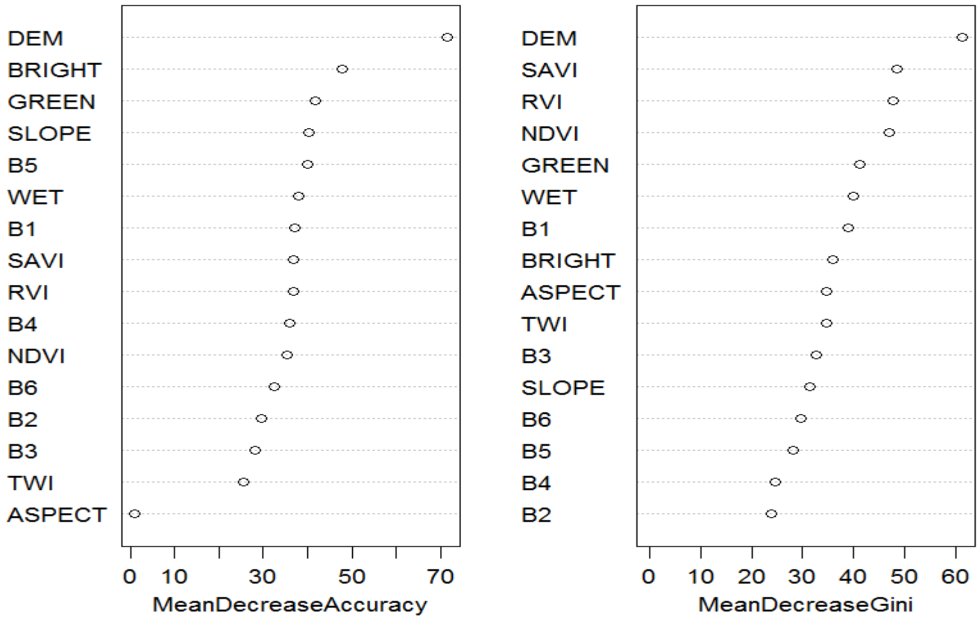

Table 9.a
Error matrix of patch-based steppe degradation classification (Xilinhot City)

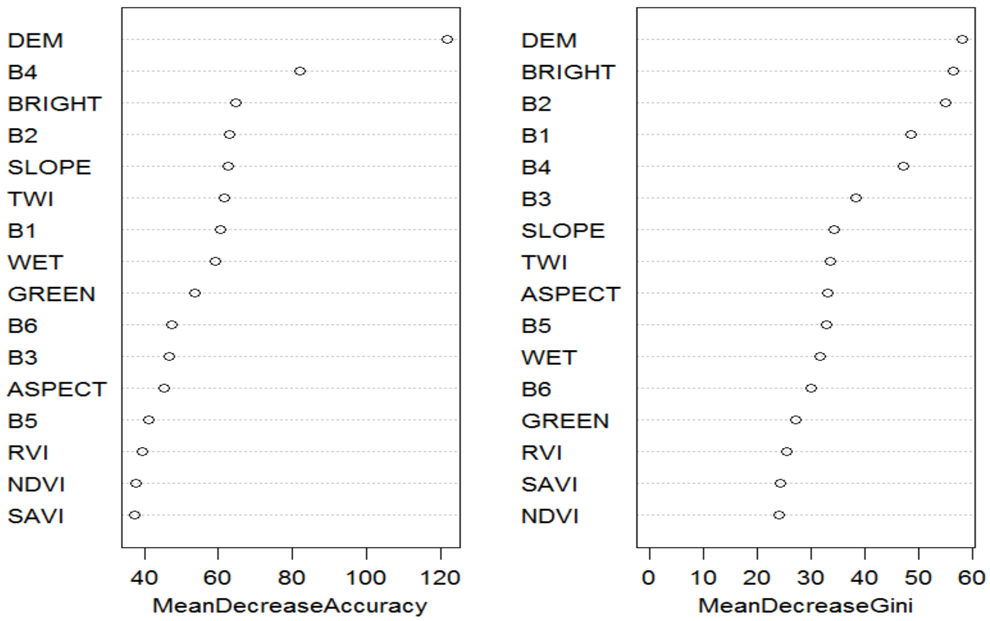

Table 9.b
Error matrix of pixel-based steppe degradation classification (Xilinhot City)

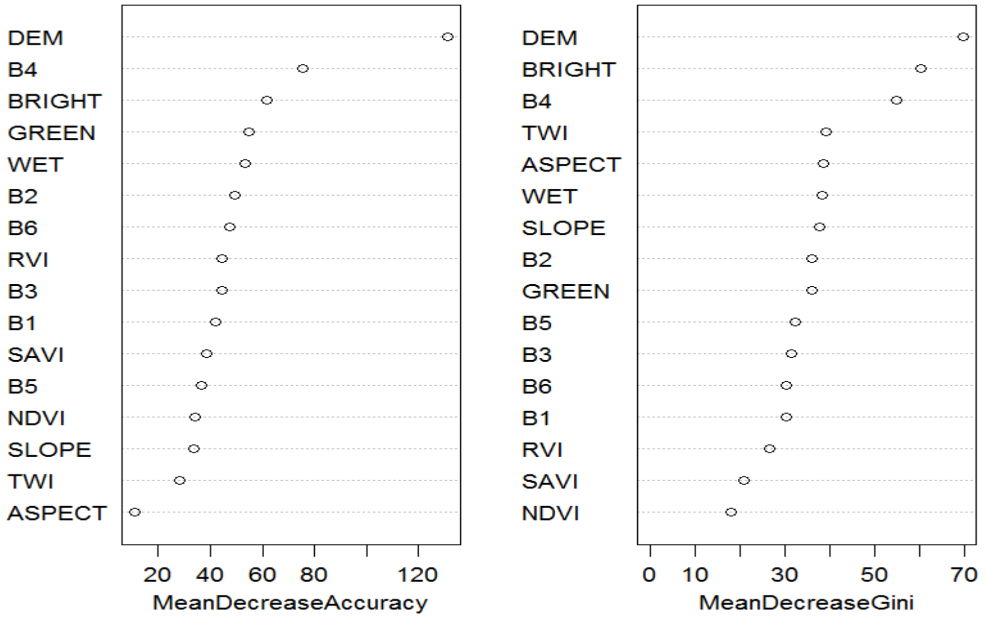

Table 9.c

Error matrix of pixel-based steppe degradation classification from reduced dataset of pixel samples (Xilinhot City)

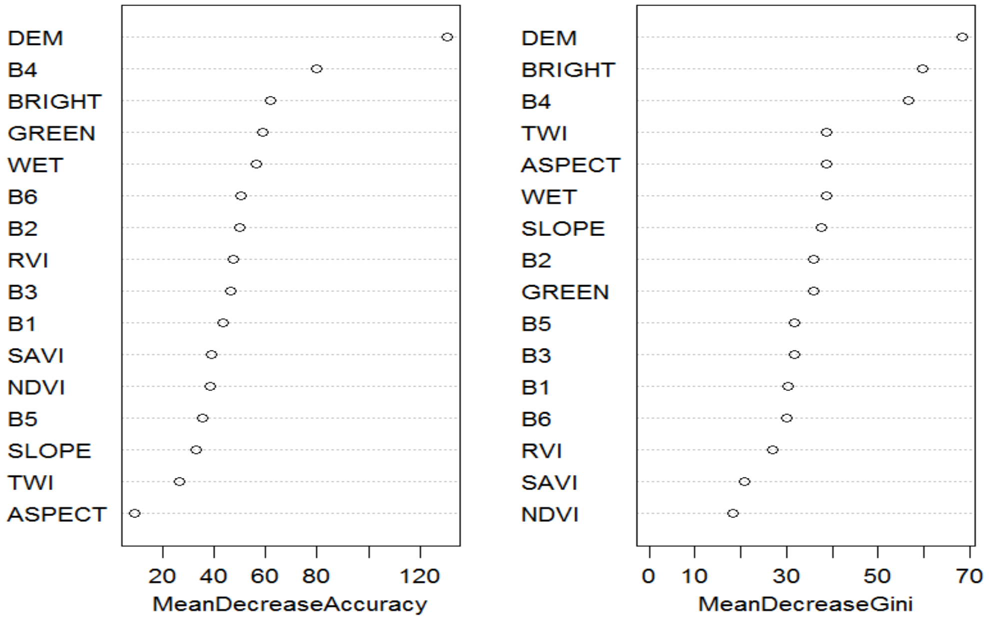

Table 10.a

Error matrix of patch-based steppe degradation classification (Urat Middle Banner)

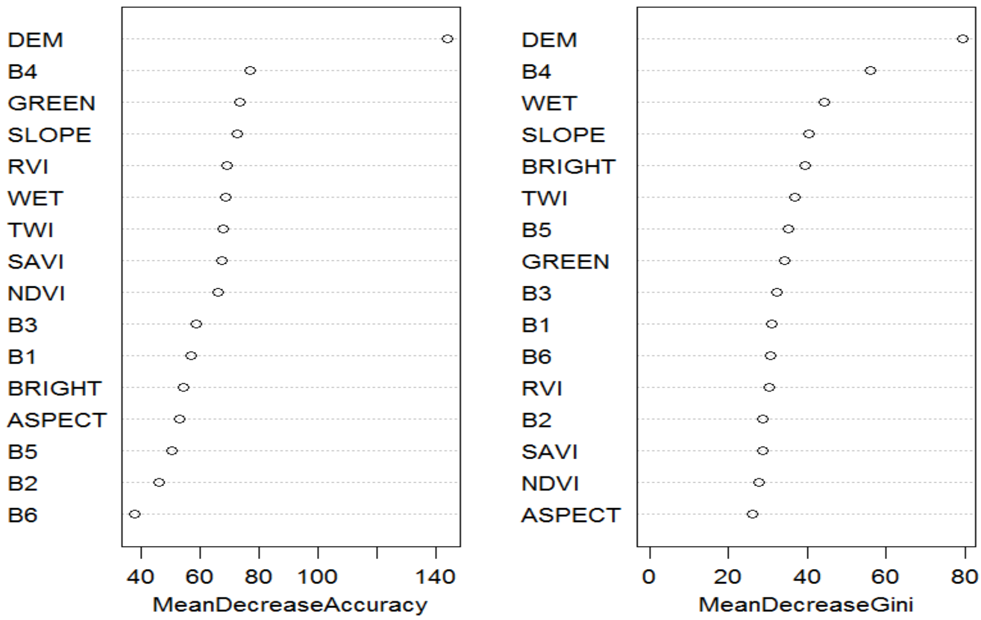

Table 10.b
Error matrix of pixel-based steppe degradation classification (Urat Middle Banner)

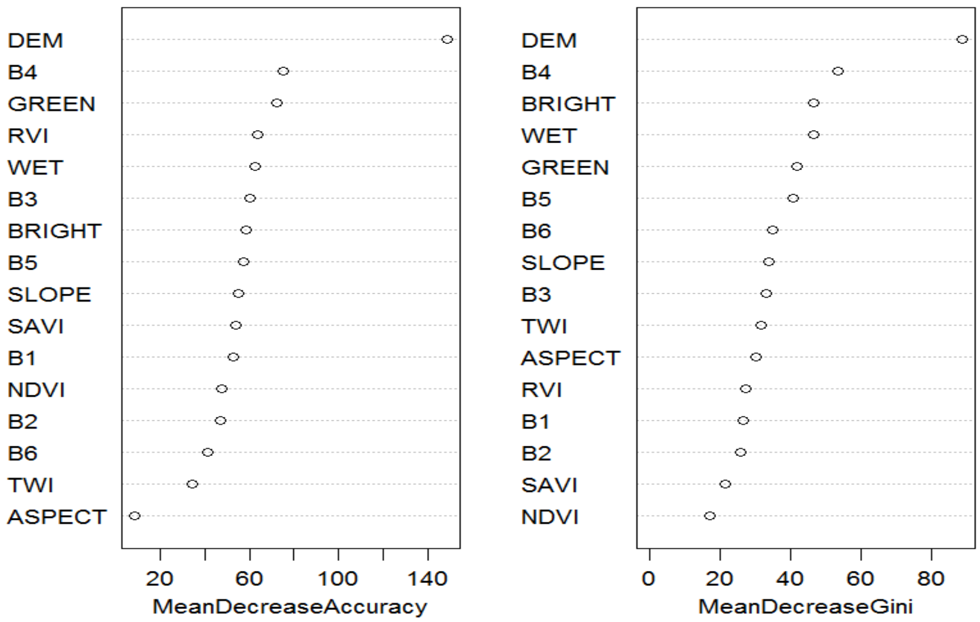

Table 10.c
Error matrix of pixel-based steppe degradation classification from reduced dataset of pixel samples (Urat Middle Banner)

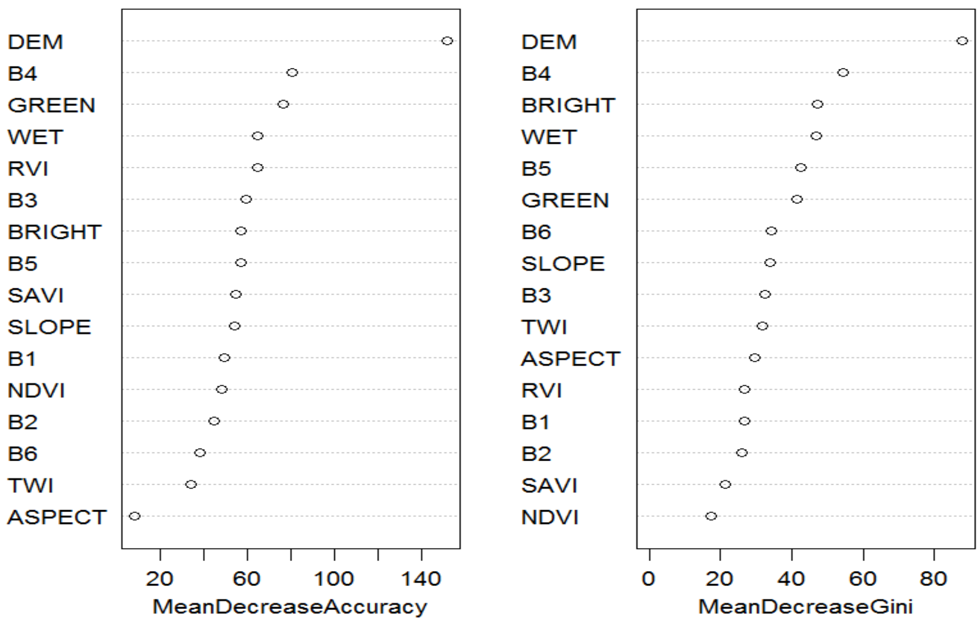

Table 11.a

Error matrix of patch-based steppe classification with texture features (Evenk Autonomous)

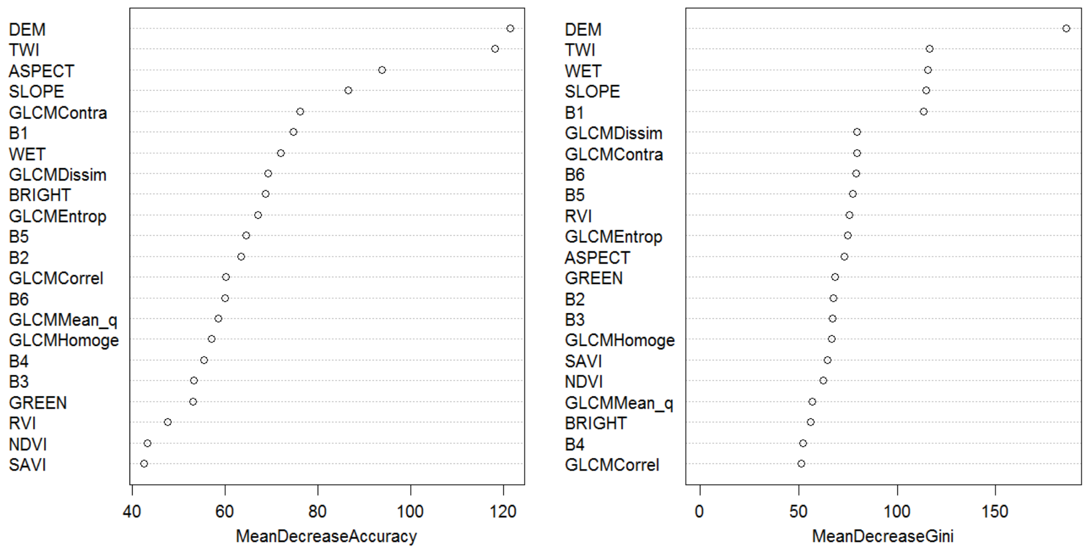

Table 11.b

Error matrix of patch-based steppe vegetation classification with texture features (Xilinhot City)

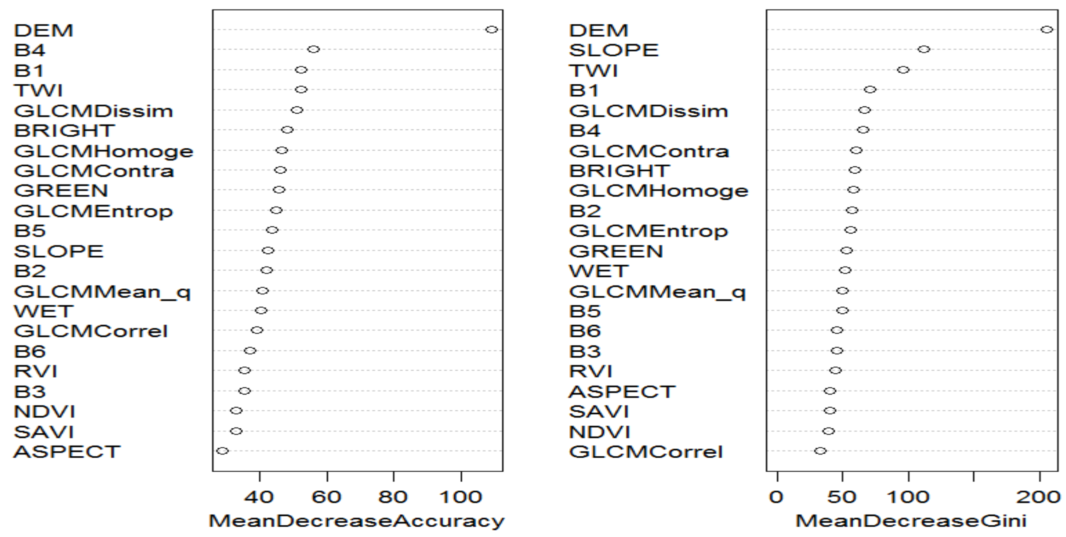

Table 11.c

Error matrix of patch-based steppe vegetation classification with texture features (Uraq Middle Banner)

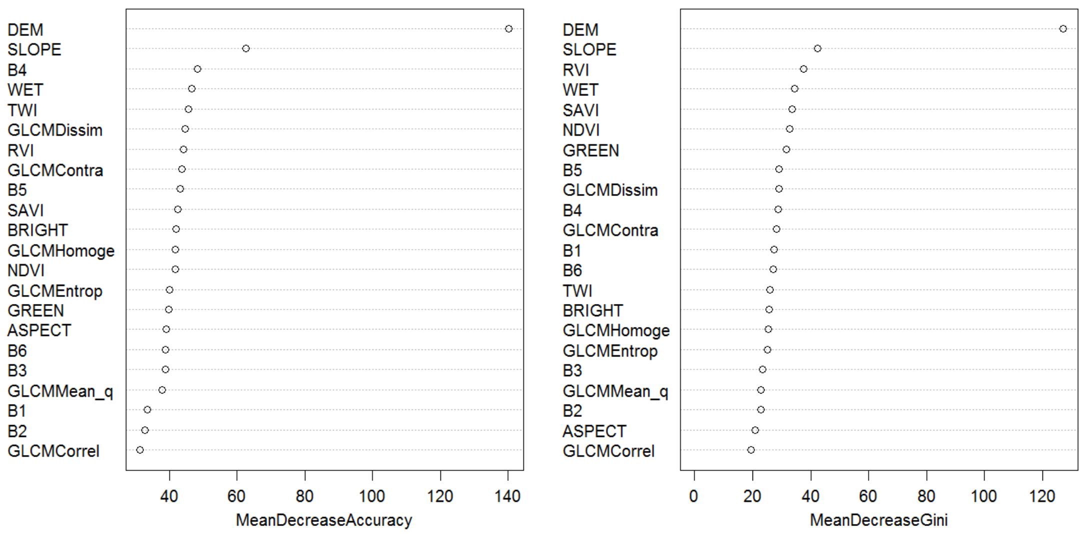

Table 12.a

Error matrix of patch-based steppe degradation classification with texture features (Evenk Autonomous)

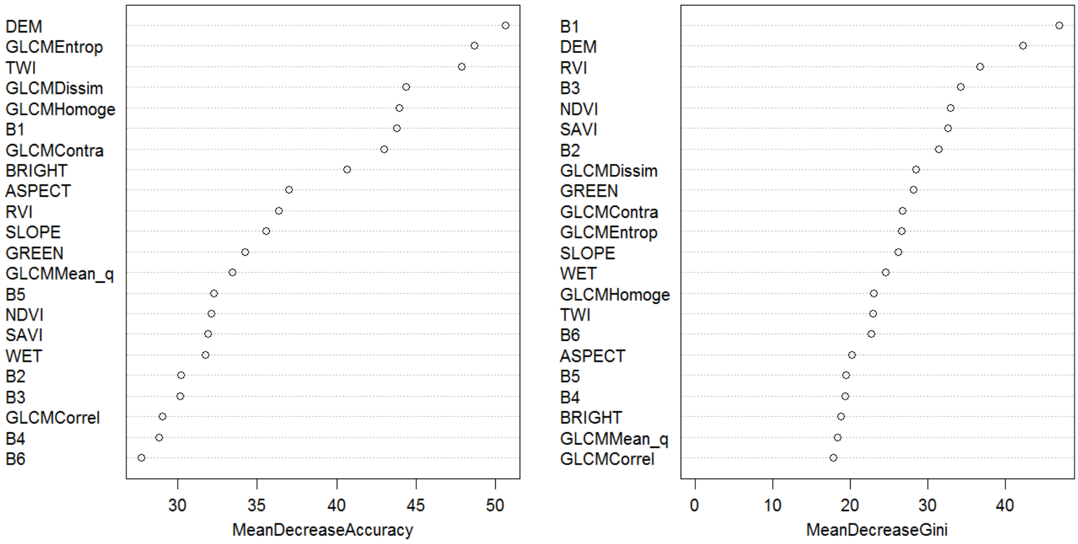

Table 12.b

Error matrix of patch-based steppe degradation classificationwith texture features (XilinhotCity)

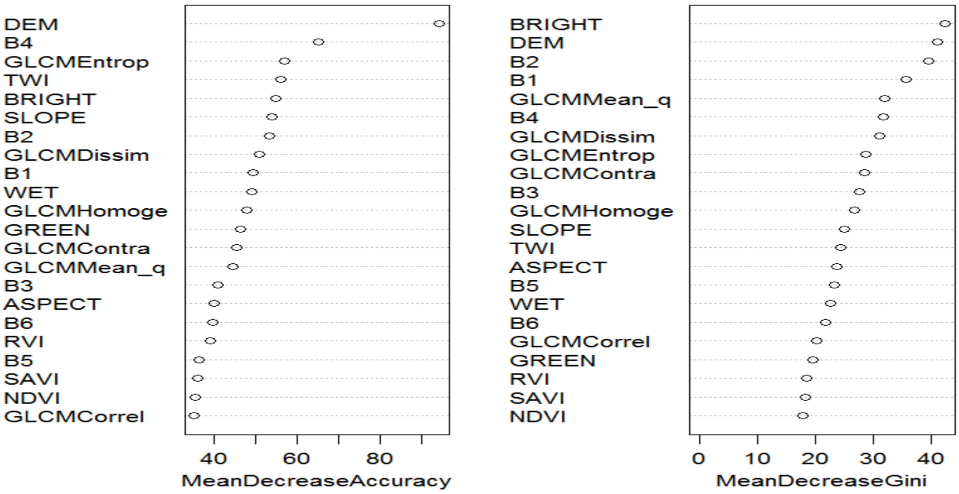

Table 12.c

Error matrix of patch-based steppe degradation classification with texture features (Urat Middle Banner)

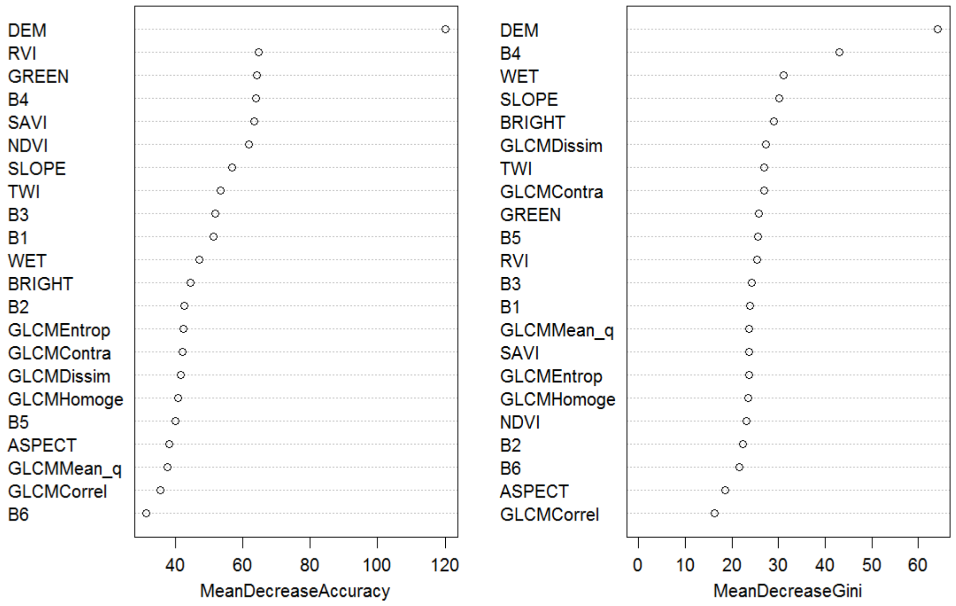

Table 13.a

Error matrix of patch-based steppe vegetation classification at scale of 40 (Evenk Autonomous)

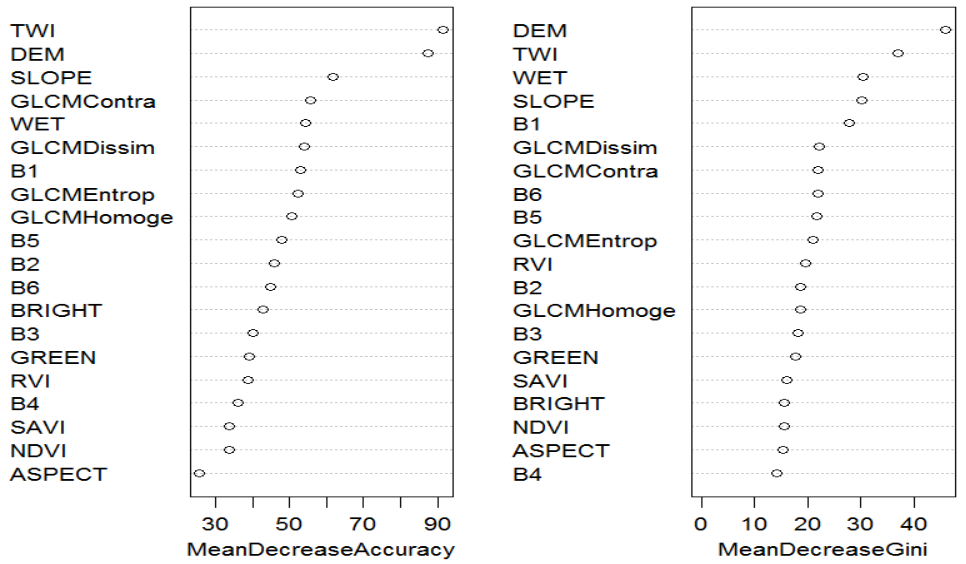

Table 13.b

Error matrix of pixel-based steppe degradation classification at scale of 40 (Evenk Autonomous)

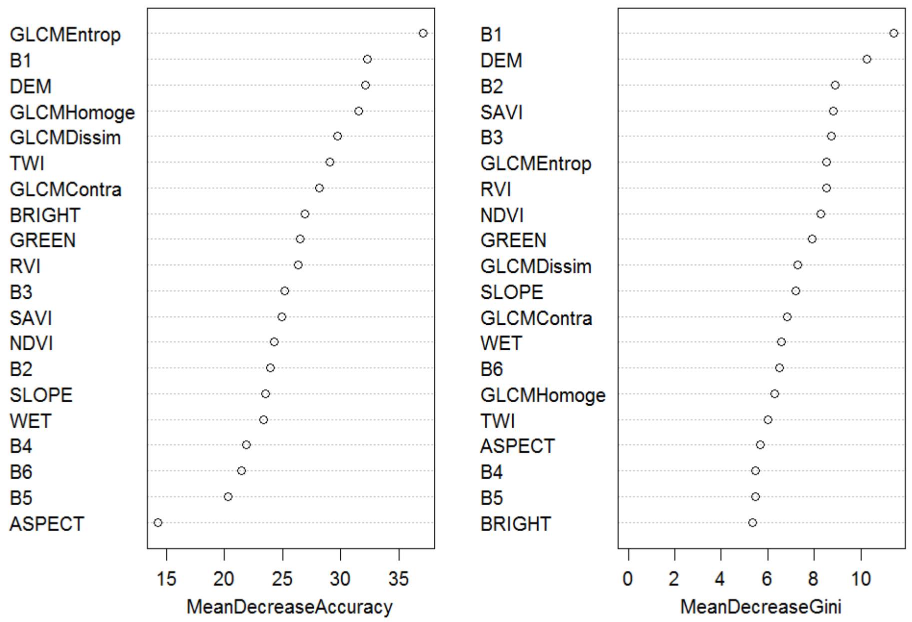

Table 14.a

Error matrix of patch-based steppe vegetation classification at scale of 40 (Xilinhot City)

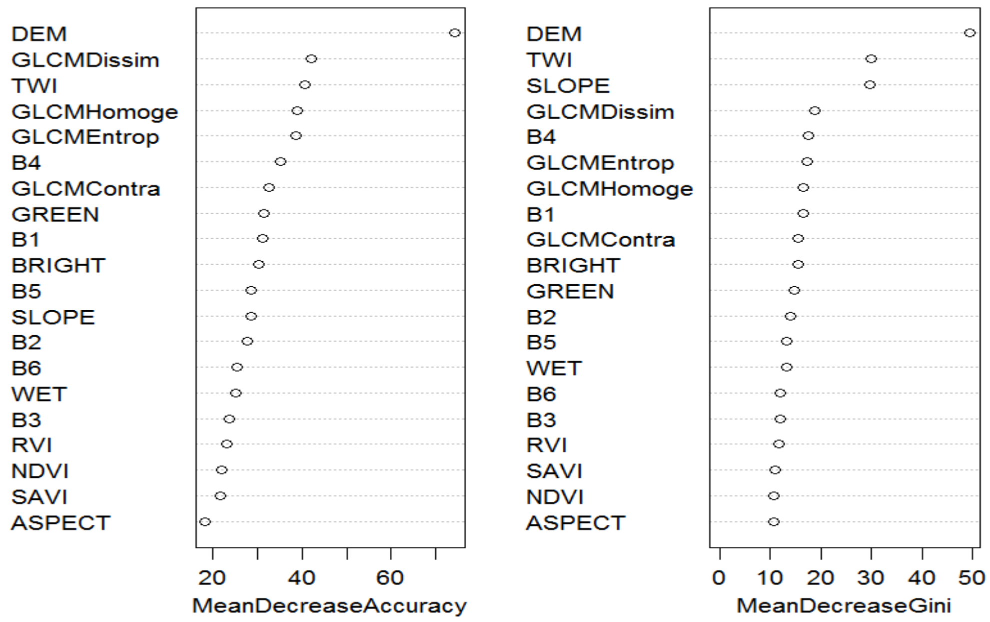

Table 14.b

Error matrix of patch-based steppe degradation classification at scale of 40 (Xilinhot City)

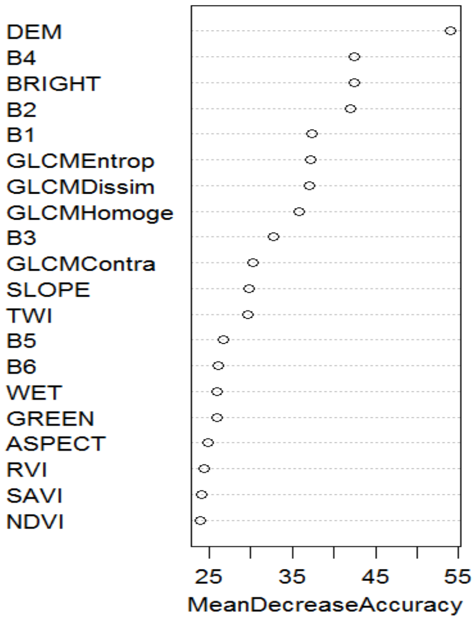

Table 15.a

Error matrix of patch-based steppe vegetation classification at scale of 40(Uraq Middle Banner)

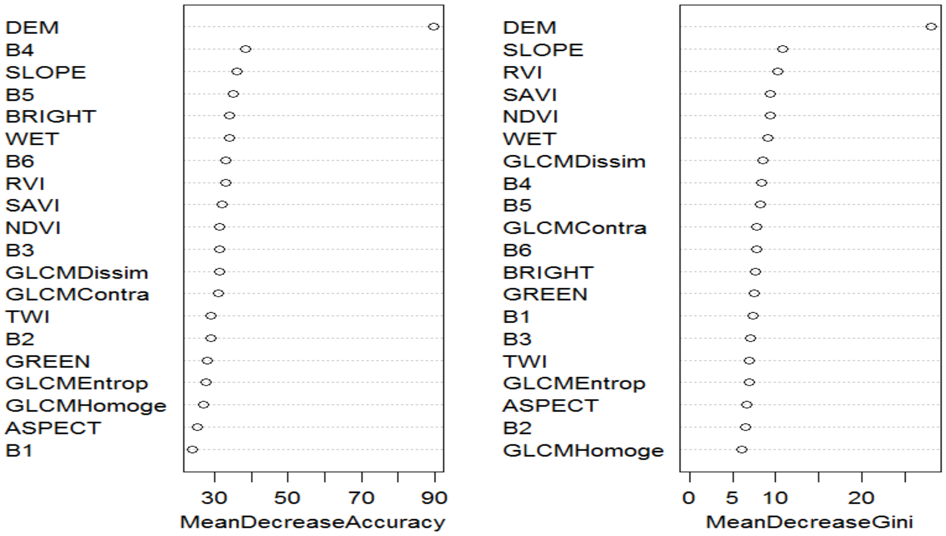

Table 15.b

Error matrix of patch-based steppe degradation classification at scale 40(Urat Middle Banner)

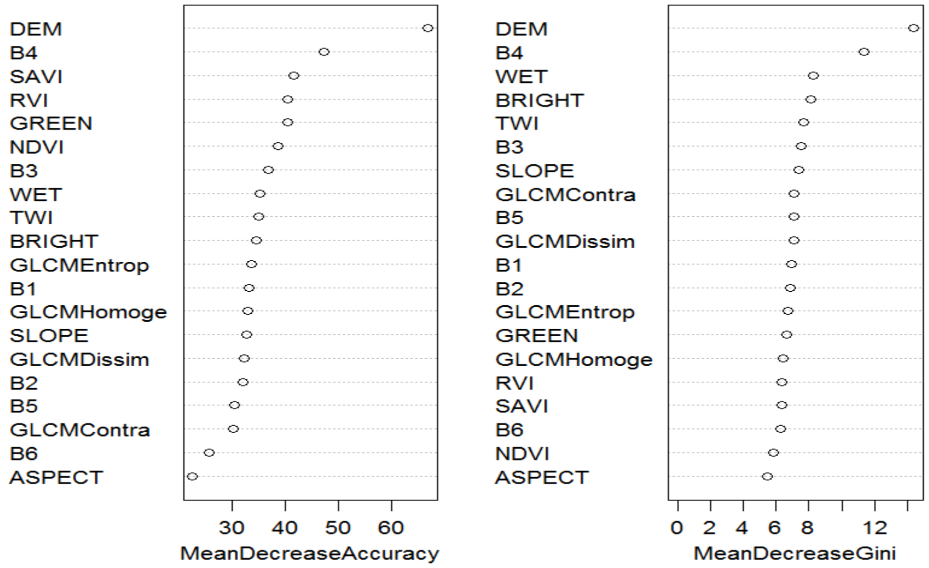

Table 16.a
Error matrix of local prediction of steppe types (Evenk Autonomous)

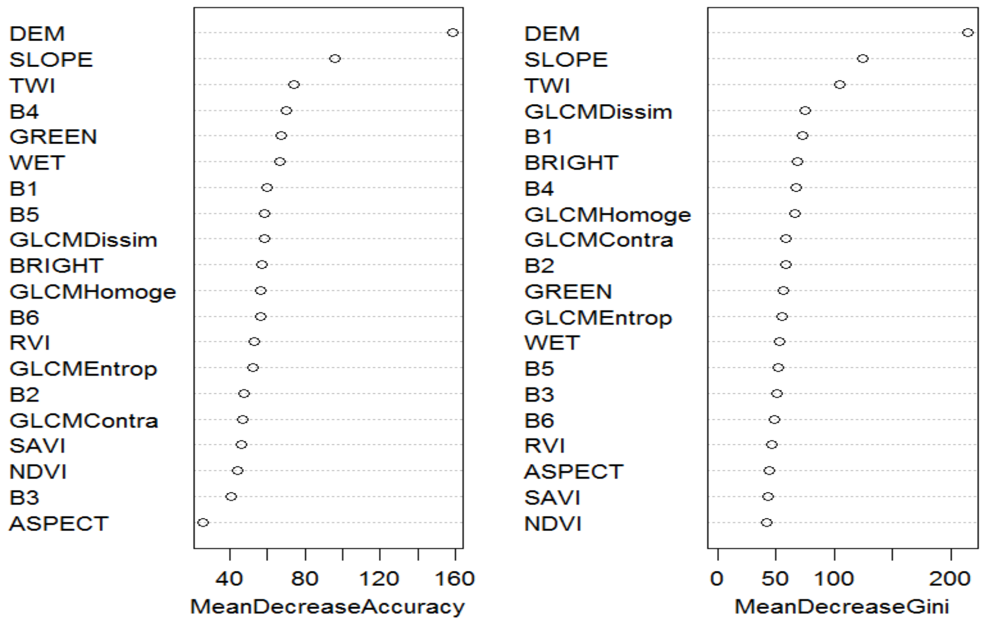

Table 16.b
Error matrix of local prediction of degradation (Evenk Autonomous)

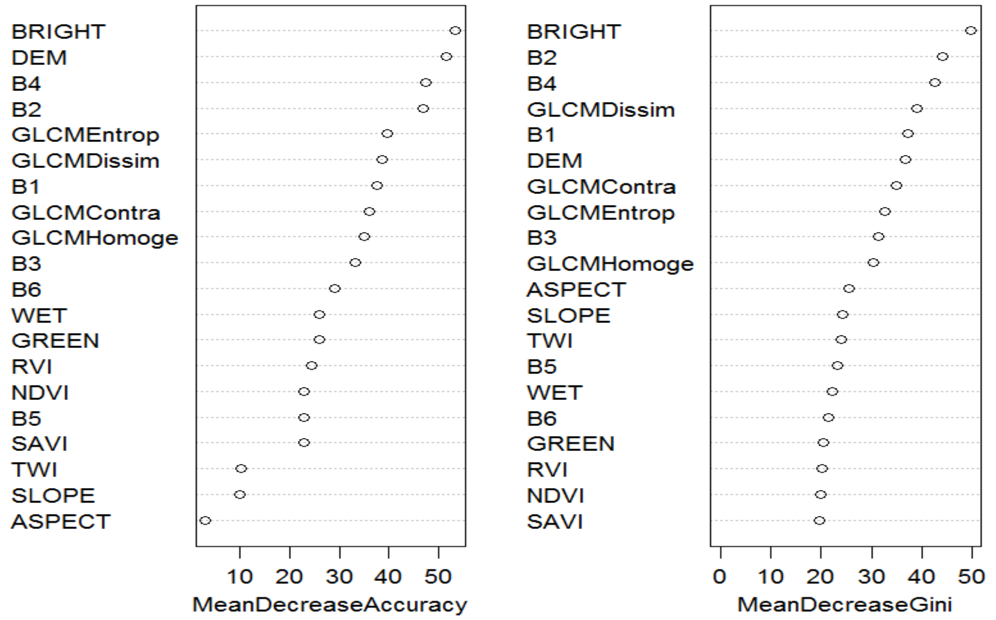

Table 17.a
Error matrix of local prediction of steppe types (Xilinhot City)

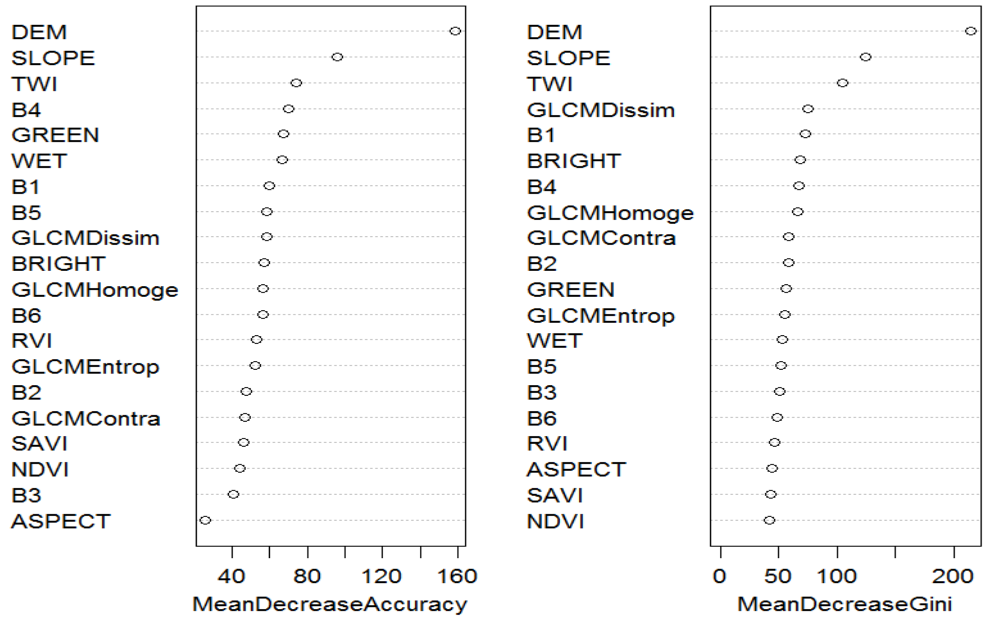

Table 17.b
Error matrix of local prediction of degradation (Xilinhot City)

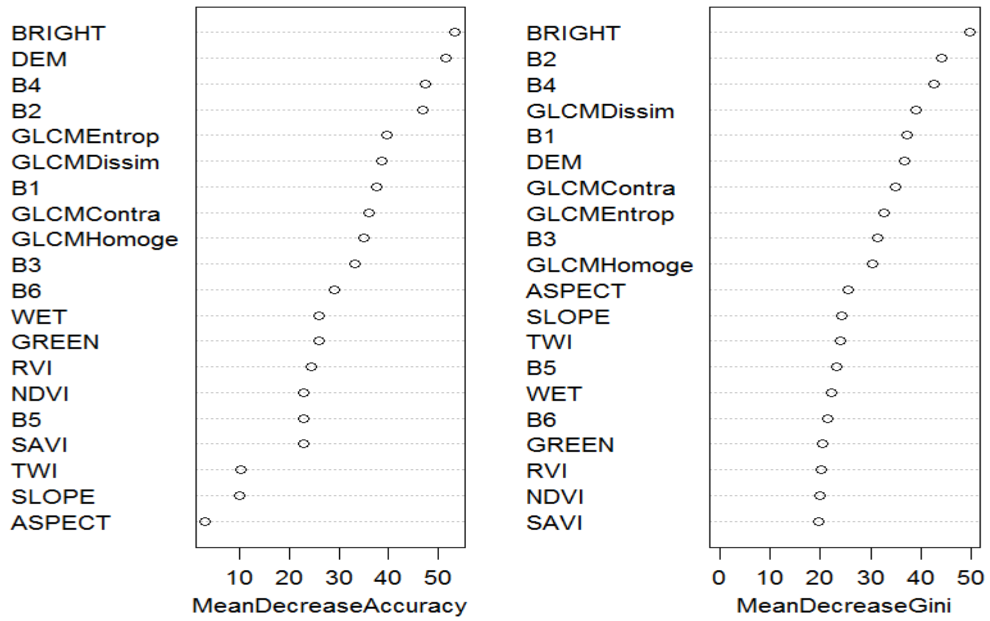

Table 18.a
Error matrix of local prediction of steppe types (Urat Middle Banner)

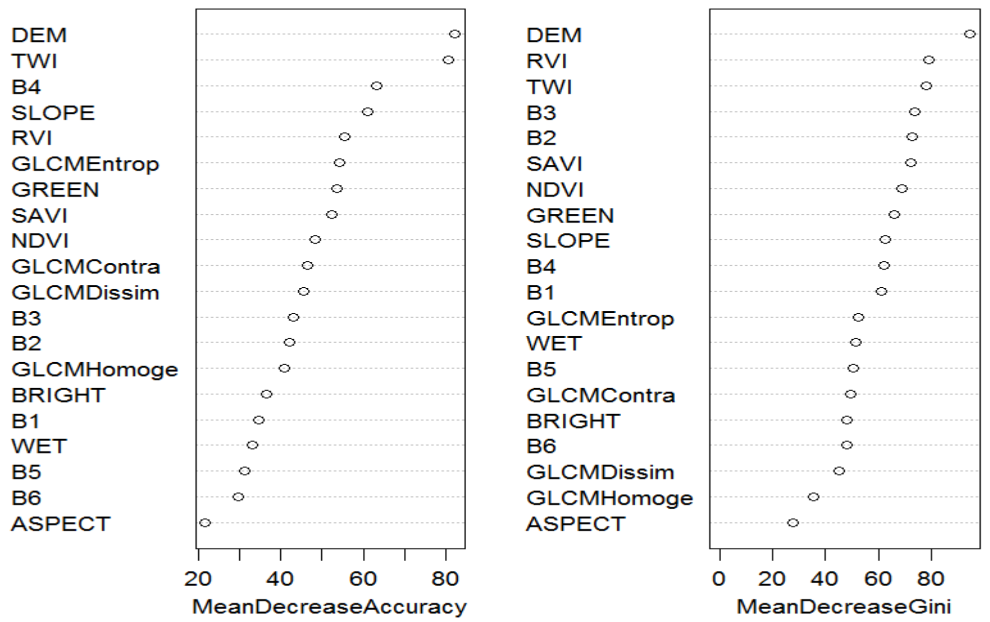

Table 18.b
Error matrix of local prediction of steppe degradation (Urat Middle Banner)

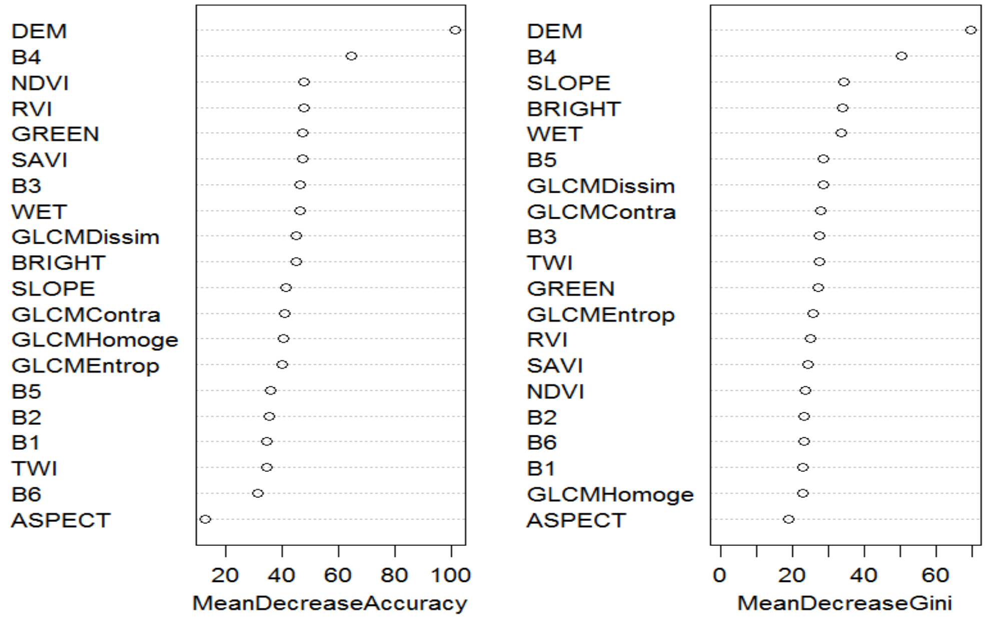

Table 19.a
Error matrix of local prediction of degradation with steppe class added into model (Ewenk Autonomous Region)

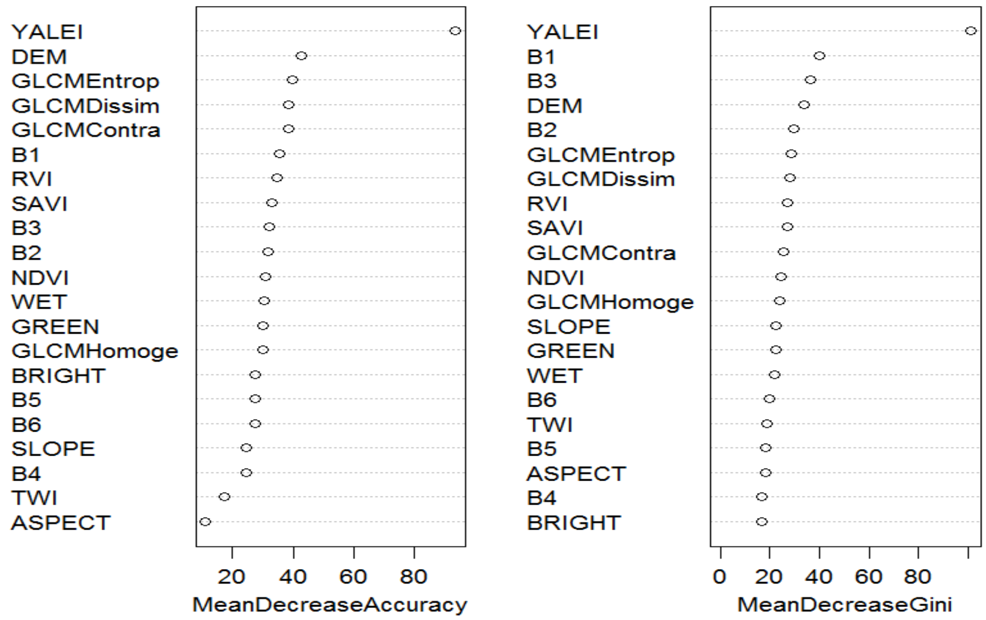

Table 19.b
Error matrix of local prediction of degradation with steppe class added into model and by using predicted steppe class for degradation prediction (Ewenk Autonomous Region)

See Table 19. a

Table 20.a

Error matrix of steppe type prediction within eco-region -- train on north and predict on south (Ewenk Autonomous Region)

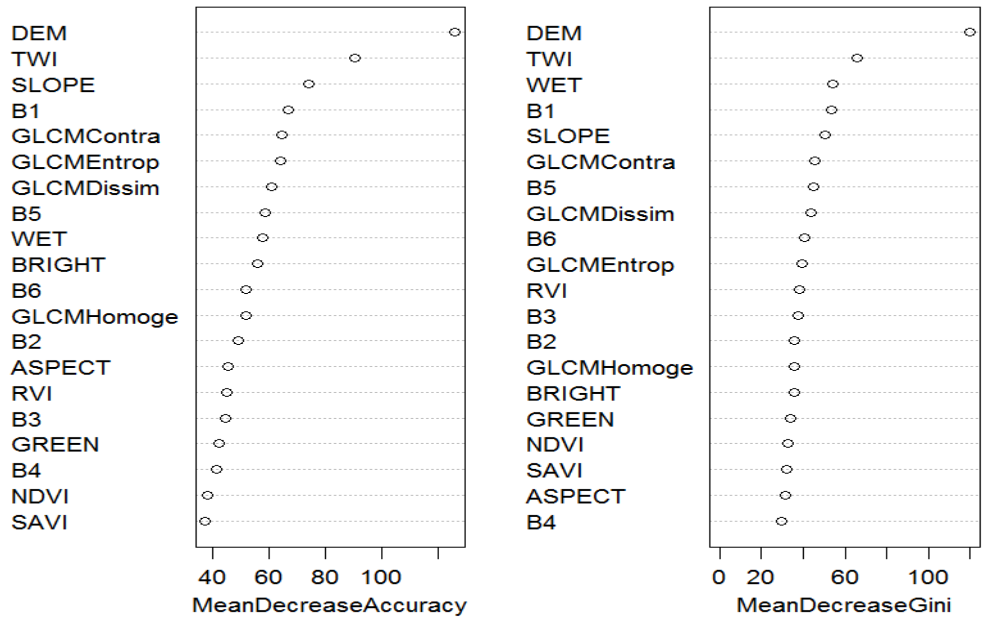

Table 20.b

Error matrix of degradation prediction within eco-region -- train on north and predict on south (Ewenk Autonomous Region)

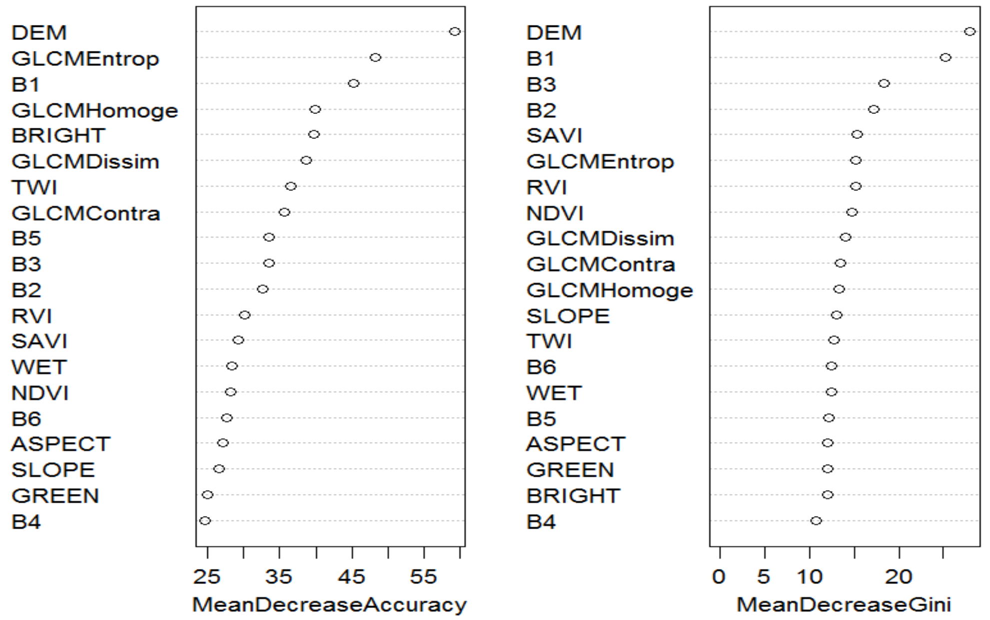

Table 20.c

Error matrix of steppe type prediction within eco-region -- train on south and predict on north (Ewenk Autonomous Region)

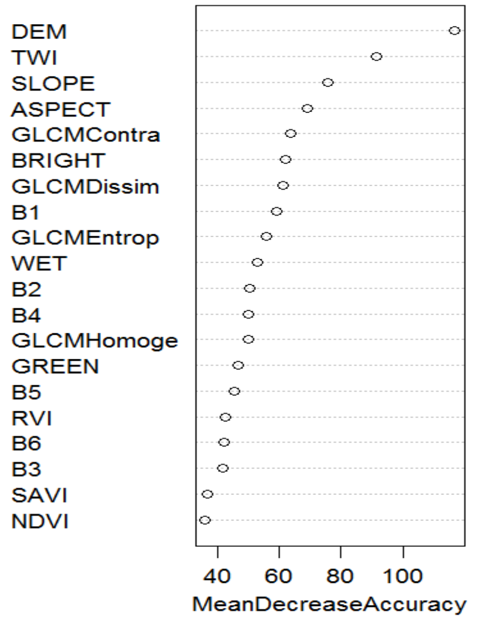

Table 20.d

Error matrix of degradation prediction within eco-region -- train on south and predict on north (Ewenk Autonomous Region)

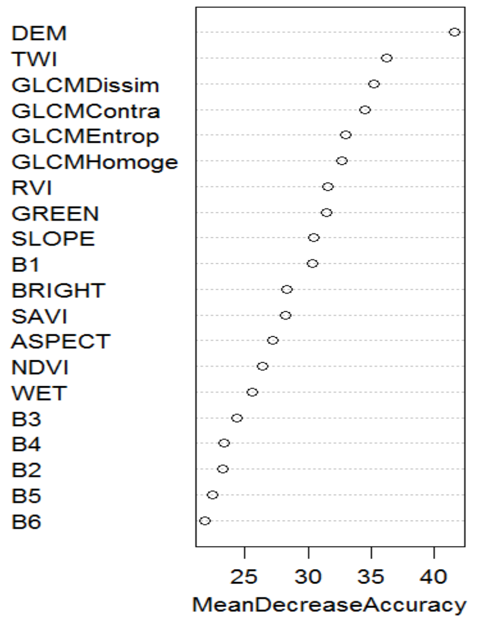

Table 21.a

Error matrix of steppe type prediction within eco-region -- train on east and predict on west (Xilinhot City)

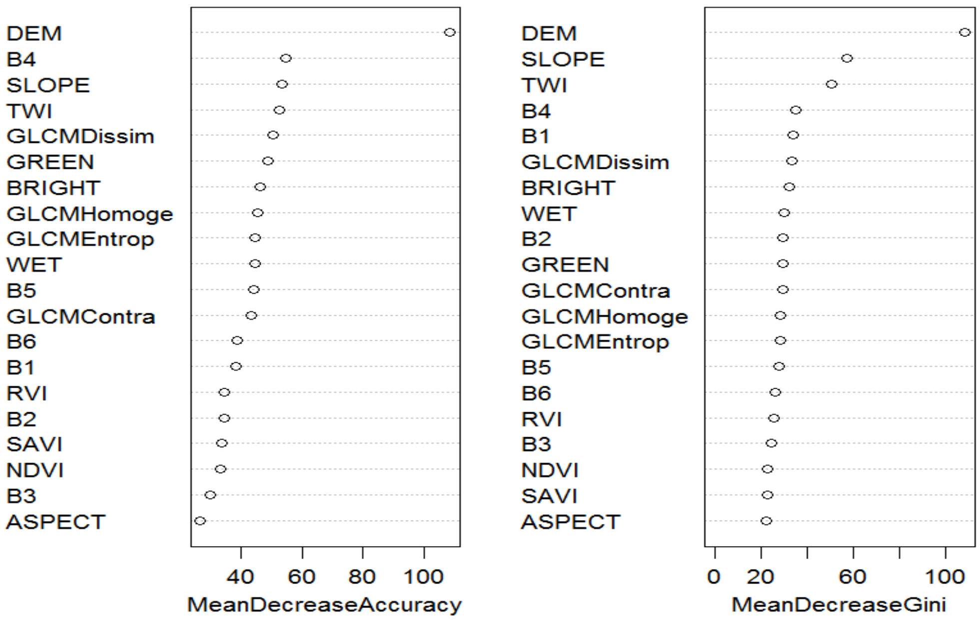

Table 21.b

Error matrix of degradation prediction within eco-region -- train on east and predict on west (Xilinhot City)

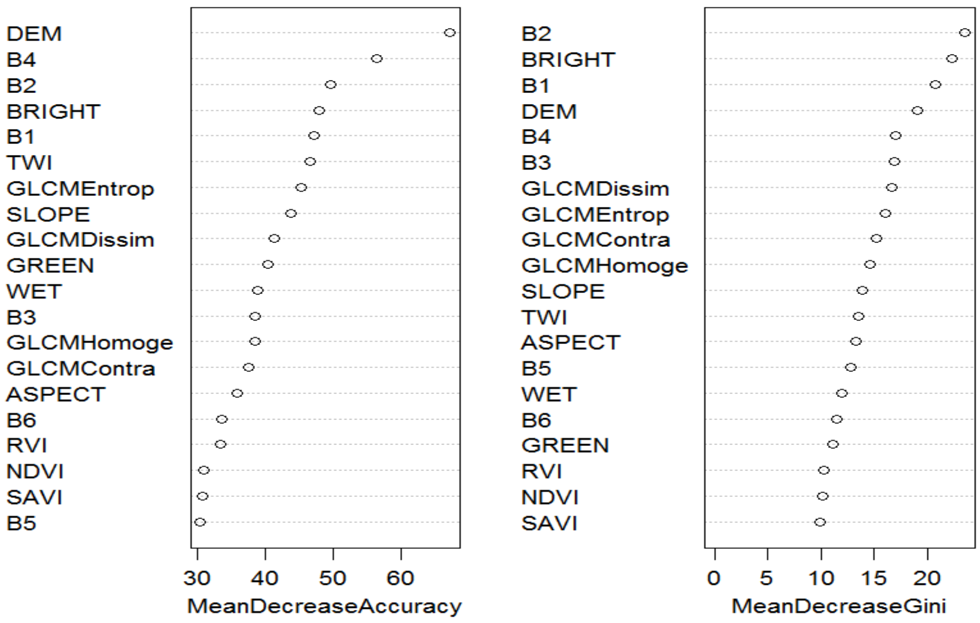

Table 21.c

Error matrix of steppe type prediction within eco-region -- train on west and predict on east (Xilinhot City)

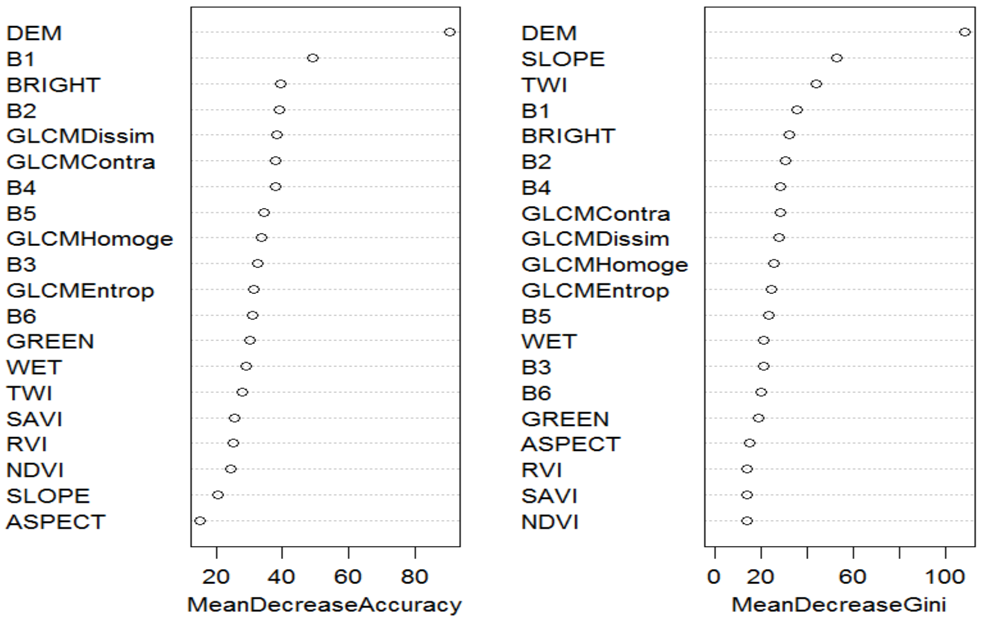

Table 21.d

Error matrix of degradation prediction within eco-region -- train on west and predict on east (Xilinhot City)

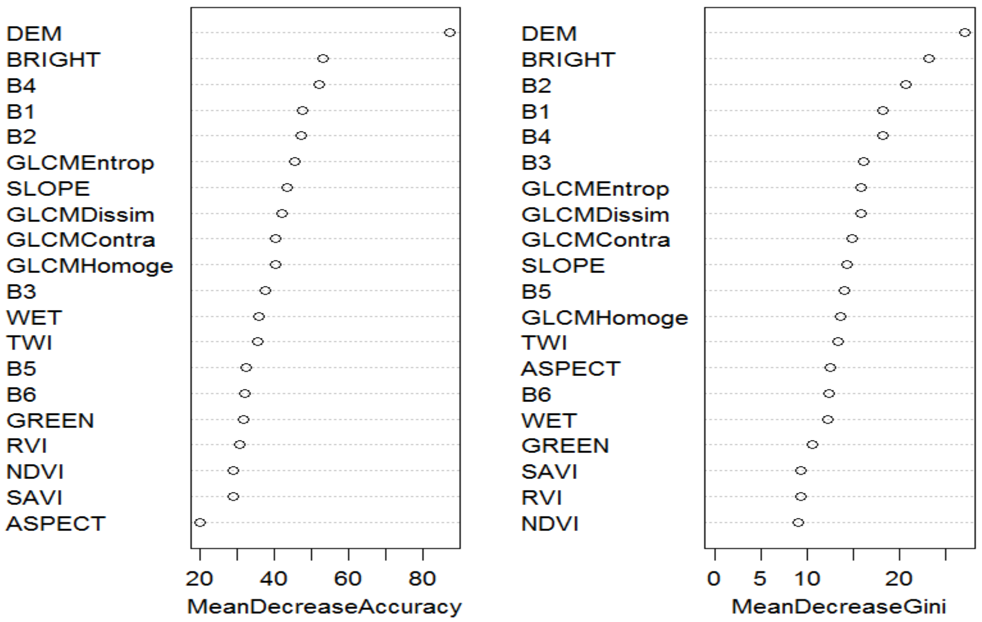

Table 22.a

Error matrix of steppe type prediction within eco-region -- train on northeast and predict on southwest (Urat Middle Banner)

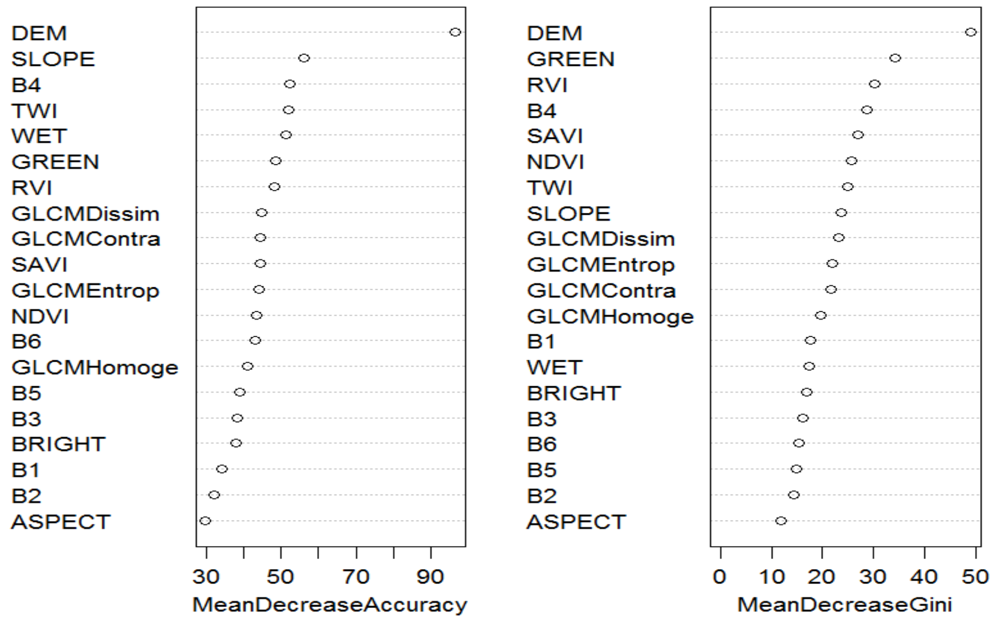

Table 22.b

Error matrix of degradation prediction within eco-region -- train on northeast and predict on southwest (Urat Middle Banner)

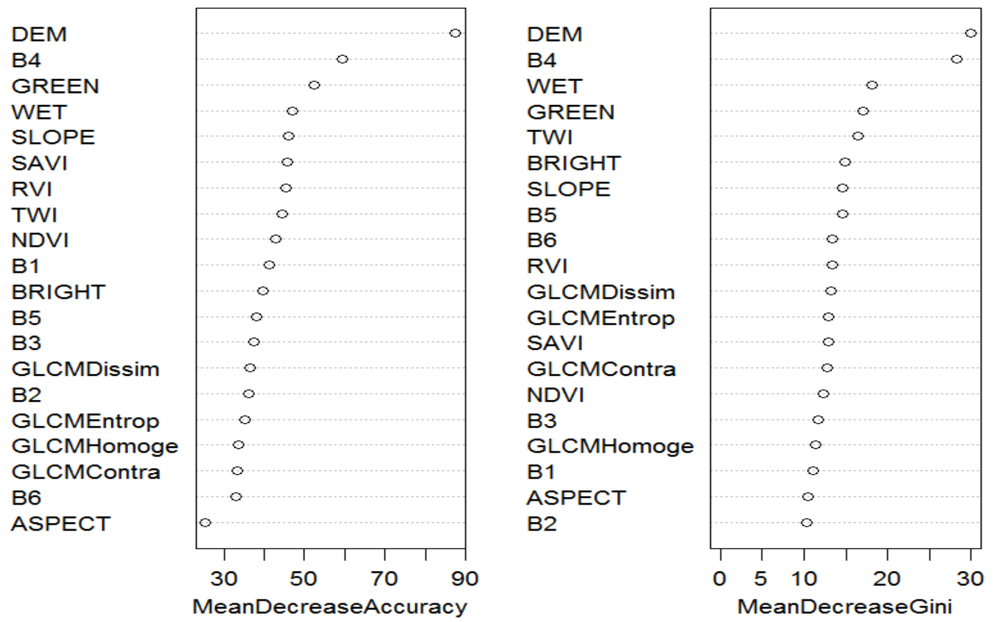

Table 22.c

Error matrix of steppe type prediction within eco-region -- train on southwest and predict on northeast (Urat Middle Banner)

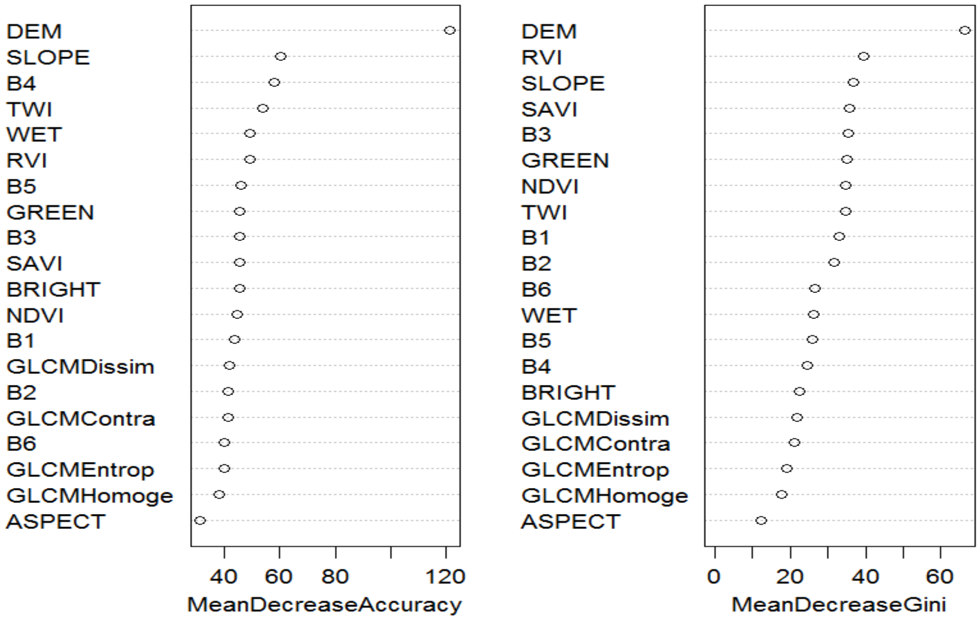

Table 22.d

Error matrix of degradation prediction within eco-region -- train on southwest and predict on northeast (Urat Middle Banner)

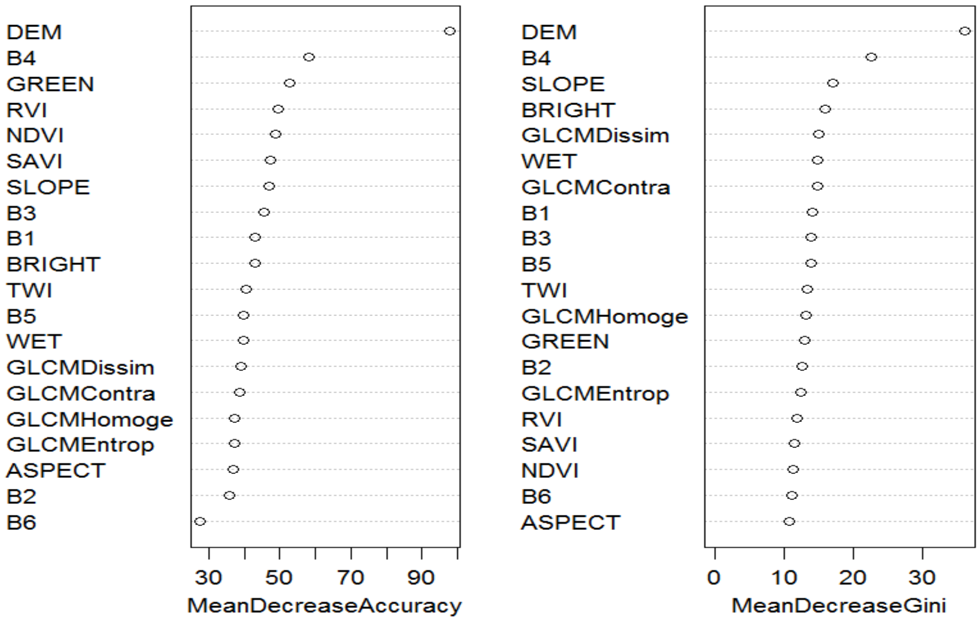

Table 23.a

Prediction across eco-region of steppe type (train on samples of Ewenk Autonomous Region, predict on all patches of Xilinhot City)

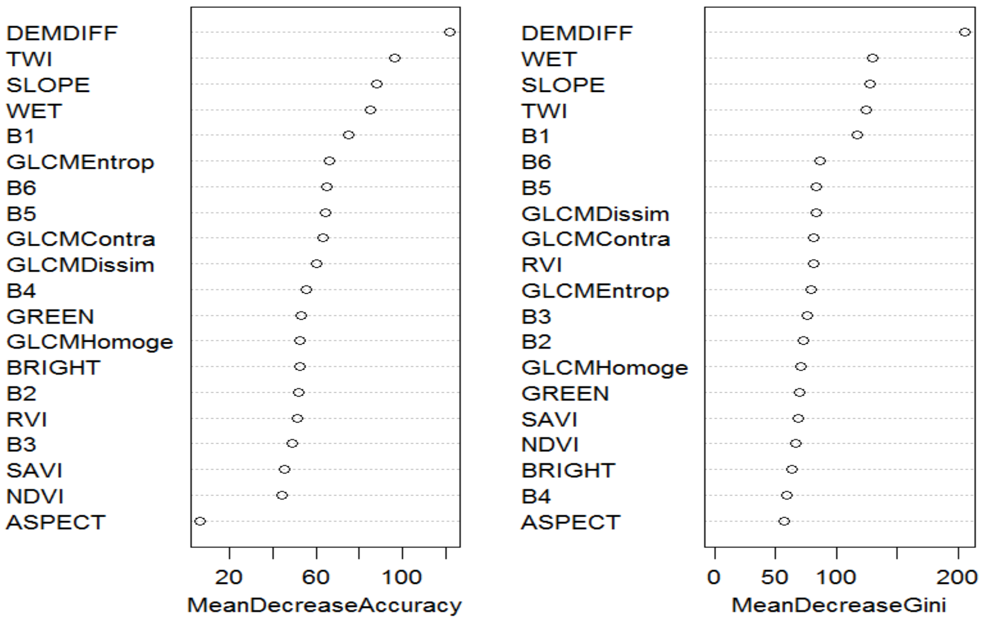

Table 23.b

Prediction across eco-region of steppe type (train on samples of Xilinhot City, predict on all patches of Ewenk Autonomous Region)

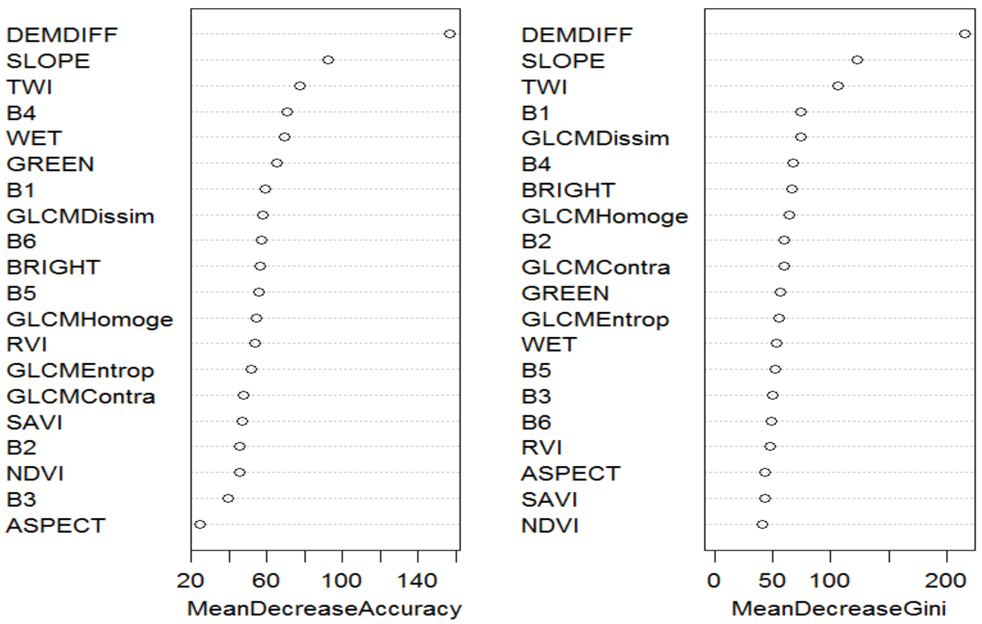

Table 23.c

Prediction across eco-region of degradation (train on samples of Ewenk Autonomous Region, predict on all patches of Xilinhot City)

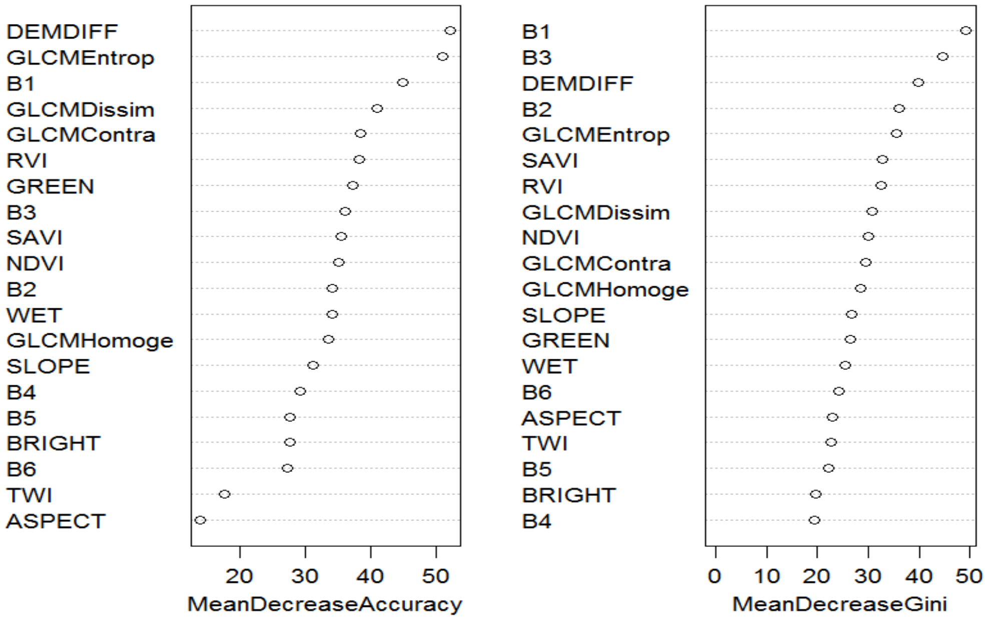

Table 23.d

Prediction across eco-region of degradation (train on samples of Xilinhot City, predict on all patches of Ewenk Autonomous Region)

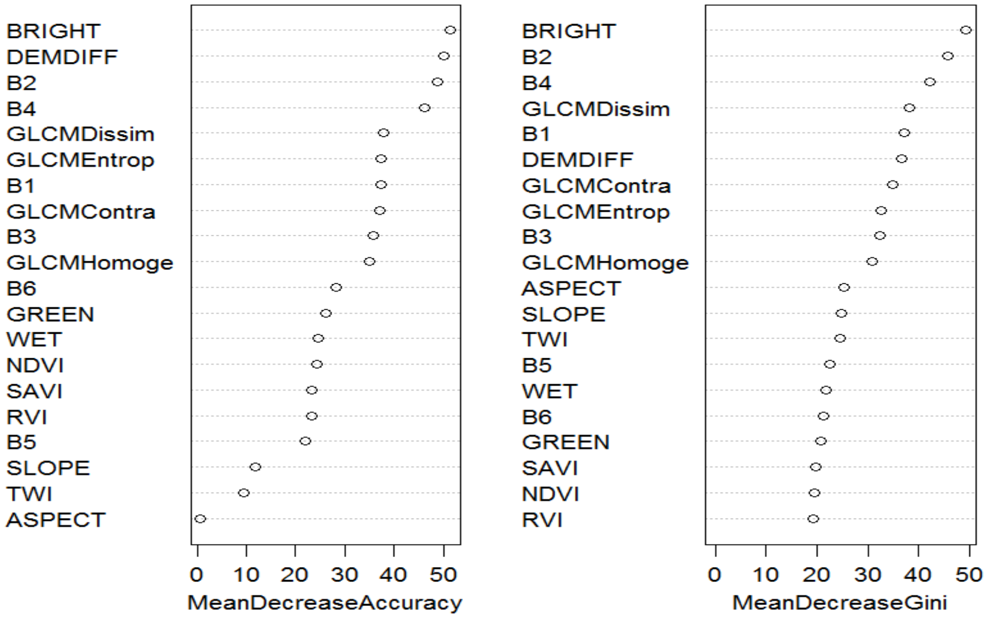

Table 24.a

Pooling and predicting on Ewenk Autonomous Region - steppe type classification

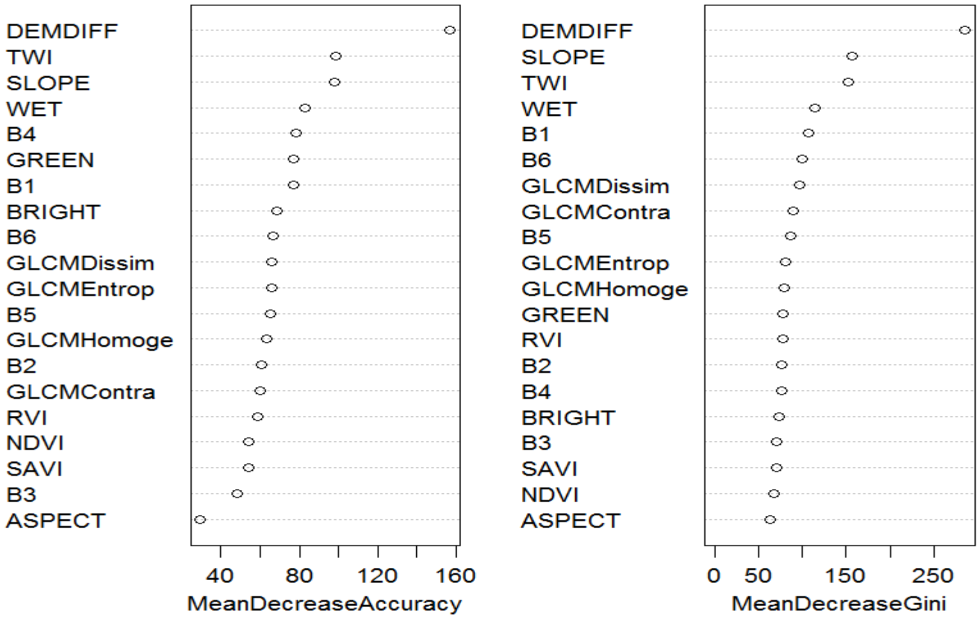

Table 24.b
Pooling and predicting on Xilinhot City - steppe type classification

See Table 24. a

Table 24.c
Pooling and predicting on Ewenk Autonomous Region - steppe degradation classification

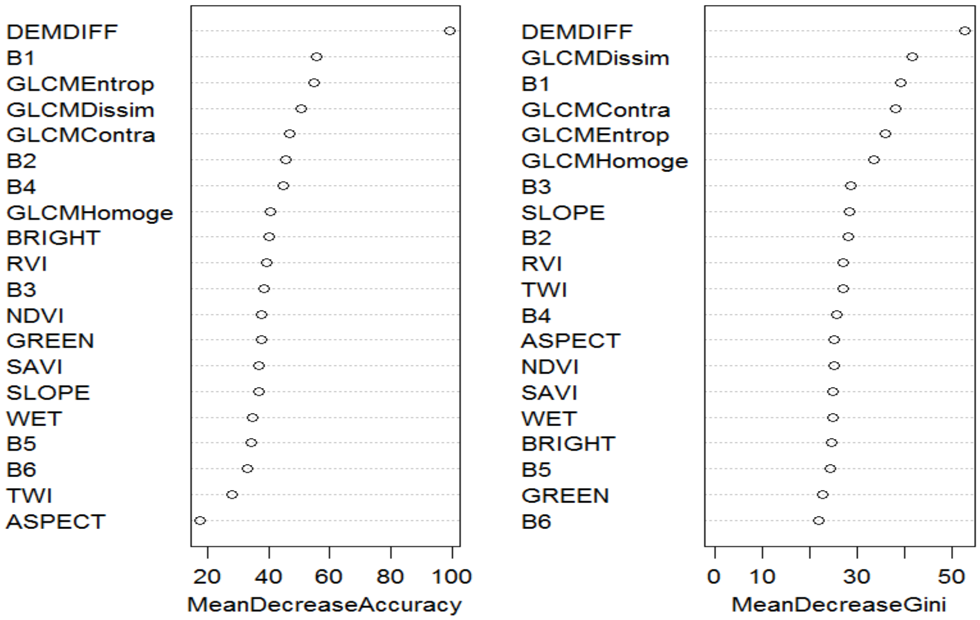

Table 24.d
Pooling and predicting on Xilinhot City - steppe degradation classification

See Table 24. c

Table 25.a

Pooling of filtered sample patches from Ewenk Autonomous Region and Xilinhot City

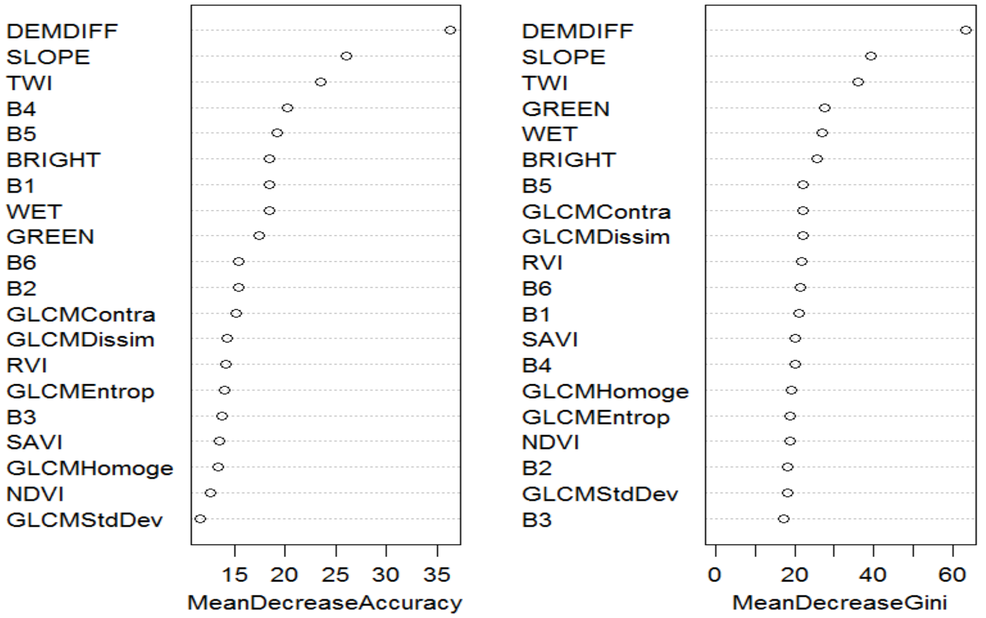

Table 25.b

Pooling of purified samples and predicting on Ewenk Autonomous Region - steppe type classification

See Table 25. a

Table 25.c

Pooling of purified samples and predicting on Xilinhot City - steppe type classification

See Table 25. a

Appendix B Mongolia Field Survey Data (for validating classification results)

Site_ID	vege-community	vege-community (in CHN)	1st_guess	Code	2nd_guess	Code	notes for ?	
1	Stipa gobica-Anabasis brevifolia-Salsola collina	戈壁针茅-短叶假木贼-猪毛菜	30032	M	30070	O		
2	Stipa gobica-Cleistogenes songorica-Salsola collina	戈壁针茅-无芒隐子草-猪毛菜	30032	M	30070	O		
3	Eurotia ceratoides-Kochia prostrata-Salsola collina	驼绒藜(?)-木地肤-猪毛菜	30031	L			not find	suspect:Krascheninnikovia ceratoides驼绒藜
4	Cleistogenes songorica-Caragana stenophylla-Eurotia ceratoides	无芒隐子草-狭叶锦鸡儿-驼绒藜(?)	30031	L			not find	suspect:Krascheninnikovia ceratoides驼绒藜
5	Cleistogenes songorica-Caragana pygmaea-Eurotia ceratoides	无芒隐子草-矮锦鸡儿-驼绒藜(?)	30031	L			not find	suspect:Krascheninnikovia ceratoides驼绒藜
6	Stipa gobica-Artemisia adamsii	戈壁针茅-丝裂(叶)蒿	30032	M				
7	Haloxylon ammodendron	梭梭	30082	Q				
8	Caragana pugmaea-Artemisia adamsii-Stipa gobica	矮锦鸡儿(?)-丝裂(叶)蒿-戈壁针茅	30070	O			typo	Caragana pygmaea
9	Allium polyrrhizum-Eurotia ceratoides	碱韭(多根葱)(?)-驼绒藜(?)	30082	Q	30021	D	typo,not find	Allium polyrhizum;suspect:Krascheninnikovia
10	Stipa gobica-Caragana pygmaea	戈壁针茅-矮锦鸡儿	30032	M				
11	Stipa gobica-Cleistogenes songorica-Allium mongolicum	戈壁针茅-无芒隐子草-蒙古韭(蒙古葱）	30032	M				
12	Stipa gobica-Convolvulus ammanii	戈壁针茅-银灰旋花(?)	30032	M			typo	Convolvulus ammannii
13	Convolvulus ammanii-Stipa gobica-Cleistogenes songorica	银灰旋花(?)-戈壁针茅-无芒隐子草	30031	L	30032	M	typo	Convolvulus ammannii
14	shrubs (Eurotia ceratoides, Artemisia xerophytica, Reaumurea songorica)	?-旱蒿-红砂(?)	30081	P			typo	Reaumuria soongarica
15	Anabasis brevifolia-Allium polyrrhizum	短叶假木贼-碱韭(多根葱)(?)	30070	O	30081	P	typo	Allium polyrhizum

16	Anabasis brevifolia-Stipa glareosa	短叶假木贼-沙生针茅	30070	O				
17	Haloxylon ammodendron with shrubs	梭梭(及灌木)	30082	Q				
18	Reaumurea songoorica-Anabasis brevifolia-Allium	红砂(?)-短叶假木贼-葱属(?)	30081	P			typo, not find	Reaumuria soongarica
19	Nitraria sibirica-Cleistogenes songorica	(小果)白刺?-无芒隐子草	30082	Q	30070	O	same genus	
20	Ajania achilleoides-Salsola collina-Eurotia ceratoides	蓍状亚菊-猪毛菜-？	30031	L			not find,susp	
21	Stipa gobica-Anabasis brevifolia	戈壁针茅-短叶假木贼	30032	M	30070	O		
22	Stipa gobica-Artemisia frigida	戈壁针茅-冷蒿	30032	M				
23	Allium polyrrhizum-Stipa gobica	碱韭(多根葱)(?)-戈壁针茅	30031	L			typo	Allium polyrhizum
24	Stipa gobica-Cleistogenes songorica-Allium mongolicum with shrubs	戈壁针茅-无芒隐子草-蒙古韭(蒙古葱）(及灌木）	30031	L				
25	Allium polyrrhizum-Allium mongolicum-Cleistogenes songorica	碱韭(多根葱)(?)-蒙古韭(蒙古葱）-无芒隐子草	30031	L			typo	Allium polyrhizum
26	Allium mongolicum-Allium polyrrhizum-Cleistogenes songorica	蒙古韭(蒙古葱）-碱韭(多根葱)(?)-无芒隐子草	30031	L			typo	Allium polyrhizum
27	Cleistogenes songorica with shrubs	无芒隐子草(及灌木）	30031	L				
28	shrubs with Allium mongolicum and Cleistogenes songorica	灌木(及蒙古韭(蒙古葱）-无芒隐子草）	30031	L	30070	O		
29	Anabasisi brevifolia-Stipa gobica	短叶假木贼(?)-戈壁针茅	30070	O			typo	Anabasis brevifolia
30	Stipa gobica-Cleistogenes songorica with shrubs	戈壁针茅-无芒隐子草(及灌木)	30032	M				
31	Stipa gobica-Cleistogenes songorica	戈壁针茅-无芒隐子草	30032	M				
32	Allium mongolicum-Stipa gobica	蒙古韭(蒙古葱）-戈壁针茅	30081	P	30031	L		
33	Stipa gobica-Cleistogenes songorica	戈壁针茅-无芒隐子草	30032	M				

34	Allium mongolicum-Stipa gobica-Artemisia frigida	蒙古韭(蒙古葱）-戈壁针茅-冷蒿	30081	P	30031	L		
35	Stipa gobica-Allium mongolicum	戈壁针茅-蒙古韭(蒙古葱）	30032	M				
36	Stipa gobica-Cleistogenes squarrosa with Caragana microphylla	戈壁针茅-糙隐子草(及小叶锦鸡儿)	30032	M				
37	Stipa gobica-Anabasis brevifolia	戈壁针茅-短叶假木贼	30032	M				
38	Stipa gobica-Cleistogenes squarrosa	戈壁针茅-糙隐子草	30032	M				
39	Stipa krylovii-Allium polyrrhizum-Carex duriuscula	克氏针茅-碱韭(多根葱)(?)-寸草苔	30021	D			typo	Allium polyrhizum
40	Stipa krylovii-Allium polyrrhizum	克氏针茅-碱韭(多根葱)(?)	30021	D			typo	Allium polyrhizum
41	Caragana microphylla-Allium odorum-Artemisia frigida with Chenopodium viride	小叶锦鸡儿-?-冷蒿(及野韭？)	30021	D			typo, not find	Allium odorumsuspect：野韭
42	Elymus chinensis-Stipa-Cleistogenes squarrosa	羊草(?)-糙隐子草	30021	D			not find	suspect：Leymus chinensis羊草
43	Elymus chinensis-Cleistogenes squarrosa-Artemisia frigida	羊草(?)-糙隐子草-冷蒿	30021	D			not find	suspect：Leymus chinensis羊草
44	Cleistogenes squarrosa-Allium with Chenopodium viride	糙隐子草-葱属(及?)	30021	D			not find	
45	Cleistogenes squarrosa-Allium with Chenopodium viride	糙隐子草-葱属(及?)	30021	D			not find	
46	Allium polyrrhizum-Caragana microphylla with annual plants	碱韭(多根葱)(?)-小叶锦鸡儿(及一年生杂类草）	30021	D			typo	Allium polyrhizum
47	Allium polyrrhizum-Caragana stenophylla	碱韭(多根葱)(?)-狭叶锦鸡儿	30021	D			typo	Allium polyrhizum
48	Stipa krylovii-Allium polyrrhizum-Cleistogenes squarrosa	克氏针茅-碱韭(多根葱)(?)-糙隐子草	30021	D			typo	Allium polyrhizum
49	Allium polyrrhizum	碱韭(多根葱)(?)	30021	D			typo	Allium polyrhizum

50	Artemisia frigida-Leymus chinensis-Allium polyrrhizum with Chenopodium viride	冷蒿-羊草-碱韭(多根葱)(?)(及？)	30021	D			typo, not find	Allium polyrhizum
51	Allium polyrrhizum-Convolvulus ammanii	碱韭(多根葱)(?)-银灰旋花(?)	30021	D	30031	L	typo	Allium polyrhizum, Convolvulus ammannii
52	Allium polyrrhizum-Convolvulus ammanii	碱韭(多根葱)(?)-银灰旋花(?)	30021	D	30031	L	typo	Allium polyrhizum, Convolvulus ammannii
53	Allium-Elymus chinensis	葱属(?)-羊草(?)	30021	D			not find	suspect：Leymus
54	Allium polyrrhizum-Convolvulus ammanii-Caragana	碱韭(多根葱)(?)-银灰旋花(?)-锦鸡儿属(?)	30021	D			typo, not find	Allium polyrhizum, Convolvulus ammannii
55	Allium polyrrhizum-Convolvulus ammanii-Caragana	碱韭(多根葱)(?)-银灰旋花(?)-锦鸡儿属(?)	30021	D			typo, not find	Allium polyrhizum, Convolvulus ammannii
56	Leymus chinensis-Cleistogenes squarrosa with Chenopodium viride	羊草-糙隐子草(及？)	30021	D			not find	
57	Allium polyrrhizum	碱韭(多根葱)(?)	30021	D			typo	Allium polyrhizum
58	Allium polyrrhizum	碱韭(多根葱)(?)	30021	D			typo	Allium polyrhizum
59	Artemisia frigida-Leymus chinensis-Cleistogenes squarrosa with Chenopodium viride	冷蒿-羊草-糙隐子草(及？)	30021	D			not find	
60	Stipa krylovii-Cleistogenes squarrosa-Carex duriuscula	克氏针茅-糙隐子草-寸草苔	30021	D				
61	Allium polyrrhizum-Carex duriuscula	碱韭(多根葱)(?)-寸草苔	30152	G	30021	D	typo	Allium polyrhizum, Convolvulus ammannii
62	Stipa grandis-Cleistogenes squarrosa with annual plants	大针茅-糙隐子草(及一年生杂类草）	30021	D				
63	Stipa krylovii-Carex duriuscula-Caragna microphylla	克氏针茅-寸草苔-小叶锦鸡儿	30021	D				
64	Stipa krylovii-Elymus chinensis	克氏针茅-羊草(?)	30021	D			not find	suspect：Leymus chinensis羊草
65	Cleistogenes squarrosa-Stipa krylovii-Kochia prostrata with Salsola collina	糙隐子草-克氏针茅-木地肤(及猪毛菜）	30021	D				

66	Stipa krylovii-Corispermum mongolicum-chenopodium viride	克氏针茅-蒙古虫实-?	30023	M	30021	D	not find	
67	Stipa krylovii-Cleistogenes squarrosa with annual plants	克氏针茅-糙隐子草(及一年生杂类草)	30021	D				
68	Carex duriuscula-Stipa krylovii with annul plants	寸草苔-克氏针茅(及一年生杂类草)	30152	G				
69	Stipa krylovii with Salsola collina	克氏针茅(及猪毛菜)	30021	D	30022	K		
70	Allium-Caragana pygmaea	葱属(?)-矮锦鸡儿	30031	L			not find	
71	Salsola collina-Carex duriumscula with Chenopodium viride	猪毛菜-寸草苔(及?)	30031	L			not find	
72	Stipa krylovii-Elymus chinensis-Cleistogenes squarrosa	克氏针茅-羊草(?)-糙隐子草	30021	D			not find	suspect：Leymus chinensis羊草
73	Stipa krylovii-Salsola collina-Convolvulus ammanii	克氏针茅-猪毛菜-银灰旋花(?)	30021	D	30031	L	typo	Convolvulus ammannii
74	Allium polyrrhizum-Elymus chinensis-Cleistogenes squarrosa	碱韭(多根葱)(?)-羊草(?)-糙隐子草	30021	D			typo, not find	Allium polyrhizum，suspect：Leymus chinensis羊草
75	Artemisia frigida-Leymus chinensis with Chenopodium viride	冷蒿-羊草(?)(及？)	30023	E	30021	D	not find	suspect：Leymus chinensis羊草
76	Stipa krylovii-Carex stenophylloides-Salsola collina	克氏针茅-中亚苔草(砾苔草)-猪毛菜	30021	D				
77	Elymus chinensis-Artemisia frigida-Cleistogenes squarrosa	羊草(?)-冷蒿-糙隐子草	30021	D	30023	E	not find	suspect：Leymus chinensis羊草
78	Lappula intermedia-Caragana microphylla-Artemisia frigida with Chenopodium album	东北鹤虱(中间鹤虱)-小叶锦鸡儿-冷蒿(及藜(白藜,灰菜))	30021	D				
79	Allium polyrrhizum-Stipa grandis-Cleistogenes squarrosa with Chenopodium viride	碱韭(多根葱)(?)-大针茅-糙隐子草(及?)	30021	D			typo, not find	Allium polyrhizum

80	Cleistogenes squarrosa-Carex duriuscula-Haplophyllum dauricum	糙隐子草-寸草苔-假芸香(北芸香）	30021	D				
81	Allium polyrrhizum-Caragana pygmaea-Carex duriuscula	碱韭(多根葱)(?)-矮锦鸡儿-寸草苔	30021	D			typo, not find	Allium polyrhizum
82	Carex duriuscula-Cleistogenes squarrosa-Carex stenophylloides	寸草苔-糙隐子草-中亚苔草(砾苔草)	30152	G				
83	Cleistogenes squarrosa-Carex duriuscula-Salsola collina	糙隐子草-寸草苔-猪毛菜	30021	D				
84	Carex duriuscula-Caragana microphylla-Convolvulus ammanii	寸草苔-小叶锦鸡儿-银灰旋花(?)	30152	G			typo	Convolvulus ammannii
85	Carex duriuscula-Cleistogenes squarrosa with Chenopodium viride	寸草苔-糙隐子草(及?)	30152	G			not find	
86	Carex duriuscula-Salsola collina-Allium polyrrhizum	寸草苔-猪毛菜-碱韭(多根葱)(?)	30152	G			typo	Allium polyrhizum
87	Stipa krylovii-Elymus chinensis-Allium polyrrhizum	克氏针茅-羊草(?)-碱韭(多根葱)(?)	30021	D			typo, not find	Allium polyrhizum,suspect：Leymus chinensis羊草
88	Cleistogenes squarrosa-Carex duriuscula with Chenopodium album	糙隐子草-寸草苔(及藜(白藜,灰菜))	30021	D	30023	E		
89	Cleistogenes squarrosa-Carex duriuscula-Caragana korshinskii	糙隐子草-寸草苔-柠条锦鸡儿	30021	D	30023	E		
90	Stipa krylovii-Convolvulus ammanii-Allium polyrrhizum	克氏针茅-银灰旋花(?)-碱韭(多根葱)(?)	30021	D	30023	E	typo	Convolvulus ammannii,Allium
91	Allium polyrrhizum-Carex duriuscula-Cleistogenes squarrosa	碱韭(多根葱)(?)-寸草苔-糙隐子草	30021	D	30031	L	typo	Allium polyrhizum
92	Convolvulus ammanii-Carex duriuscula-Allium polyrrhizum	银灰旋花(?)-寸草苔-碱韭(多根葱)(?)	30031	L	30021	L	typo	Convolvulus ammannii,Allium polyrhizum

93	Convolvulus ammanii-Carex duriuscula-Elymus chinensis with Chenopodium viride	银灰旋花(?)-寸草苔-羊草(?)(及?)	30031	L	30021	L	typo, not find	Convolvulus ammannii,suspect：Leymus chinensis羊草
94	Stipa krylovii-Cleistogenes squarrosa-Dasiphora fruticosa	克氏针茅-糙隐子草-？	30021	D			not find	suspect：金露梅
95	Stipa krylovii-Agropyron cristatum-Allium mongolicum with Chenopodium album	克氏针茅-冰草-蒙古韭(蒙古葱）(及藜(白藜,灰菜))	30021	D				
96	Allium polyrrhizum-Stipa krylovii-Convolvulus ammanii-Cleistogenes squarrosa	碱韭(多根葱)(?)-克氏针茅-银灰旋花(?)-糙隐子草	30021	D	30023	E	typo	Convolvulus ammannii,Allium polyrhizum
97	Allium mongolicum-Stipa krylovii-Carex duriuscula	蒙古韭(蒙古葱)-克氏针茅-寸草苔	30021	D				
98	Stipa krylovii	克氏针茅	30021	D				
99	Cleistogenes squarrosa-Artemisia adamsii-Medicago ruthenica	糙隐子草-丝裂(叶)蒿-花苜蓿	30021	D				
100	Salsola collina-Cleistogenes squarrosa-Elymus chinensis	猪毛菜-糙隐子草-羊草(?)	30023	E	30021	D	not find	suspect：Leymus chinensis羊草
101	Elymus chinensis with Salsola collina and Chenopodium viride	羊草(?)(及猪毛菜-？）	30021	D			not find	suspect：Leymus chinensis羊草
102	Cleistogenes squarrosa-Artemisia frigida with annual plants	糙隐子草-冷蒿(及一年生杂类草)	30021	D				
103	Cleistogenes squarrosa-Caragana microphylla-Allium tenuissimum	糙隐子草-小叶锦鸡儿-细叶韭(细叶葱）	30021	D				
104	Stipa krylovii-Artemisia adamsii-Allium polyrrhizum with Chenopodium album	克氏针茅-丝裂(叶)蒿-碱韭(多根葱)(?)(及藜(白藜,灰菜))	30021	D			typo	Allium polyrhizum
105	Carex -Cleistogenes squarrosa	苔草类(?)-糙隐子草	30152	G	30021	D	not find	

106	Carex duriuscula-Convolvulus ammanii with Chenopodium viride	寸草苔-糙隐子草	30152	G	30021	D		
107	Stipa grandis-Elymus chinensis-Caragana microphylla	大针茅-羊草(?)-小叶锦鸡儿	30021	D			not find	suspect：Leymus chinensis羊草
108	Elymus chinensis-Cleistogenes squarrosa-Salsola collina	羊草(?)-糙隐子草-猪毛菜	30021	D			not find	suspect：Leymus chinensis羊草
109	Stipa grandis-Elymus chinensis-Cleistogenes squarrosa with Chenopodium album	大针茅-羊草(?)-糙隐子草(及藜(白藜,灰菜))	30021	D				
110	Cleistogenes squarrosa-Carex korshinskyi with Chenopodium album	糙隐子草-黄囊苔草(及藜(白藜,灰菜))	30023	E	30021	D		
111	Stipa grandis- Cleistogenes squarrosa-Salsola collina with Chenopodium album	大针茅-糙隐子草-猪毛菜(及藜(白藜,灰菜))	30021	D				
112	Stipa krylovii-Allium polyrrhizum-Heteropappus hispidus	克氏针茅-碱韭(多根葱)(?)-狗娃花	30021	D			typo	Allium polyrhizum
113	Salsola collina-Cleistogenes squarrosa-Carex duriuscula with Chenopodium viride	猪毛菜-糙隐子草-寸草苔(及?)	30031	L	30023	E	not find	
114	Stipa krylovii-Carex korshinskyi-Elymus chinensis	克氏针茅-黄囊苔草-羊草(?)	30021	D			not find	suspect：Leymus chinensis羊草
115	Cleistogenes squarrosa-Stipa grandis-Elymus chinensis	糙隐子草-大针茅-羊草(?)	30021	D			not find	suspect：Leymus chinensis羊草
116	Cleistogenes squarrosa-Stipa -Elymus chinensis	糙隐子草-针茅(?)-羊草(?)	30021	D			not find	suspect：Leymus chinensis羊草
117	Stipa krylovii-Cleistogenes squarrosa-Artemisia adamsii with Chenopodium album	克氏针茅-糙隐子草-丝裂(叶)蒿(及藜(白藜,灰菜))	30021	D				

118	Stipa grandis-Cleistogenes squarrosa-Allium polyrrhizum with Chenopodium album	大针茅-糙隐子草-碱韭(多根葱)(?)(及藜(白藜,灰菜))	30021	D			typo	Allium polyrhizum
119	Allium-Carex duriuscula-Stipa krylovii	葱属(?)-寸草苔-克氏针茅	30152	G	30021	D	not find	
120	Allium senescens-Medicago ruthenica-Carex duriuscula	山韭-花苜蓿-寸草苔	30013	C				
121	Elymus chinensis-Stipa sibirica-Artemisia frigida with Chenopodium virides	羊草(?)-羽茅(光颖芨芨草)(?)-冷蒿(及?)	30021	D			not find	suspect：Leymus chinensis羊草；suspect：Achnatherum
122	Elymus chinensis-Stipa sibirica with Chenopodium viride	羊草(?)-羽茅(光颖芨芨草)(?)(及?)	30021	D			not find	suspect：Leymus chinensis羊草；suspect：Achnatherum
123	Cleistogenes squarrosa-Allium senescens-Grasses	糙隐子草-山韭-杂类草	30021	D				
124	Allium senescens-Cleistogenes squarrosa-forbs	山韭-糙隐子草-非禾本草本植物	30021	D				
125	Cleistogenes squarrosa-Elymus chinensis-Carex duriuscula-Allium polyrrhizum	糙隐子草-羊草(?)-寸草苔-碱韭(多根葱)(?)	30021	D			typo, not find	Allium polyrhizum,suspect：Leymus chinensis羊草
126	Caragana microphylla-Stipa sibirica-Allium senescens	小叶锦鸡儿-羽茅(光颖芨芨草)(?)-山韭	30021	D				
127	Elymus chinensis-Cleistogenes sguarrosa-Salsola collina-Allium	羊草(?)-糙隐子草-猪毛菜-葱属(?)	30021	D			not find	suspect：Leymus chinensis羊草
128	Carex duriuscula-Stipa krylovii-Allium senescens	寸草苔-克氏针茅-山韭	30152	G				
129	Cleistogenes squarrosa-Stipa krylovii-Elymus chinensis	糙隐子草-克氏针茅-羊草(?)	30021	D			not find	suspect：Leymus chinensis羊草
130	Carex duriuscula-Artemisia frigida-Stipa	寸草苔-冷蒿-针茅(?)	30152	G			not find	
131	Carex duriuscula-Stipa krylovii-Iris tigridia-Forbs	寸草苔-克氏针茅-粗根鸢尾-非禾本草本植物	30152	G				
132	Carex duriuscula-Stipa krylovii-Iris tigridia-Forbs	寸草苔-克氏针茅-粗根鸢尾-非禾本草本植物	30152	G				

133	Elymus chinensis-Cleistogenes squarrosa with Chenopodiun virides	羊草(?)-糙隐子草(及？)	30021	D			not find	suspect：Leymus chinensis羊草
134	Cleistogenes squarrosa-Elymus chinensis-Allium	糙隐子草-羊草(?)-葱属(?)	30021	D			not find	suspect：Leymus chinensis羊草
135	Cleistogenes squarrosa-Allium- Stipa krylovii	糙隐子草-葱属(?)-克氏针茅	30021	D			not find	suspect：Leymus chinensis羊草
136	Carex duriuscula-Cleistogenes squarrosa-Stipa krylovii-Allium	寸草苔-糙隐子草-克氏针茅-葱属(?)	30152	G			not find	
137	Cleistogenes squarrosa-Artemisia frigida-Allium	糙隐子草-冷蒿-葱属(?)	30021	D			not find	

Appendix C 2009 Steppe Type and Degradation Map of IMAR

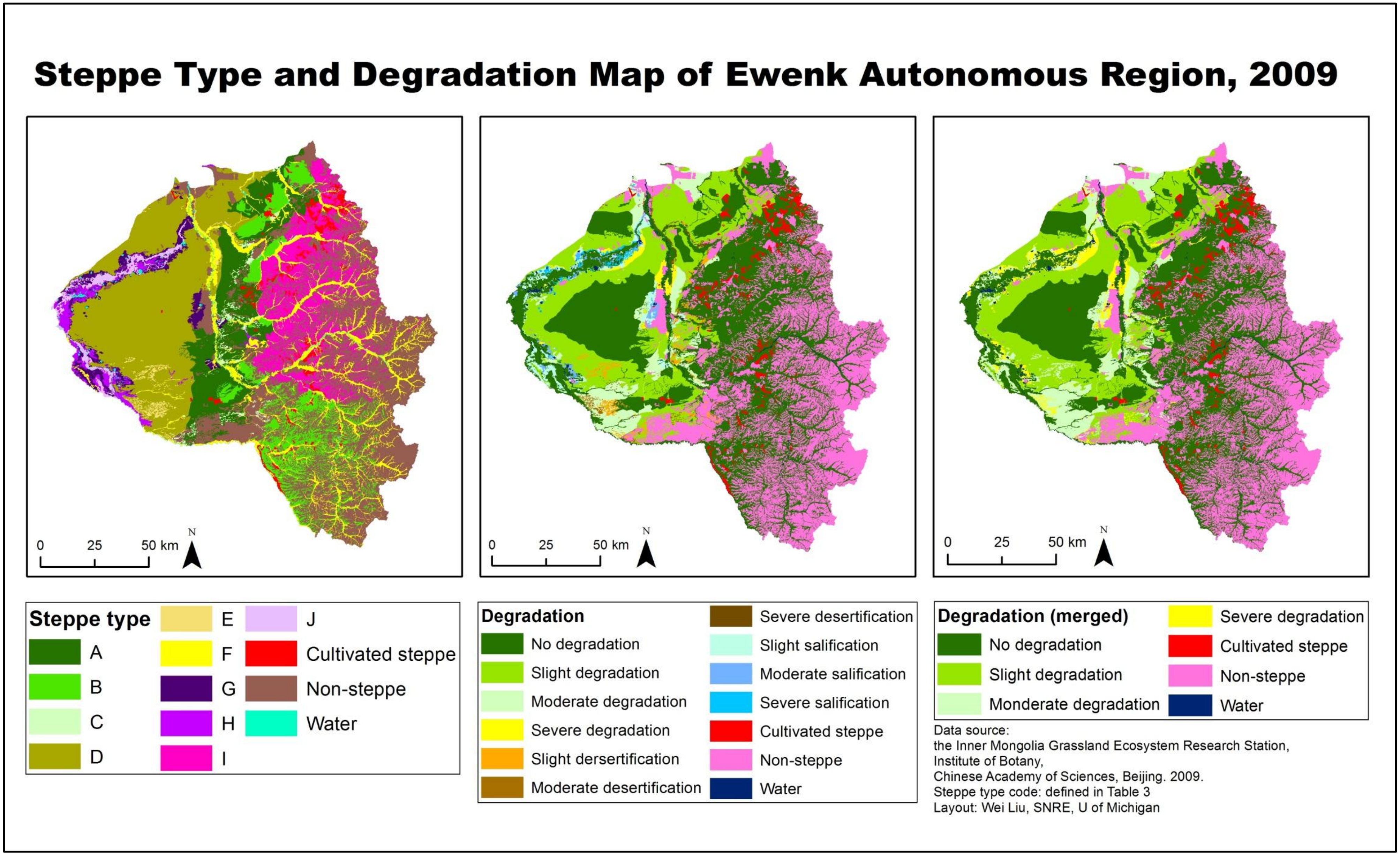

Steppe Type and Degradation Map of Xilinhot City, 2009

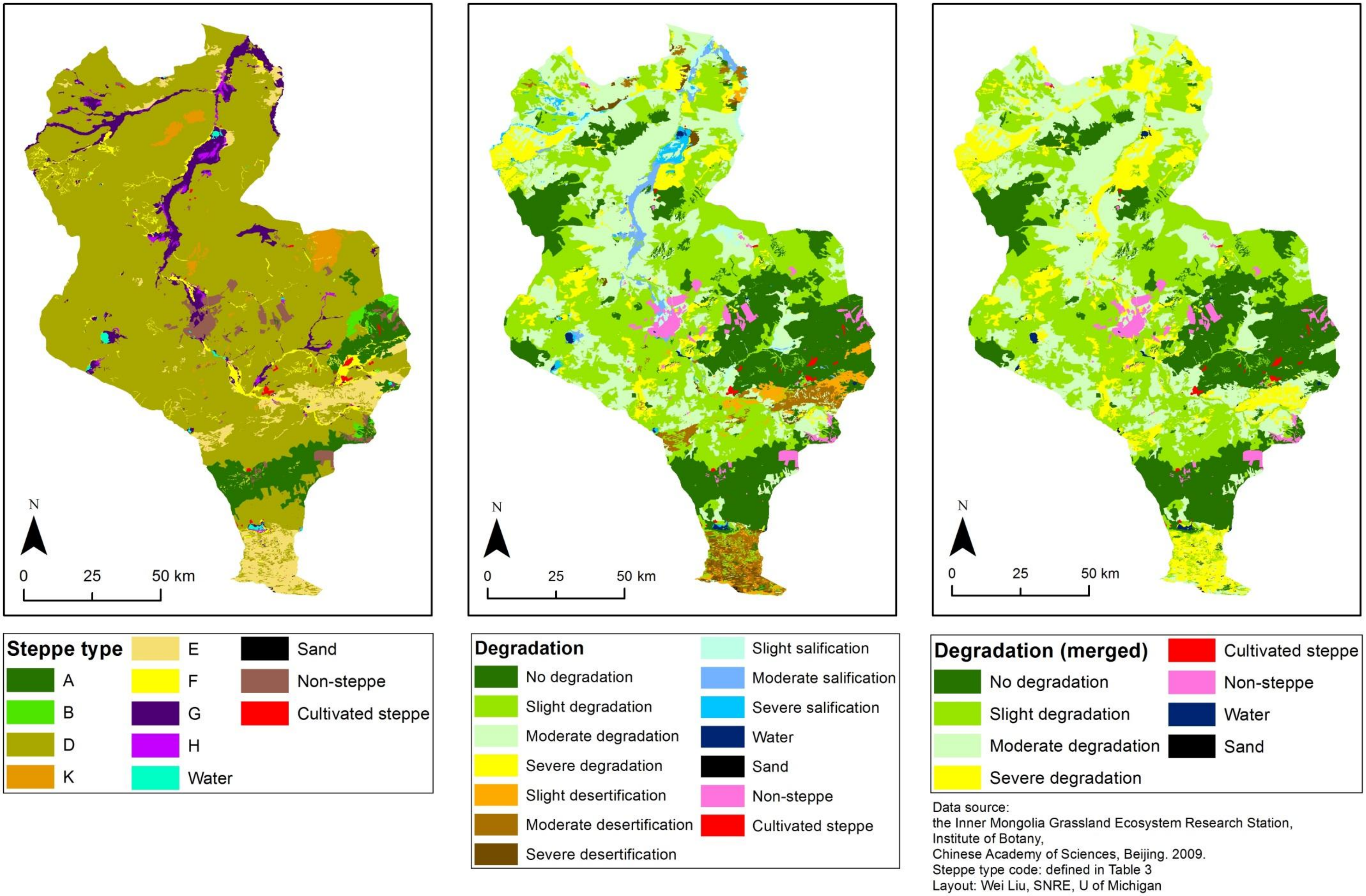

Steppe Type and Degradation Map of Urat Middle Banner, 2009

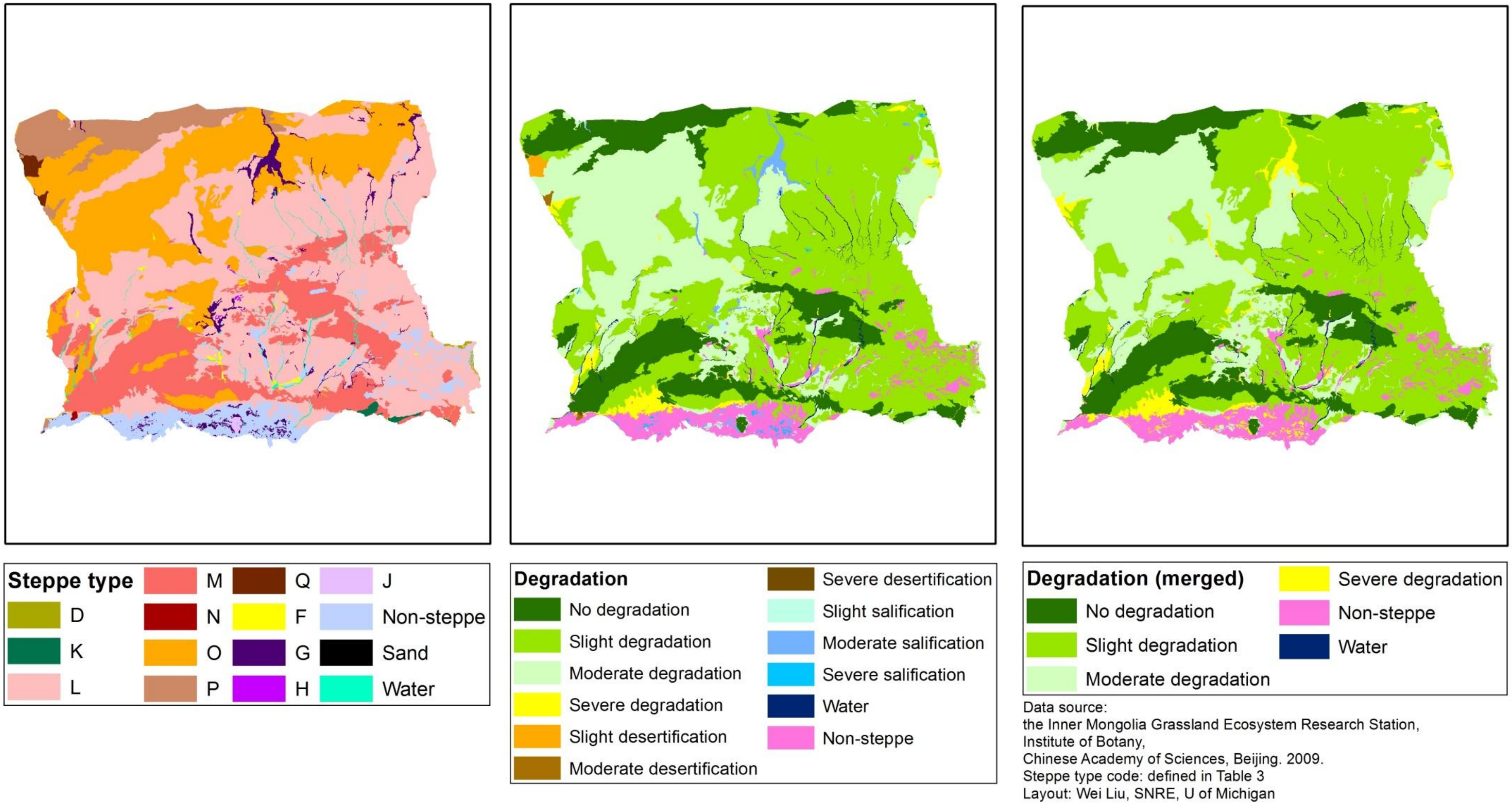

Appendix D

Steppe Type and Vegetation Match Table

Type code	Class	Subclass	Association group	Association
Ⅰ	Temperate meadow steppe			
A		Plain/hill meadow steppe		
1			Gramineae with shrubs group	
(1)				Prunus sibirica-Stipa baicalensis+Cleistogenes polyphylla
2			Forbs with shrubs group	
(1)				Prunus sibirica-Filifolium sibiricum+Carex pediformis
(2)				Prunus sibirica-Lespedeza hedysaroides+forbs
3			Semi-brush group	
(1)				Lespedeza hedysaroides-Cleistogenes polyphylla
4			Rhizomatous grass group	
(1)				Leymus chinensis+Stipa baicalensis
(2)				Leymus chinensis+Cleistogenes chinensis
(3)				Leymus chinensis+forbs
(4)				Calamagrostis epigejos+Filifolium sibiricum+Leymus chinensis
(5)				Arundinella hirta+Cleistogenes chinensis
5			Bunch grass group	
(1)				Stipa baicalensis+Leymus chinensis
(2)				Stipa baicalensis+Cleistogenes polyphylla+Arundinella hirta
(3)				Stipa baicalensis+Filifolium sibiricum
(4)				Stipa baicalensis+Carex pediformis
(5)				Cleistogenes polyphylla+Artemisia frigida+Carex pediformis
(6)				Cleistogenes polyphylla+Lespedeza hedysaroides
6			Eleocharis acicularis group	
(1)				Carex pediformis+Filifolium sibiricum+Stipa baicalensis
7			Erect forbs group	
(1)				Filifolium sibiricum+Stipa baicalensis
(2)				Filifolium sibiricum+Leymus chinensis
(3)				Filifolium sibiricum+Stipa grandis
(4)				Filifolium sibiricum+Lespedeza hedysaroides+Cleistogenes polyphylla
(5)				Sanguisorba officinalis+Artemisia tanacetifolia
(6)				Sanguisorba officinalis+Stipa baicalensis
B		Mountain meadow steppe		
1			Sage semi-brush rangeland with shrubs and trees group	
(1)				Populus davidiana（Betula platyphylla）-Prunus sibirica-Artemisia gmelinii+Lespedeza hedysaroides
(2)				Populus davidiana（Betula platyphylla）-Corylus davidiana-Artemisia gmelinii+Carex pediformis
2			Gramineae with shrubs and trees	

			group	
(1)				Populus davidiana（Betula platyphylla）-Spiraea pubescens-Stipa baicalensis
3			Gramineae with trees group	
(1)				Populus davidiana（Betula platyphylla）-Stipa baicalensis+Filifolium sibiricum+Carex pediformis
4			Forbs with trees and shrubs group	
(1)				Populus davidiana（Betula platyphylla）-Spiraea pubescens-Filifolium sibiricum-Carex pediformis
(2)				Populus davidiana（Betula platyphylla）-Corylus davidiana-Filifolium sibiricum+Stipa baicalensis
5			Sage semi-brush rangeland with shrubs group	
(1)				Prunus sibirica-Artemisia gmelinii+forbs
(2)				Corylus davidiana-Artemisia gmelinii
6			Gramineae with shrubs group	
(1)				Prunus sibirica-Leymus chinensis+Stipa baicalensis
(2)				Rosa davurica-Leymus chinensis+Carex pediformis
(3)				Prunus sibirica-Stipa baicalensis+Cleistogenes chinensis
(4)				Prunus sibirica-Cleistogenes polyphylla+Lespedeza davurica
(5)				Corylus davidiana-Stipa baicalensisCarex
(6)				Corylus davidiana-Cleistogenes polyphylla
(7)				Lespedeza nivolot-Cleistogenes chinensis
7			Cyperaceae with shrubs group	
(1)				Prunus sibirica-Carex pediformis+Sanguisorba officinalis
(2)				Corylus davidiana-Carex lanceolata+forbs
(3)				Corylus davidiana-Carex pediformis+forbs
(4)				Spiraea pubescens-Carex pediformis+forbs
(5)				Spiraea trilobata-Carex lanceolata
(6)				Potentilla fruticosa-Carex lanceolata
8			Forbs with shrubs group	
(1)				Prunus sibirica-Filifolium sibiricum+forbs
(2)				Corylus davidiana-Filifolium sibiricum+forbs
(3)				Spiraea pubescens-Filifolium sibiricum+Stipa baicalensis
(4)				Lespedeza nivolot-Filifolium sibiricum+Sanguisorba officinalis
9			Rhizomatous grass group	
(1)				Leymus chinensis+Stipa baicalensis+Cleistogenes polyphylla
(2)				Leymus chinensis+Cleistogenes polyphylla
(3)				Leymus chinensis+Festuca ovina
(4)				Leymus chinensis+Arundinella hirta
(5)				Leymus chinensis+Carex pediformis
(6)				Arundinella hirta+Stipa baicalensis+Cleistogenes chinensis
10			Bunch grass group	
(1)				Stipa baicalensis+Filifolium sibiricum
(2)				Stipa baicalensis+Leymus chinensis
(3)				Stipa baicalensis+Cleistogenes polyphylla

(4)				Cleistogenes polyphylla+Artemisia frigida
(5)				Cleistogenes polyphylla+Lespedeza hedysaroides
11			Semi-brush group	
(1)				Lespedeza davurica+Lespedeza hedysaroides-Agropyron cristatum
12			sagesemi-brush rangeland group	
(1)				Artemisia gmelinii-Stipa baicalensis
(2)				Artemisia gmelinii-Carex pediformis+Cleistogenes polyphylla
13			Eleocharis acicularis group	
(1)				Carex pediformis+forbs
(2)				Carex lanceolata+forbs
14			Erect forbs group	
(1)				Filifolium sibiricum+Stipa baicalensis
(2)				Filifolium sibiricum+Cleistogenes caespitosa
(3)				Filifolium sibiricum+Festuca ovina
(4)				Filifolium sibiricum+Spodiopogon sibiricus
(5)				Filifolium sibiricum+Carex pediformis
(6)				Artemisia tanacetifolia+Carex lanceolata
C		Sand land meadow steppe		
1			Sage semi-brush rangeland with shrubs group	
(1)				Salix gordejevii-Artemisia halodendron-Agropyron cristatum
(2)				Lespedeza nivolot-Artemisia halodendron-Allium senescens
2			sagesemi-brush rangeland group	
(1)				Artemisia halodendron-Leymus chinensis+forbs
Ⅱ	Temperate typical steppe			
A		Plain/hill typical steppe		
1			Semi-brush with shrubs group	
(1)				Caragana microphylla-Ceratoides latens+Artemisia frigida
(2)				Caragana intermedia-Oxytropis aciphylla
(3)				Caragana intermedia-Thymus serpyllum var. mongolicus+Stipa bungeana
2			Sage semi-brush rangeland with shrubs group	
(1)				Ulmus macrocarpa-Artemisia gmelinii-Cleistogenes chinensis
(2)				Caragana microphylla-Artemisia frigida+Stipa krylovii
(3)				Caragana stenophylla-Artemisia frigida+Leymus chinensis
3			Gramineae with shrubs group	
(1)				Caragana microphylla-Leymus chinensis+forbs
(2)				Caragana microphylla-Leymus chinensis+Allium polyrhizum
(3)				Prunus sibirica-Stipa grandis+Cleistogenes squarrosa
(4)				Prunus sibirica-Cleistogenes squarrosa+Lespedeza davurica
(5)				Ulmus macrocarpa-Cleistogenes chinensis+Stipa grandis
(6)				Caragana microphylla-Stipa grandis+Agropyron cristatum

(7)				Caragana microphylla-Stipa krylovii+Cleistogenes squarrosa
(8)				Caragana microphylla-Cleistogenes squarrosa+Stipa grandis
(9)				Caragana microphylla-Agropyron cristatum+Cleistogenes squarrosa
(10)				Caragana stenophylla-Stipa krylovii+Cleistogenes squarrosa
(11)				Caragana stenophylla-Cleistogenes squarrosa
(12)				Caragana intermedia-Stipa bungeana+Cleistogenes squarrosa
4			Semi-brush group	
(1)				Thymus serpyllum var. asiaticus+Stipa krylovii
(2)				Thymus serpyllum var. asiaticus+Stipa bungeana
(3)				Thymus serpyllum var. asiaticus+Stipa breviflora
(4)				Thymus serpyllum var. asiaticus+Cleistogenes squarrosa+Lespedeza davurica
(5)				Thymus serpyllum var. asiaticus+Artemisia frigida+Stipa krylovii
(6)				Lespedeza davurica+Cleistogenes squarrosa
(7)				Oxytropis aciphylla+Oxytropis psammocharis
(8)				Ephedra sinica+Lespedeza davurica+forbs
5			Sagesemi-brush rangeland group	
(1)				Artemisia gmelinii-Lespedeza davurica+Cleistogenes squarrosa
(2)				Artemisia frigida+Stipa grandis+Cleistogenes squarrosa
(3)				Artemisia frigida+Stipa krylovii+Leymus chinensis
(4)				Artemisia frigida+Stipa bungeana
(5)				Artemisia frigida+Cleistogenes squarrosa
(6)				Artemisia frigida+Leymus chinensis+Cleistogenes squarrosa
(7)				Artemisia frigida+Festuca ovina
(8)				Artemisia brachyloba+Stipa gobica
(9)				Artemisia giraldii+Thymus serpyllum var. asiaticus
6			Rhizomatous grass group	
(1)				Leymus chinensis+Stipa grandis
(2)				Leymus chinensis+Stipa krylovii
(3)				Leymus chinensis+Cleistogenes squarrosa+Agropyron cristatum
(4)				Leymus chinensis+Artemisia frigida
(5)				Leymus chinensis+forbs
(6)				Leymus chinensis+Artemisia capillaris+Cleistogenes squarrosa
7			Bunch grass group	
(1)				Stipa grandis+Leymus chinensis
(2)				Stipa grandis+Cleistogenes squarrosa
(3)				Stipa grandis+Artemisia frigida
(4)				Stipa krylovii+Leymus chinensis+Cleistogenes squarrosa
(5)				Stipa krylovii+Cleistogenes squarrosa
(6)				Stipa krylovii+Artemisia frigida
(7)				Stipa bungeana+Cleistogenes squarrosa+Thymus serpyllum var. mongolicus

(8)				Stipa bungeana+Lespedeza davurica+Artemisia scoparia
(9)				Cleistogenes squarrosa+Stipa grandis+Agropyron cristatum
(10)				Cleistogenes squarrosa+Stipa krylovii+Carex duriuscula
(11)				Cleistogenes squarrosa+Artemisia frigida
(12)				Cleistogenes squarrosa+Polygonum divaricatum+Digitaria ischaemum
(13)				Cleistogenes squarrosa+Lespedeza davurica+Stipa grandis
(14)				Cleistogenes squarrosa+Leymus chinensis
(15)				Agropyron cristatum+Stipa grandis
(16)				Agropyron cristatum+Artemisia frigida+Allium polyrhizum
(17)				Festuca ovina+Leymus chinensis
8			erect leguminous grass group	
(1)				Glycyrrhiza uralensis
(2)				Sophora alopecuroides
9			bulbousforbsgroup	
(1)				Allium polyrhizum+Leymus chinensis+Stipa grandis
(2)				Allium polyrhizum+Cleistogenes squarrosa
(3)				Allium ramosum+Stipa krylovii+Leymus chinensis
10			erect 杂草 group	
(1)				Cynanchum komarovii+annual forbs
B		Mountain typical steppe		
1			Gramineae with shrubs group	
(1)				Prunus sibirica-Cleistogenes polyphylla
(2)				Prunus pedunculata-Stipa krylovii
(3)				Prunus pedunculata-Stipa gobica
2			Sage semi-brush rangeland with shrubs group	
(1)				Corylus davidiana-Artemisia gmelinii+Carex lanceolata
(2)				Prunus pedunculata-Artemisia gmelinii
3			Semi-brush group	
(1)				Thymus serpyllum var. asiaticus+Stipa krylovii
(2)				Lespedeza davurica+Cleistogenes squarrosa+Stipa grandis
4			Sage semi-brush rangeland group	
(1)				Artemisia gmelinii+Thymus serpyllum var. asiaticus+Cleistogenes squarrosa
(2)				Artemisia gmelinii+Lespedeza davurica+Stipa grandis
(3)				Artemisia gmelinii+Artemisia frigida+Cleistogenes squarrosa
(4)				Artemisia gmelinii+Artemisia dracunculus+Stipa bungeana
(5)				Artemisia brachyloba+Lespedeza davurica+Cleistogenes squarrosa
5			Rhizomatous grass group	
(1)				Leymus chinensis+Cleistogenes squarrosa
(2)				Leymus chinensis+Artemisia frigida
6			Bunch grass group	
(1)				Stipa grandis+Cleistogenes squarrosa

(2)				Stipa krylovii+Artemisia frigida
(3)				Stipa krylovii+Thymus serpyllum var. asiaticus
(4)				Stipa krylovii+Potentilla acaulis
(5)				Cleistogenes squarrosa+Lespedeza davurica
C		Sand land typical steppe		
1			Sage semi-brush rangeland with trees and shrubs group	
(1)				Ulmus-Betula gmelinii+Artemisia frigida
(2)				Ulmus-Caragana microphylla-Artemisia halodendron+Pennisetum flaccidum
(3)				Ulmus-Caragana microphylla-Artemisia intramongolica
2			Sage semi-brush rangeland with trees group	
(1)				Ulmus-Artemisia frigida+Poa sphondylodes+Carex
(2)				Ulmus-Artemisia frigida+Cleistogenes squarrosa+Carex
(3)				Ulmus-Artemisia frigida+Artemisia halodendron+Pennisetum flaccidum
(4)				Ulmus-Artemisia halodendron+Melissitus ruthenicus var. oblongifolius
(5)				Ulmus-Ephedra sinica-Artemisia frigida+Pennisetum flaccidum
3			Gramineae with trees and shrubs group	
(1)				Ulmus-Prunus sibirica-Cleistogenes squarrosa+Lespedeza davurica
4			Gramineae with trees group	
(1)				Ulmus-Agropyron cristatum+Melissitus ruthenicus var. oblongifolius
(2)				Ulmus-Pennisetum flaccidum+Cleistogenes squarrosa
(3)				Ulmus-Cleistogenes squarrosa+annual forbs
5			Scale-leaf shrubsgroup	
(1)				Sabina vulgaris+forbs
6			Semi-brush with shrubs group	
(1)				Salix gordejevii-Ephedra sinica+Lespedeza davurica
(2)				Caragana microphylla-Ephedra sinica-Cleistogenes squarrosa
(3)				Caragana microphylla-Lespedeza davurica
(4)				Caragana microphylla-Hedysarum fruticosum
7			Sage semi-brush rangeland with shrubs group	
(1)				Prunus sibirica-Artemisia halodendron+Polygonum divaricatum
(2)				Spiraea trilobata-Artemisia frigida+Agropyron desertorum
(3)				Ulmus macrocarpa-Artemisia halodendron+Cleistogenes polyphylla
(4)				Atraphaxis manshurica-Artemisia halodendron+Artemisia frigida
(5)				Salix gordejevii-Artemisia halodendron
(6)				Salix gordejevii-Artemisia intramongolica
(7)				Caragana microphylla-Artemisia halodendron
(8)				Caragana microphylla-Artemisia frigida+Agropyron desertorum
(9)				Caragana intermedia-Artemisia intramongolica-Psammochloa villosa
(10)				Caragana intermedia-Artemisia ordosica

8			Gramineae with shrubs group	
(1)				Salix gordejevii-Pennisetum flaccidum
(2)				Caragana microphylla-Leymus chinensis+Agropyron desertorum
(3)				Caragana microphylla-Psammochloa villosa+Agropyron desertorum
(4)				Caragana microphylla-Pennisetum flaccidum
(5)				Caragana intermedia-Pennisetum flaccidum
(6)				Ulmus macrocarpa-Stipa grandis+Cleistogenes polyphylla
(7)				Atraphaxis manshurica-Agropyron desertorum+Lespedeza davurica
(8)				Lespedeza nivolot-Agropyron desertorum
(9)				Caragana microphylla-Agropyron desertorum+Lespedeza davurica
9			Semi-brush group	
(1)				Lespedeza davurica-Agropyron desertorum
(2)				Lespedeza davurica-Cleistogenes squarrosa
(3)				Hedysarum fruticosum-Pennisetum flaccidum
(4)				Oxytropis aciphylla-forbs
(5)				Ephedra sinica-Artemisia halodendron
(6)				Ephedra sinica-Cleistogenes squarrosa
10			Sage semi-brush rangeland group	
(1)				Artemisia oxycephala-Cleistogenes squarrosa+Lespedeza davurica
(2)				Artemisia halodendron-Artemisia frigida+Pennisetum flaccidum
(3)				Artemisia halodendron-Polygonum divaricatum
(4)				Artemisia halodendron-Agropyron desertorum
(5)				Artemisia ordosica-Psammochloa villosa
(6)				Artemisia ordosica-Artemisia frigida
(7)				Artemisia ordosica+Salix psammophyla
(8)				Artemisia ordosica-forbs
(9)				Artemisia frigida+Agropyron desertorum+Cleistogenes squarrosa
(10)				Artemisia intramongolica+Hedysarum fruticosum var. lignosum+Thymus serpyllum var. asiaticus
(11)				Artemisia intramongolica-Psammochloa villosa+Agropyron cristatum
11			Rhizomatous grass group	
(1)				Leymus chinensis+Stipa grandis+Artemisia frigida
(2)				Leymus chinensis+Poa annua+Artemisia frigida
(3)				Leymus chinensis+Lespedeza davurica+Cleistogenes squarrosa
(4)				Aneurolepidium dasystachys+annual forbs
(5)				Pennisetum flaccidum+Artemisia frigida+Phragmites australis
(6)				Psammochloa villosa+Agropyron desertorum+Artemisia frigida
(7)				Psammochloa villosa+Agriophyllum pungens
12			Bunch grass group	
(1)				Agropyron desertorum+Cleistogenes squarrosa+Artemisia frigida
(2)				Agropyron desertorum+Melissitus ruthenicus var.

				oblongifolius+Cleistogenes squarrosa
(3)				Cleistogenes squarrosa+Lespedeza davurica+forbs
(4)				Cleistogenes squarrosa+Polygonum divaricatum+Agropyron desertorum
13			Erect leguminous grass group	
(1)				Glycyrrhiza uralensis+annual forbs
14			Annualforbs group	
(1)				Artemisia scoparia+Cleistogenes squarrosa
(2)				Artemisia scoparia+Artemisia frigida
(3)				Agriophyllum pungens+Setaria viridis
III	Temperate desert steppe			
A		Plain/hill desert steppe		
1			Semi-brush with shrubs group	
(1)				Caragana stenophylla-Oxytropis aciphylla
(2)				Caragana stenophylla-Atraphaxis pungens
2			Gramineae with shrubs group	
(1)				Caragana stenophylla-Aneurolepidium dasystachys
(2)				Caragana intermedia-Psammochloa villosa
(3)				Prunus pedunculata-Stipa tianschanica var. klemenzii+Agropyron cristatum
(4)				Caragana microphylla-Stipa tianschanica var. klemenzii+Artemisia frigida
(5)				Caragana microphylla-Stipa breviflora+Artemisia frigida
(6)				Caragana microphylla-Cleistogenes songorica+Artemisia frigida
(7)				Caragana stenophylla-Stipa tianschanica var. klemenzii+Cleistogenes songorica
(8)				Caragana stenophylla-Stipa breviflora+Artemisia frigida
(9)				Caragana stenophylla-Agropyron desertorum+Cleistogenes songorica
(10)				Caragana stenophylla-Stipa breviflora+Cleistogenes squarrosa
3			Semi-brush group	
(1)				Hippolytia trifida+Stipa tianschanica var. klemenzii
(2)				Ceratoides latens+Stipa tianschanica var. klemenzii
(3)				Oxytropis aciphylla+Stipa tianschanica var. klemenzii
(4)				Ephedra sinica+forbs
4			Sagesemi-brush rangeland group	
(1)				Artemisia frigida+Stipa breviflora+Stipa tianschanica var. klemenzii
(2)				Artemisia frigida+Agropyron desertorum
(3)				Artemisia frigida+Lespedeza nivolot
5			Bunch grass group	
(1)				Stipa breviflora+Artemisia frigida
(2)				Stipa breviflora+Cleistogenes songorica
(3)				Stipa tianschanica var. klemenzii+Artemisia frigida+Cleistogenes songorica
(4)				Stipa tianschanica var. klemenzii+Cleistogenes songorica
(5)				Stipa tianschanica var. klemenzii+Ajania achilloides+Allium polyrhizum

(6)				Stipa tianschanica var. klemenzii+Convolvulus ammannii
(7)				Cleistogenes songorica+Stipa tianschanica var. klemenzii
6			Erect leguminous grass group	
(1)				Glycyrrhiza uralensis+forbs
(2)				Sophora alopecuroides+forbs
(3)				Astragalus melilotoides+Artemisia capillaris
7			Erectforbs group	
(1)				Iris bungei+Stipa tianschanica var. klemenzii+Cleistogenes songorica
(2)				Iris bungei+forbs
8			Bulbousforbs group	
(1)				Allium polyrhizum+Stipa tianschanica var. klemenzii+Cleistogenes songorica
(2)				Allium polyrhizum+Allium mongolicum
9			Annual forbs group	
(1)				Salsola collina+forbs
B		Mountain desert steppe		
1			Forbs with trees group	
(1)				Ulmus glaucescens+Prunus ansu-forbs
2			Gramineae with shrubs group	
(1)				Prunus mongolica-Stipa gobica
3			Bunch grass group	
(1)				Stipa tianschanica var. klemenzii+Agropyron desertorum
(2)				Stipa tianschanica var. klemenzii+Ajania achilloides
(3)				Stipa gobica+Convolvulus tragacanthoides
(4)				Stipa breviflora+Artemisia frigida
C		Mountain desert steppe		
1			Sage semi-brush rangeland with shrubs group	
(1)				Caragana stenophylla-Artemisia ordosica
(2)				Caragana intermedia-Artemisia ordosica
2			Semi-brush group	
(1)				Hedysarummongolicum turcz+Artemisia ordosica
3			Sagesemi-brush rangeland group	
(1)				Artemisia ordosica-Psammochloa villosa
(2)				Artemisia ordosica-Glycyrrhiza uralensis
(3)				Artemisia ordosica-forbs
4			Rhizomatous grass group	
(1)				Pennisetum flaccidum+Setaria viridis
(2)				Psammochloa villosa+forbs
Ⅳ	Temperate steppe desert			
A		Gravelly steppe desert		
1			Succulent shrub group	
(1)				Caragana korshinskii

(2)				Caragana intermedia+Caragana tibetica
(3)				Caragana korshinskii+Nitraria sphaerocarpa-Psammochloa villosa
2			Semi-brush with shrubs group	
(1)				Caragana korshinskii-Oxytropis aciphylla
3			Sage semi-brush rangeland with shrubs group	
(1)				Caragana korshinskii-Artemisia ordosica
4			Gramineae with shrubs group	
(1)				Caragana stenophylla+Reaumuria soongarica-Stipa tianschanica var. klemenzii
(2)				Caragana korshinskii-Cleistogenes songorica
(3)				Caragana intermedia-sand Gramineae
(4)				Caragana brachypoda-Potaninia mongolica-Cleistogenes songorica
(5)				Caragana brachypoda-Stipa tianschanica var. klemenzii
(6)				Caragana opulens-Stipa breviflora+Cleistogenes songorica
(7)				Ammopiptanthus mongolicus-Ceratoides latens+Stipa tianschanica var. klemenzii
(8)				Nitraria tangutorum+Reaumuria soongarica-Cleistogenes songorica
(9)				Zygophyllum xanthoxylon+Reaumuria soongarica-Cleistogenes songorica
(10)				Reaumuria soongarica+Stipa tianschanica var. klemenzii+Cleistogenes songorica
5			Bulbous forbs with shrubs group	
(1)				Nitraria tangutorum+Reaumuria soongarica-Allium polyrhizum
6			Succulent shrub group	
(1)				Nitraria tangutorum+Zygophyllum xanthoxylon
(2)				Zygophyllum xanthoxylon+Ammopiptanthus mongolicus
(3)				Zygophyllum xanthoxylon+Caragana brachypoda
(4)				Reaumuria soongarica+Potaninia mongolica
(5)				Tetraena mongolica+Potaninia mongolica
(6)				Tetraena mongolica+Reaumuria soongarica
7			Cushion-like shrub and semi-brush group	
(1)				Caragana tibetica+Reaumuria soongarica
(2)				Caragana tibetica+Zygophyllum xanthoxylon
8			Sage semi-brush rangeland with cushion-like shrubs group	
(1)				Caragana tibetica-Artemisia frigida+Stipa gobica
9			Gramineae with cushion-like shrubs group	
(1)				Caragana tibetica-Stipa tianschanica var. klemenzii+Cleistogenes songorica
(2)				Helianthemum songaricum-Stipa tianschanica var. klemenzii
10			Semi-brush group	
(1)				Ceratoides latens+Hippolytia trifida+Ajania achilloides
(2)				Ceratoides latens+Stipa tianschanica var. klemenzii
(3)				Oxytropis aciphylla-Stipa tianschanica var. klemenzii
11			Saltsemi-brush group	

(1)				Salsola passerina+Reaumuria soongarica-Allium polyrhizum
B		Terrene steppe desert		
1			Saltsemi-brush group	
(1)				Kalidium foliatum+Salsola passerina+Reaumuria soongarica
(2)				Kalidium foliatum+Nitraria sibirica
(3)				Kalidium foliatum+Suaeda glauca
(4)				Salsola passerina-Stipa tianschanica var. klemenzii+Allium polyrhizum
C		Gravelly steppe desert		
1			Gramineae with shrubs group	
(1)				Prunus mongolica+Reaumuria soongarica+Stipa tianschanica var. klemenzii
(2)				Salsola laricifolia+Stipa gobica
2			Bulbous forbs with shrubs group	
(1)				Salsola laricifolia-Allium polyrhizum
3			Saltsemi-brush group	
(1)				Salsola passerina+Reaumuria soongarica-Stipa tianschanica var. klemenzii
(2)				Salsola passerina+Reaumuria soongarica-Allium polyrhizum
(3)				Salsola passerina+Sympegma regelii-Stipa bungeana
(4)				Salsola passerina+Sympegma regelii+Brachanthemum mongolicum
(5)				Sympegma regelii+Nitraria sibirica-Ptilagrostis pelliotii
(6)				Anabasis brevifolia-Stipa gobica
V	Temperate desert			
A		Sandy desert		
1			Shrubs with trees group	
(1)				Haloxylon ammodendron
(2)				Haloxylon ammodendron-Nitraria tangutorum
(3)				Haloxylon ammodendron-Calligonum mongolicum+Zygophyllum xanthoxylon
2			Succulent shrub group	
(1)				Nitraria sibirica
(2)				Nitraria tangutorum+Ammopiptanthus mongolicus
3			Semi-brush group	
(1)				Calligonum mongolicum+Zygophyllum xanthoxylon+Nitraria sphaerocarpa
4			Sagesemi-brush rangeland group	
(1)				Artemisia desertorum+Zygophyllum xanthoxylon+Reaumuria soongarica
(2)				Artemisia desertorum+Ammopiptanthus mongolicus
(3)				Artemisia desertorum+Psammochloa villosa
(4)				Artemisia desertorum+Nitraria tangutorum
(5)				Artemisia ordosica+Zygophyllum xanthoxylon+Ammopiptanthus mongolicus
(6)				Artemisia ordosica+Glycyrrhiza uralensis
(7)				Artemisia ordosica+forbs

(8)				Artemisia sphaerocephala+forbs
5			Rhizomatous grass group	
(1)				Psammochloa villosa
B		Sandy and gravelly desert		
1			Shrubs with trees group	
(1)				Haloxylon ammodendron+Reaumuria soongarica
2			Succulent shrub group	
(1)				Caragana leucophloea+Nitraria sibirica
(2)				Caragana leucophloea+Zygophyllum xanthoxylon+Stipa gobica
(3)				Ammopiptanthus mongolicus+Reaumuria soongarica+Nitraria sibirica
(4)				Potaninia mongolica+Salsola passerina+Reaumuria soongarica
(5)				Potaninia mongolica+Zygophyllum xanthoxylon+Ceratoides latens
(6)				Potaninia mongolica+Caragana brachypoda
(7)				Potaninia mongolica+Tetraena mongolica
(8)				Sympegma regelii+Zygophyllum xanthoxylon+Anabasis brevifolia
(9)				Zygophyllum xanthoxylon+Potaninia mongolica
(10)				Zygophyllum xanthoxylon+Ceratoides latens+Oxytropis aciphylla
(11)				Nitraria sphaerocarpa+Zygophyllum xanthoxylon
(12)				Nitraria sphaerocarpa+Salsola passerina+Kalidium sinicum
3			Semi-brush group	
(1)				Oxytropis aciphylla+Zygophyllum xanthoxylon+Ceratoides latens
(2)				Ceratoides latens+Nitraria sphaerocarpa
C		Gravelly desert		
1			Succulent shrub group	
(1)				Zygophyllum xanthoxylon+Prunus mongolica+Reaumuria soongarica
(2)				Nitraria sphaerocarpa+Reaumuria soongarica
(3)				Reaumuria soongarica
(4)				Reaumuria soongarica+Salsola passerina
(5)				Brachanthemum gobicum
(6)				Brachanthemum mongolicum+Zygophyllum xanthoxylon+Oxytropis aciphylla
(7)				Brachanthemum mongolicum+Reaumuria soongarica+Salsola passerina
(8)				Brachanthemum mongolicum+Ceratoides latens
2			Scale-leaf shrubsgroup	
(1)				Ephedra przewalskii+Reaumuria soongarica+Zygophyllum xanthoxylon
(2)				Ephedra przewalskii+Artemisia desertorum+Stipa gobica
3			Semi-brush group	
(1)				Convolvulus tragacanthoides+Artemisia xerophytica
(2)				Convolvulus tragacanthoides+Potaninia mongolica
(3)				Convolvulus gortschakovii+Brachanthemum gobicum
4			Saltsemi-brush group	

(1)				Salsola passerina+Reaumuria soongarica
(2)				Salsola passerina+Anabasis brevifolia
(3)				Anabasis brevifolia+Salsola laricifolia
5			Annualforbs group	
(1)				Elachanthemum intricatum+annual forbs
D		Saline desert		
1			Succulent shrub group	
(1)				Nitraria roborowskii+Reaumuria soongarica
2			Saltsemi-brush group	
(1)				Kalidium sinicum+Sympegma regelii
(2)				Kalidium sinicum+Salsola passerina
(3)				Kalidium gracile
(4)				Kalidium gracile+Nitraria tangutorum
(5)				Salsola passerina+Kalidium foliatum+Sympegma regelii
(6)				Salsola passerina+Kalidium sinicum+Reaumuria soongarica
(7)				Salsola passerina+Nitraria sphaerocarpa
Ⅵ	Mountain meadow			
A		Subalpine meadow		
1			Cyperaceae group	
(1)				Kobresia bellardii+Festuca ovina
(2)				Kobresia pygmaea+Kobresia bellardii
B		Mountain meadow		
1			Gramineae with trees and shrubs group	
(1)				Quercus mongolica+Corylus heterophylla+Lespedeza nivolot+Calamagrostis arundinacea
2			Eleocharis acicularis with trees and shrubs group	
(1)				Quercus mongolica-Lespedeza nivolot-Carex pediformis+Sanguisorba officinalis
3			Gramineae with trees group	
(1)				Populus davidiana-Spodiopogon sibiricus+Arundinella hirta
4			Eleocharis acicularis with trees group	
(1)				Populus davidiana-Carex pediformis+Vicia gigantea
(2)				Pinaceae-Carex caespitosa+forbs
5			Erectforbs with shrubs	
(1)				Populus davidiana-Sanguisorba officinalis+Carex pediformis
(2)				Populus davidiana-Filifolium sibiricum+Spodiopogon sibiricus+Arundinella hirta
(3)				Populus davidiana+Hemerocallis citrina+Carex pediformis
6			Eleocharis acicularis with shrubs group	
(1)				Salix+Spiraea salicifolia-Carex
(2)				Rosa davurica-Carex pediformis+Vicia gigantea
7			Forbs with shrubs group	
(1)				Salix+Spiraea salicifolia-Sanguisorba

				officinalis+Artemisia tanacetifolia
8			Rhizomatous grass group	
(1)				Calamagrostis epigejos+Sanguisorba officinalis
(2)				Bromus inermis+Leymus chinensis
9			Bunch grass group	
(1)				Roegneria kamoji+Sanguisorba officinalis
(2)				Poa annua+forbs
10			Eleocharis acicularis group	
(1)				Carex pediformis+Sanguisorba officinalis
(2)				Carex pediformis+Poa annua
(3)				Carex lanceolata+forbs
11			Erectforbs group	
(1)				Sanguisorba officinalis+Carex pediformis
Ⅶ	Lowland meadow			
A		Lowland and wetland meadow		
1			Gramineae with trees group	
(1)				Salix-Roegneria kamoji+Artemisia tanacetifolia+Sanguisorba officinalis
2			Cyperaceae with shrubs group	
(1)				Salix-Carex+Calamagrostis purpurea+forbs
(2)				Salix-Carex+forbs
3			Forbs with trees and shrubs group	
(1)				Populus cuphratica-Tamarix chinensis-Sophora alopecuroides+forbs
(2)				Populus cuphratica-forbs
(3)				Elaeagnus angustifolia-Tamarix chinensis-Sophora alopecuroides+forbs
(4)				Ulmus-forbs
4			Gramineae with shrubs group	
(1)				Salix bush-Leymus chinensis+forbs
(2)				Salix bush-Phragmites australis
(3)				Salix bush-Calamagrostis purpurea+Artemisia lavandulaefolia
(4)				Salix bush-Miscanthus sacchariflorus+Hemarthria compressa var. fasciculata
(5)				Salix bush-Arundinella hirta+Sanguisorba officinalis
(6)				Salix bush-Agrostis gigantea+forbs
5			Cyperaceae with shrubs group	
(1)				Salix bush-Scirpus triqueter+forbs
(2)				Salix bush-Carex appendiculata
6				
(1)				Salix bush-Sanguisorba officinalis+forbs
(2)				Spiraea salicifolia-forbs
(3)				Betula fruticosa-forbs
7			Rhizomatous grass group	
(1)				Calamagrostis epigejos+Carex+forbs

(2)				Calamagrostis epigejos+Arundinella hirta
(3)				Calamagrostis epigejos+Phragmites australis+forbs
(4)				Phragmites australis+Leymus chinensis+forbs
(5)				Agrostis gigantea+Scirpus triqueter+forbs
(6)				Agrostis gigantea+Calamagrostis epigejos+forbs
(7)				Arundinella hirta+Leymus chinensis
(8)				Arundinella hirta+Sanguisorba officinalis
(9)				Leymus chinensis+Arundinella hirta+forbs
(10)				Leymus chinensis+Phragmites australis+Calamagrostis epigejos
(11)				Leymus chinensis+Carex+forbs
(12)				Leymus chinensis+Sanguisorba officinalis+forbs
(13)				Leymus chinensis+Iris lactea var. chinensis+forbs
(14)				Poa subfastigiata+Hordeum brevisubulatum+Leymus chinensis
8			Bunch grass group	
(1)				Elymus dahuricus+Leymus chinensis+Carex
(2)				Elymus dahuricus+Phragmites australis
9			Eleocharis vivipara group	
(1)				Carex meyeriana+forbs
10			Creepingforbs group	
(1)				Potentilla ansrina+forbs
B		Swampy lowland meadow		
1			Rhizomatous grass group	
(1)				Phragmites australis+Scirpus triqueter+forbs
(2)				Phragmites australis+Calamagrostis epigejos+forbs
(3)				Calamagrostis epigejos+Agrostis gigantea+Scirpus triqueter
(4)				Agrostis gigantea+Scirpus triqueter+Leymus chinensis
(5)				Calamagrostis purpurea+Carex+forbs
(6)				Agrostis mongolica+Potentilla ansrina+Eleocharis intersita
2			Cyperaceae group	
(1)				Carex+Hemarthria compressa var. fasciculata+Scirpus planiculmis
(2)				Carex+Phragmites australis+forbs
(3)				Carex+forbs
(4)				Eleocharis intersita+Potentilla ansrina+forbs
C		Salinized lowland meadow		
1			Gramineae with shrubs group	
(1)				Nitraria tangutorum-Achnatherum splendens+forbs
(2)				Reaumuria soongarica-Leymus chinensis+Allium polyrhizum
2			Forbs with shrubs group	
(1)				Nitraria tangutorum-Salineforbs
(2)				Reaumuria soongarica-forbs
3			Saltsemi-brush group	

(1)				Kalidium foliatum+Reaumuria soongarica-forbs
(2)				Kalidium gracile-Phragmites australis
(3)				Kalidium foliatum-forbs
4			Rhizomatous grass group	
(1)				Phragmites australis+Puccinellia distans+Hordeum brevisubulatum
(2)				Leymus chinensis+Calamagrostis epigejos+Puccinellia tenuiflora
(3)				Leymus chinensis+Puccinellia distans+Suaeda glauca
(4)				Leymus chinensis+Iris lactea var. chinensis+Suaeda glauca
(5)				Leymus chinensis+Carex+forbs
(6)				Hordeum brevisubulatum+forbs
(7)				Hordeum brevisubulatum+Leymus chinensis+forbs
5			Bunch grass group	
(1)				Puccinellia distans+Suaeda glauca+forbs
(2)				Puccinellia distans+forbs
(3)				Puccinellia tenuiflora+Phragmites australis
(4)				Achnatherum splendens+Leymus chinensis+forbs
(5)				Achnatherum splendens+Iris lactea var. chinensis+forbs
(6)				Achnatherum splendens+Suaeda glauca
(7)				Achnatherum splendens+Puccinellia distans
(8)				Achnatherum splendens+Reaumuria soongarica+Salsola passerina
(9)				Achnatherum splendens+Nitraria sibirica
(10)				Achnatherum splendens+Kalidium foliatum-forbs
(11)				Achnatherum splendens-Allium polyrhizum+forbs
(12)				Achnatherum splendens-Allium mongolicum+forbs
(13)				Achnatherum splendens-Carex+forbs
6			Eleocharis acicularis group	
(1)				Carex duriuscula+forbs
(2)				Carex+Hordeum brevisubulatum+forbs
(3)				Carex+Puccinellia distans+forbs
7			Erectforbs groups	
(1)				Iris lactea var. chinensis+Leymus chinensis+forbs
(2)				Iris lactea var. chinensis+Carex+forbs
(3)				Iris lactea var. chinensis+Hordeum brevisubulatum+forbs
(4)				Iris lactea var. chinensis+Suaeda glauca+forbs
8			Annualforbs group	
(1)				Suaeda glauca+Artemisia anethifolia+forbs
(2)				Suaeda corniculata+forbs
Ⅷ	Swamp/marsh			
1			Rhizomatous grass group	
(1)				Phragmites australis+Scirpus triqueter+Carex
(2)				Phragmites australis+Typha orientalis
(3)				Phragmites australis
2			Eleocharis vivipara group	

(1)				Carex meyeriana+Calamagrostis purpurea
(2)				Eleocharis intersita+forbs
(3)				Scirpus triqueter+forbs
(4)				Scirpus tabernaemontani+forbs
(5)				Carex appendiculata+Carex meyeriana
3			Erectforbs group	
(1)				Typha orientalis+forbs
Ⅸ	Supplementary grassland			